2011

The Hos2p Histone De-acetylase Promotes the Successful Completion of Cytokinesis in Schizosaccharomyces pombe.

Charnpal Grewal

The Hos2p Histone De-acetylase Promotes the Successful Completion of Cytokinesis in *Schizosaccharomyces pombe.*

(Spine title: A Histone De-acetylase with a Role in Cytokinesis)

(Thesis format: Monograph)

by

Charnpal Grewal

Graduate Program in Biology

A thesis submitted in partial fulfillment
of the requirements for the degree of
Master of Science

The School of Graduate and Postdoctoral Studies
The University of Western Ontario
London, Ontario, Canada

THE UNIVERSITY OF WESTERN ONTARIO
SCHOOL OF GRADUATE AND POSTDOCTORAL STUDIES

CERTIFICATE OF EXAMINATION

Supervisor:

Dr. Jim Karagiannis

Supervisory Committee:

Dr. Sashko Damjanovski

Dr. Greg Kelly

Examiners:

Dr. Sashko Damjanovski

Dr. Shiva Singh

Dr. Mark Bernards

The thesis by

Charnpal Grewal

entitled:

The Hos2p Histone De-acetylase Promotes the Successful Completion of Cytokinesis in *Schizosaccharomyces pombe.*

is accepted in partial fulfillment of the requirements for the degree of

Master of Science

Date

Chair of the Thesis Examination Board

ABSTRACT

A cell cycle checkpoint at the G2/M boundary of fission yeast cells ensures that the G2/M transition of daughter cells only occurs after successful cytokinesis in the mother cell. The Lst complex is necessary for proper functioning of this checkpoint and is orthologous to a human histone de-aceylase complex (HDAC3/NCOR2-SMRT), with a known role in cytokinesis. However, the fission yeast orthologue of the human HDAC3 histone de-acetylase, Hos2p, was never previously characterized with respect to the Lst complex. Through a combination of phenotypic analyses on *hos2* mutants, live-cell imaging of Hos2p localization, live-cell imaging of cytokinesis dynamics as they relate to Hos2p's cytokinetic regulatory function, and co-immunoprecipitation experiments, I showed that Hos2p is indeed a member of the Lst complex, and ensures faithful cytokinesis through its de-acetylase activity. Additionally, I used Western Blotting to show that the Lst complex is a stress-responsive complex that up-regulates expression of its Lst1p sub-unit in response to a sub-set of environmental stressors known to turn on the fission yeast core environmental stress response (CESR). Finally, I show that Hos2p inhibits growth and produces various abnormal phenotypes in a dose-dependent manner, although the biological significance of these observations is unclear.

Keywords: cytokinesis, *Schizosaccharomyces pombe*, cell cycle, checkpoint, transcription, histone de-acetylase, core environmental stress response (CESR)

ACKNOWLEDGMENTS

I give my utmost thanks and a great respect to my supervisor Dr. Jim Karagiannis for giving me a running start into my research career. Through realistic guidance, positive feedback and constructive criticisms, he has shaped my thinking and working patterns into that of an effective, creative and adaptable problem solver, and has ensured a timely and smooth passage through my M.Sc. by providing dependable support at sticking points. I also like to thank Dr. Sashko Damjanovski and Dr. Greg Kelly for their feedback and encouragement at various landmarks in my M.Sc. Special thanks to Stefan, Kyle, and undergraduates in the lab for enjoyable company. I thank my spiritual mentor, Baba Baldev Singh Ji for giving me tranquility, contentment and unshakeable inner strength. I thank my father who had taught me how to dream big and have the courage to relentlessly pursue those dreams, and I thank my mother for stepping in his shoes as well as her own, and being my best friend and a source of wisdom, strength and comfort ever since he had passed away.

TABLE OF CONTENTS

LIST OF FIGURES

LIST OF TABLES

APPENDIX

Please refer to the appended disc entitled:

Charnpal Grewal
M.Sc. Thesis, 2011
Supplementary Disc
Videos for:
Chapter 3
Section 3

LIST OF ABBREVIATIONS

Ade: adenine

APC: anaphase promoting complex

BRCA2: breast cancer 2

Cdc: cell division cycle

Cdk1: cyclin-dependent kinase 1

Cdr: changed division response

CESR: core environmental stress response

Clp1: cdc14p-like protein 1

DAPI: 4'6,-diamidino-2-phenylindole

DMSO: dimethyl sulfoxide

DNA: deoxyribonucleic acid

E3: enzyme 3

EDTA:ethylenediaminetetraacetic acid

EMM: edinburgh minimal medium

G1: gap 1

G2: gap 2

GFP: green fluorescent protein

H: histone OR heterothallic (depending on context)

HA: hemagglutinin

HAT: histone acetyltransferase

HDAC: histone de-acetylase

His: histidine

Hos2: HDA (histone de-acetylase) one similar 2

HU: hydroxyurea

IP: immunoprecipitation

JNK: c-Jun N-terminal kinase

Kif-4: kinesin family member 4

LatA: latrunculin A

LATS1: large tumor suppressor 1

LB: Luria-Bertani medium

Leu: leucine

Lsk1: latrunculin sensitive kinase 1

Lst: latrunculin sensitive transcription factor

M: mitosis

MAPK: mitogen-activated protein kinase

Mid1: division in the middle 1

MKLP1: mitotic kinesin-like protein 1

MLL5: mixed lineage leukemia 5

MMS: methyl methanesulfonate

Myc: myelocytomatosis viral oncogene

NCOR2: nuclear co-receptor 2

nmt: no message in thiamine

OD_{600}: optical density at 600 nm

ORF: open reading frame

p38: protein 38 kilodaltons

p53: protein 53 kilodaltons

PBS: phosphate buffered saline

PCR: polymerase chain reaction

PHD: plant homeodomain

Plo1: *S. pombe* orthologue of polokinase

PMSF: phenylmethanesulphonylfluoride

Polo: kinase needed to form normal spindle poles

PRC1: protein regulator of cytokinesis 1

Pom1: polarity misplaced 1

pREP: exosomally replicating plasmids

PVDF: polyvinylidene fluoride

Rho: ras homolog

Rlc1: regulatory light chain of myosin 1

RNAi: ribonucleic acid interference

rpm: revolutions per minute

S: synthesis

SANT: switching-defective protein 3, adaptor 2, nuclear receptor co-repressor, transcription factor

SDS-PAGE: sodium dodecyl sulfate polyacrylamide gel electrophoresis

SET: su(var)3-9, enhancer-of-zeste and trithorax

SIF2: sir4p-interacting factor 2

SIN: septation initiation network

SMRT: silencing mediator of retinoid and thyroid receptors

SNARE: SNAP [soluble NSF (N-ethylmaleimide-sensitive factor) attachment protein] REceptor

SNT1: sant domains protein 1

SPB: spindle pole body

Sty1: serine threonine tyrosine kinase 1

TBL1X: transducin β like 1 X-linked

Ura: uracil

UV: ultraviolet

WD40: ~40 domain amino acid motif, often terminating in a Trp-Asp (W-D) dipeptide.

Wee1: named for the small (i.e. wee) phenotype of the deletion mutant

Y321H: tyrosine residue 321 of Hos2p replaced with histidine

YES: yeast extract and supplements

CHAPTER 1: INTRODUCTION

1.1 Cytokinesis in metazoans

Cytokinesis is a fundamental part of the cell cycle in all eukaryotes and must be fully understood to complete the foundation for basic eukaryotic cell biology. Despite this, cytokinesis is riddled with many unanswered questions regarding how its known parts function together to ensure reliable cell division. This is partly explained by the fact that cytokinesis involves many spatially and temporally co-ordinated processes, making it a challenging research topic. That being said however, a number of broad generalizations can be made for cytokinesis in metazoans (Eggert *et al.* 2006).

Cytokinesis is temporally regulated and cleavage furrow assembly only occurs within a tightly restricted window of time, determined by both kinase-phosphatase and regulated proteolysis systems. Reduced Cdc2/Cdk1 activity (the master regulator for G2 exit) irreversibly commits a cell to divide, and APC (anaphase promoting complex, which is an E3 ligase) regulates mitotic exit by ubiquitination of cyclin B and securin for proteolysis(King *et al.* 1996) (Nigg, 2006) (Niiya *et al.* 2005). Cytokinesis is also spatially regulated and the plane of cleavage furrow formation is specified by microtubule signals to the cell cortex (Eggert *et al.* 2006).

As the cell prepares to divide, proteins necessary for furrowing accumulate at the equator in a microtubule-dependent manner (i.e. Rho, Rho regulators, Aurora B, Polo, etc.)(Bement *et al.* 2005) (Hirose *et al.* 2001) (Mabuchi *et al.* 1993) (Nigg, 2001) (Prokopenko *et al.* 1999) (Tatsumoto *et al.* 1999) (Uyeda *et al.* 2004). Additionally, a microtubule structure specialized for cytokinesis (the midzone) forms. The midzone is

self-organizing and characterized by a distinct array of microtubule-associated proteins and motors (i.e. activated PRC1, the kinesins MKLP1 and Kif-4) (Adams *et al.* 1998) (Goshima and Vale, 2003) (Mollinari *et al.* 2002) (Nislow *et al.* 1992) (Verni*et al.* 2004) (Vernos *et al.* 1995) (Williams *et al.* 1995) (Zhu and Jiang, 2005).

The actomyosin contractile ring begins to depolymerize and contract upon assembly, which generates a force that is coupled to an increase in cell surface area by membrane deposition. The contractile ring ingresses to its fullest point, after which the intercellular bridge continues to constrict, except in a region termed the stembody (a structure necessary for completion). Microtubules disappear over the length of the bridge, which has a characteristic array of proteins (i.e. anillin and septins). Finally, the completion of cytokinesis involves membrane fusion mediated by specific SNAREs (a protein superfamily mediating vesicle fusion) using mechanisms common with other types of intracellular vesicle fusion (Echard *et al.* 2004) (Low *et al.* 2003).

Despite the unanswered questions and poorly understood processes tied to cytokinesis, a survey of the processes involved reveals an important theme: many aspects of cytokinesis are controlled by multiple pathways that operate in parallel. This property confers robustness to cytokinesis; robustness is the property whereby the system is able to operate normally and dependably under a wide range of external variables that challenge the system, which is unsurprising given the complexity of cytokinesis and hints at important consequences for cytokinesis failure. The ideas discussed in Chapter 1.1 are summarized in Fig. 1.1.

1.2 The utility of *S. pombe* as a model for cytokinesis in metazoans

Figure 1.1 Generalized schematic of the sequence of events that occur during cytokinesis in metazoans. Image modified from Pollard and Wu 2010. See text for a detailed description.**(A)** In preparation for cytokinesis, microtubules form and elongate from the centrosomes, and the nuclear envelope begins to dissolve. **(B)** The microtubules lengthen. One subpopulation of microtubules does not interact with chromosomes, and has a role in the placement of the contractile ring (astral microtubules). Another subpopulation of microtubules captures the chromosomes, aligning them at the metaphase plate (spindle microtubules). The contractile ring forms in preparation for cytokinesis. **(C, D)** Upon anaphase onset, the contractile ring constricts circumferentially, while duplicated chromosomes are pulled apart. **(E)** When the contractile ring has ingressed to its fullest point, a microtubule-containing structure forms at the intercellular bridge (the midzone), which is characterized by a distinct array of proteins; the stembody is another specialized structure, found within the midzone. The midzone is necessary for abscission. **(F)** Abscission separates the plasma membrane of the two daughter cells and the nuclear envelope re-forms around the chromatin of the daughter cells.

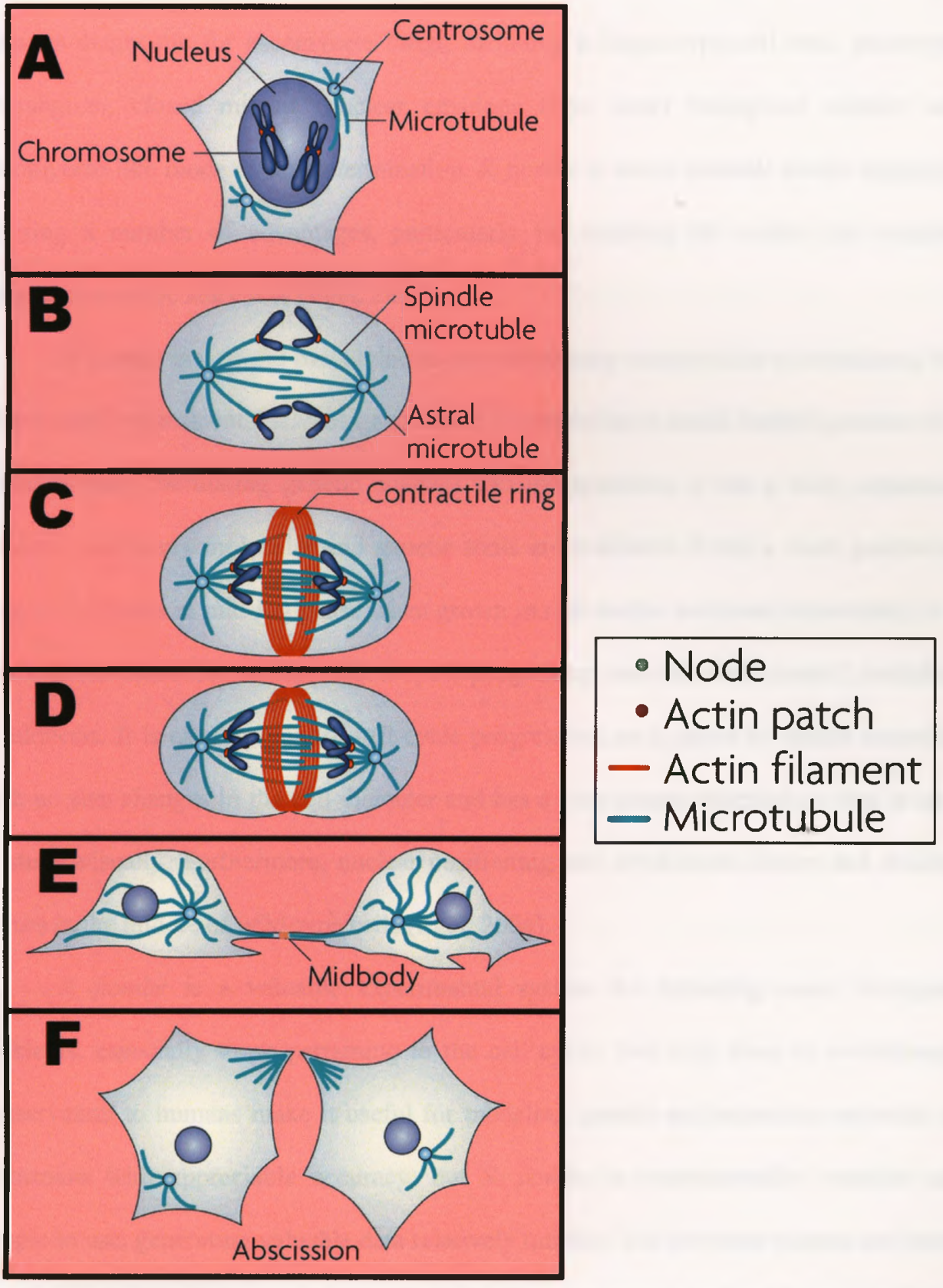
A
Nucleus
Centrosome
Microtubule
Chromosome
B
Spindle microtuble
Astral microtuble
C
Contractile ring
D
E
Midbody
F
Abscission
Node
Actin patch
Actin filament
Microtubule

S. pombe is an ascomycete, unicellular fungus, possessing a constellation of features diagnostic for ascomycete fungi, including a fungal-type cell wall, ascus-type sporangium, closed mitosis (nuclear envelope stays intact throughout mitosis) and ascomycete-like mode of sex-determination. *S. pombe* is also a valuable model organism, offering a number of advantages, particularly for studying the events that regulate progression of the cell cycle (Egel, 2004).

S. pombe is a useful model due to its evolutionary conservation to metazoans, but offers many experimental advantages as well. *S. pombe* has a small, haploid genome of 3 chromosomes, facilitating genetic analysis and manipulation. It has a fully sequenced genome, and many molecular and genetic tools are available. It has a short generation time of 2.5 hours in mid-log phase when grown in rich media, and most importantly, it is an excellent model for studies of cell cycle progression and cell cycle control, including cytokinesis. It is easy to monitor cell cycle progression, as it grows by length extension with no size changes in the cell diameter and has a very simple morphology that is easy to study visually. Furthermore, nuclear positioning and cytokinesis always and reliably occurs in the middle of wild-type cells (Egel, 2004).

S. pombe is a valuable experimental system for exploring many biological problems, especially those pertaining to the cell cycle. Not only does its evolutionary conservation to humans make it useful for modeling genetic and molecular networks in metazoans with appreciable accuracy, but *S. pombe* is experimentally versatile and simple to use, generating valuable data relatively quickly. It is for these reasons and more that it was used in the pioneering studies of cell cycle control by Paul Nurse. As it has been used extensively to study the cell cycle, networks that control cell cycle progression

and control have been extensively mapped out, facilitating further study with this organism in cell cycle control (Egel, 2004).

1.3 Cytokinesis in *S. pombe*

S. pombe, similarly to humans, undergoes cytokinesis using an actomyosin contractile ring, further supporting its value in cytokinesis research. The actomyosin contractile ring appeared 1 billion years ago in the common ancestor of fungi, amoebas and animals, and they share most of the genes used for cytokinesis by *S. pombe*. Also, like animal cells, positioning of the mitotic apparatus (inside the nucleus of fungi) determines ring positioning in *S. pombe* (Pollard and Wu, 2010).

The cascade of events that results in successful cytokinesis starts in interphase; Wee1p is a kinase that holds a cell in G2 by phosphorylating the master cell cycle kinase Cdc2p. Cdr2p is a kinase necessary for G2 exit by promoting formation of the interphase nodes; along with Cdr1p, Cdr2p phosphorylates and inactivates Wee1p; it also interacts with Mid1p. These nodes appear at the cell equator, overlying the interphase nucleus, which represent assemblies of proteins and are restricted to the equator by the Pom1p kinase and another unknown inhibitor (Almonacid *et al.* 2009) (Martin and Berthelot-Grosjean, 2009) (Moseley *et al.* 2009).

Ring assembly in *S. pombe* to the equator displays both positive and negative regulation. There is negative regulation that prevents assembly near the cell tips, thereby causing assembly to occur at the equator by default; this is conferred by Pom1p. Pom1p concentrates at the cell ends, restricting formation of nodes containing Cdr2p and Mid1p to the middle of the cell. Cell growth by tip extension causes the inhibitory activities to

Figure 1.2 Generalized schematic of the sequence of events that occur during cytokinesis in *S. pombe*. Image modified from Pollard and Wu 2010. See text for a detailed description.**(A)** Assemblies of proteins (interphase nodes) form, which overlie the equator; these assemblies form in preparation for cytokinesis. **(B)** Among other proteins, myosin II is recruited to these nodes as they continue to mature and become competent for contractile ring assembly. **(C)**As spindle pole bodies (yeast functional equivalent of centrosomes) begin to separate, actin in the cell is recruited to the nodes, and the search-capture-pull mechanism of ring formation generates a compact acto-myosin contractile ring. **(D)** Anaphase results in the pulling of the duplicated chromosomes into two independent daughter nuclei; upon being formed, the ring begins to constrict circumferentially. **(E)** The ring constricts to its fullest extent, after which abscission (separation of the plasma membrane of the two daughter cells) occurs, thereby completing cell division. **(F)** Abscission is followed by dissolution of the cell wall material connecting the two daughter cells, causing them to separate.

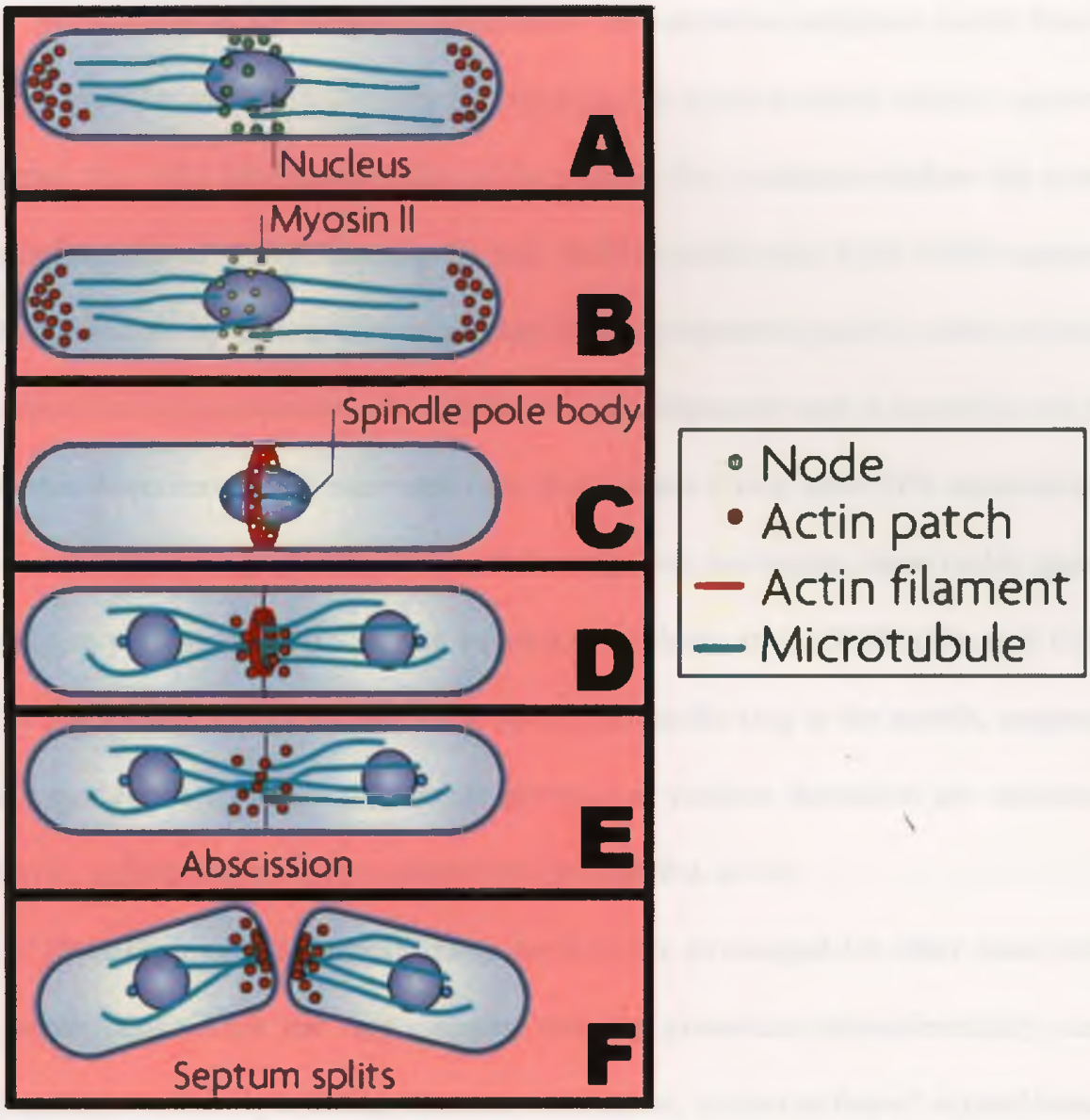
Nucleus
A
Myosin II
B
Spindle pole body
C
D
Abscission
E
Septum splits
F
Node
Actin patch
Actin filament
Microtubule

decline at the cell equator, allowing Cdr1p andCdr2p to phosphorylate and inhibit Wee1p.This releases the kinase Cdc2p to trigger the transition into mitosis, thus coupling growth to the cell cycle (Martin and Berthelot-Grosjean, 2009) (Moseley *et al.* 2009).

In addition to the 'negative regulation' that excludes interphase nodes from cell tips, the polo kinase Plo1p releases Mid1p from the nucleus before mitosis, apparently preparing the ~ 65 interphase nodes at the equator for cytokinesis before the onset of mitosis(Bähler*et al.* 1998). Starting 10 min. before spindle pole body (SPB) separation, the nodes mature by adding several proteins from cytoplasmic pools in order to become competent for actin assembly, after which the actin filaments start to assemble and grow at random directions, being nucleated from these nodes 2 min. after SPB separation; it is also noted that over a period of 10 min. following actin nucleation, these nodes appear in a nearly continuous ring around the equator (Vavylonis *et al.* 2008) (Wu and Pollard, 2005). The current model for assembly of the contractile ring is the search, capture and release model whereby actin filaments growing at random directions are captured by myosin II, pulling these nodes together (Pollard and Wu, 2010).

Once the ring has formed, many proteins are exchanged for other ones prior to ring constriction. After the ring matures, the ring constricts circumferentially, and is proposed to constrict by a sliding filament mechanism, similar to that of striated muscles; depolymerization of the ring occurs concomitantly with constriction (Pollard and Wu, 2010).

S. pombe faces an added challenge of having to couple deposition of a septum of cell wall material along with constriction of the contractile ring. The septation initiation network (SIN) is the pathway that accomplishes this goal and is also necessary for ring

constriction and disassembly but it is not fully understood how these processes are carried out by the SIN (Krapp and Simanis, 2008).

It is interesting to note that in *S. pombe*, contractile rings are able to form in a SIN-dependent pathway, without Mid1p; however, these rings do not reliably separate the two daughter nuclei during cytokinesis because they are often not perpendicular to the long axis of the cell, nor do they reliably form at the equator; this backup system nonetheless shows that cytokinesis is robust not only in metazoans, but *S. pombe* as well (Hachet and Simanis, 2008) (Schmidt *et al.* 1997). The ideas discussed in Chapter 1.3 are summarized in Fig. 1.2.

1.4 Comparisons and contrasts between cytokinesis in *S. pombe* and cytokinesis in metazoans

In order to make reliable models using *S. pombe* that can be used to generate meaningful predictions in metazoans, it is necessary to weigh both the similarities and differences between *S. pombe* and metazoan cytokinesis, as each has unique species-specific features. Both *S. pombe* and metazoans use an actomyosin ring, and the basic components of the ring are very similar in both systems, which makes *S. pombe* an excellent model. However, the assembly order of the ring components is quite different, which likely reflects the need for the actomyosin ring to coordinate with some species-specific features (Balasubramanian *et al.* 2004).

Certain obvious structural differences between metazoan and *S. pombe* cells must not be ignored, as they need to be coordinated with cell division, and therefore impinge on cytokinesis. Fission yeast grows by length extension alone, whereas animal cells

generally increase in volume without changing cell shape, meaning that animal cells face greater challenges on membrane re-organization and deposition during cytokinesis. Also, since *S. pombe* has a cell wall and animal cells do not, *S. pombe* cells must secrete a septum of cell wall material at the division site in addition to membrane material, and actomysosin ring constriction must be coupled to this. Also, the nuclear envelope stays intact during mitosis in yeast whereas it breaks down at least partially in animal cells which means there are differences in how the mitotic spindle is nucleated and how it interacts with other structural components of the cell during mitosis and cytokinesis (Balasubramanian *et al.* 2004).

Differences and similarities at the molecular level are less obvious but are nonetheless important. Animal cells determine the division site in anaphase, and it reflects the position of the spindle whereas fission yeast determines the site in G2, reflecting the position of interphase nucleus. Both animal and yeast systems are similar in that cytokinesis is tightly coordinated with the nuclear cycle. In both systems, ring constriction is dependent on the proteolysis of cyclin B, and ring constriction and its associated events can only be initiated after chromosome segregation. However, the timing of ring assembly differs; in *S. pombe*, ring assembly is dependent on mitotic entry and in animal cells, ring assembly generally does not commence until anaphase onset (Balasubramanian *et al.* 2004).

Intriguingly, a thorough comparative analysis of *S. pombe* and metazoan cytokinesis reveals that many features of cytokinesis that appear to be divergent and unrelated have conserved elements that are incorporated differently into the cytokinetic machinery. Mid1p is the critical regulator of division plane placement in fission yeast,

and is related to anillin, an early marker of the divison plane in animal cells, even though anillin isn't critical for division plane positioning in animal cells. This molecular conservation is also evident in elements of septum deposition, even though animal cells have no cell wall; there are elements of the fission yeast SIN which are conserved in animal cells, and preliminary studies indicate that these animal counterparts are also needed for cytokinesis. This brief comparative discussion makes it clear that although *S. pombe* cytokinesis differs in certain respects from metazoan cytokinesis, the similarities are strong and often not intuitively obvious, so *S. pombe*cannot be dismissed from its role as an excellent model for modeling metazoan cytokinesis (Balasubramanian *et al.* 2004).

1.5 Cytokinesis failure and cancer

As previously discussed, cytokinesis is a robust system with multiple pathways operating in parallel to carry out individual tasks. This indicates that strong selective pressures exist to ensure that cytokinesis occurs with high fidelity, so it is unsurprising that the consequences of cytokinesis failure to organismal fitness are severe. Cytokinesis failure and its consequences have been studied by many researchers, producing a large body of research that indicates a possible link between cytokinesis failure and cancer. Cytokinesis failure as one possible origin of cancerous cells was first proposed by the biologist Theodor Boveri, in his 1914 hypothesis concerning the origin of malignant tumours, the central tenets of which are presently discussed.

Boveri proposed that a multipolar mitosis in a 'tetraploid intermediate' cell is a critical first step in cancerous transformation. This tetraploid intermediate forms through either abnormal fusion of two diploid cells, or the failure of a diploid cell to execute

cytokinesis, resulting in re-entry into interphase with a doubled chromosome and centrosome content. The extra pair of centrosomes in a tetraploid intermediate produces genomic instability; if a pair of centrosomes does not cluster correctly at either end of the cell during mitosis, a multipolar mitosis is the result, with spindle microtubules being nucleated from 3-4 poles, leading to unequal partitioning of the genome into the daughter cells. Most of the progeny from such mitoses die, but if the chromosomal makeup is adequate to keep a daughter cell alive, there is a potential for carcinogenesis. Elaborating on this line of thought, Boveri explains that uncontrolled proliferation is a primitive quality of cells, and that multicellularity requires restriction of cellular proliferation to specific contexts. Loss of chromosomes can cause loss of these restrictive mechanisms; intriguingly, this idea foretells the concept of tumour suppressor genes (Boveri, 1929) (Fig. 1.3).

Boveri's ideas have received strong experimental support in a paper showing that cytokinetic failure in p53-null mouse mammary epithelial cells generates tetraploid cells, which not only produce malignant tumours when transplanted into nude mice (unlike diploid controls), but also produce increased levels of whole-chromosome mis-segregation and chromosomal rearrangements relative to diploid controls (Fujiwara *et al.* 2005).The same research group forged another study that revealed the mechanistic details of tumorigenesis via cytokinetic failure, which surprisingly showed that multipolar mitoses are not responsible for the majority of tumors that form via cytokinesis failure. Instead, extra centrosomes alone are sufficient to produce chromosome missegregation during bipolar cell division. This is because a transient 'multipolar spindle intermediate' forms prior to centrosome clustering, the geometry of which is prone to merotelic

kinetochore-microtubule attachment errors. Merotely is an error where single kinetochores attach to microtubules emanating from different poles, predisposing a cell for lagging chromosomes and segregation errors during anaphase; although these errors are often corrected prior to anaphase, merotely is poorly sensed by the spindle assembly checkpoint, causing a net increase in the frequency of lagging chromosomes and chromosome missegregation errors (Ganem *et al.* 2009). Data that corroborates these findings has also been generated in budding yeast, as tetraploidy compromises genetic stability, produces scaling defects that can contribute to genomic instability, and increases syntelic kinetochore-microtubule attachments that cause chromosome missegregation (syntelic attachment is when both sister chromosomes attach to a single spindle pole) (Fig. 1.4) (Ganem *et al.* 2007)

These findings all establish a link between cytokinesis failure and cancer and this link is further supported by various other studies, and it is unsurprising that some tumour suppressor genes (i.e. BRCA2 or LATS1) are required for the normal completion of cytokinesis. Furthermore, current research indicates that ploidy-sensing surveillance mechanisms which could rectify cytokinesis failure are unlikely to exist (Ganem *et al.* 2007). This makes cytokinesis failure a dangerous anomaly. Therefore, the mechanisms that prevent cytokinesis failure have an essential place in cancer research, as the genomic instability of progeny produced by cytokinesis failure predisposes them to aneuploidy. Aneuploidy is a characteristic feature of cancerous cells; it is an abnormal constitution of chromosomes that does not represent a multiple of the normal haploid karyotype. It is important to note that aneuploidy is neither a cause, nor a consequence of cancer; rather, aneuploidy is associated with chromosomal instability, and chromosomal instability

Figure 1.3 Progression from cytokinesis failure to aneuploidy (classical model). Cytokinesis failure generates tetraploid intermediates containing double the normal number of centrosomes. Upon progression into mitosis, chaotic multipolar chromosome segregation and aneuploidy are the result. In this model, the inherent genomic instability of aneuploid cells leads to tumourigenesis. Green lines represent microtubules, blue shapes represent DNA (chromosome assemblies or nuclei, as appropriate), and purple spheres represent centrosomes. Image modified from Storchova and Pellman 2004.

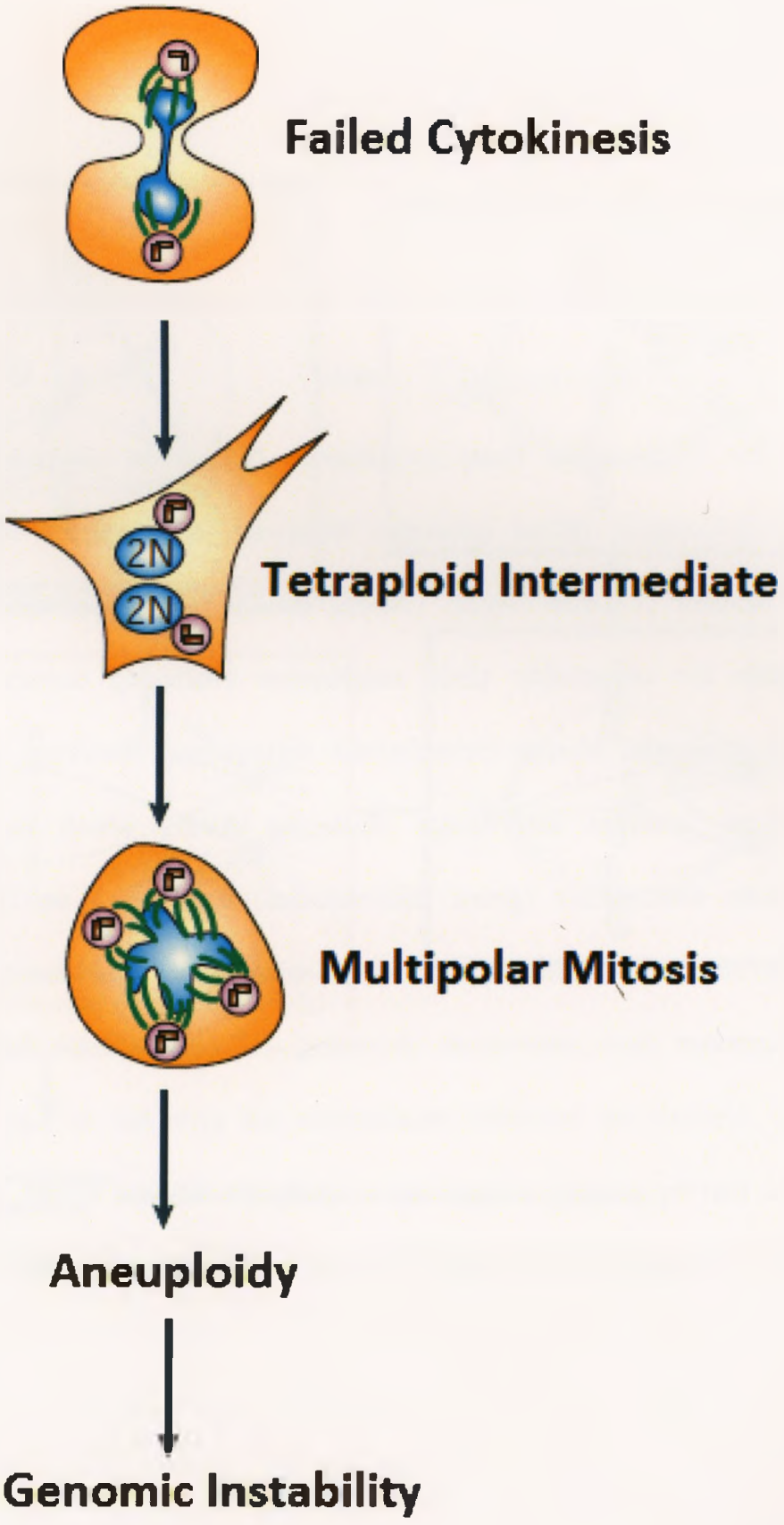
Failed Cytokinesis
2N
2N
Tetraploid Intermediate
Multipolar Mitosis
Aneuploidy
Genomic Instability

Figure 1.4 Progression from cytokinesis failure to aneuploidy (contemporary model). Cytokinesis failure generates tetraploid intermediates containing double the normal number of centrosomes. Chaotic multipolar chromosome segregation is not responsible for aneuploidy since centrosome clustering occurs prior to anaphase, resulting in normal bipolar chromosome segregation. However, a multipolar spindle intermediate precedes centrosome clustering during which merotelic kinetochore-microtubule attachments (green microtubules) form as a result of altered spindle geometry. In addition, syntelic kinetochore-microtubule attachments (blue microtubules) also accumulate upon centrosome clustering and may promote further enhancement of merotely. Unresolved merotelic attachments can give rise to lagging chromosomes at anaphase, thereby causing aneuploidy. As with the classical model, the inherent genomic instability of aneuploid cells leads to tumourigenesis. Image modified from Ganem *et al.* 2009.

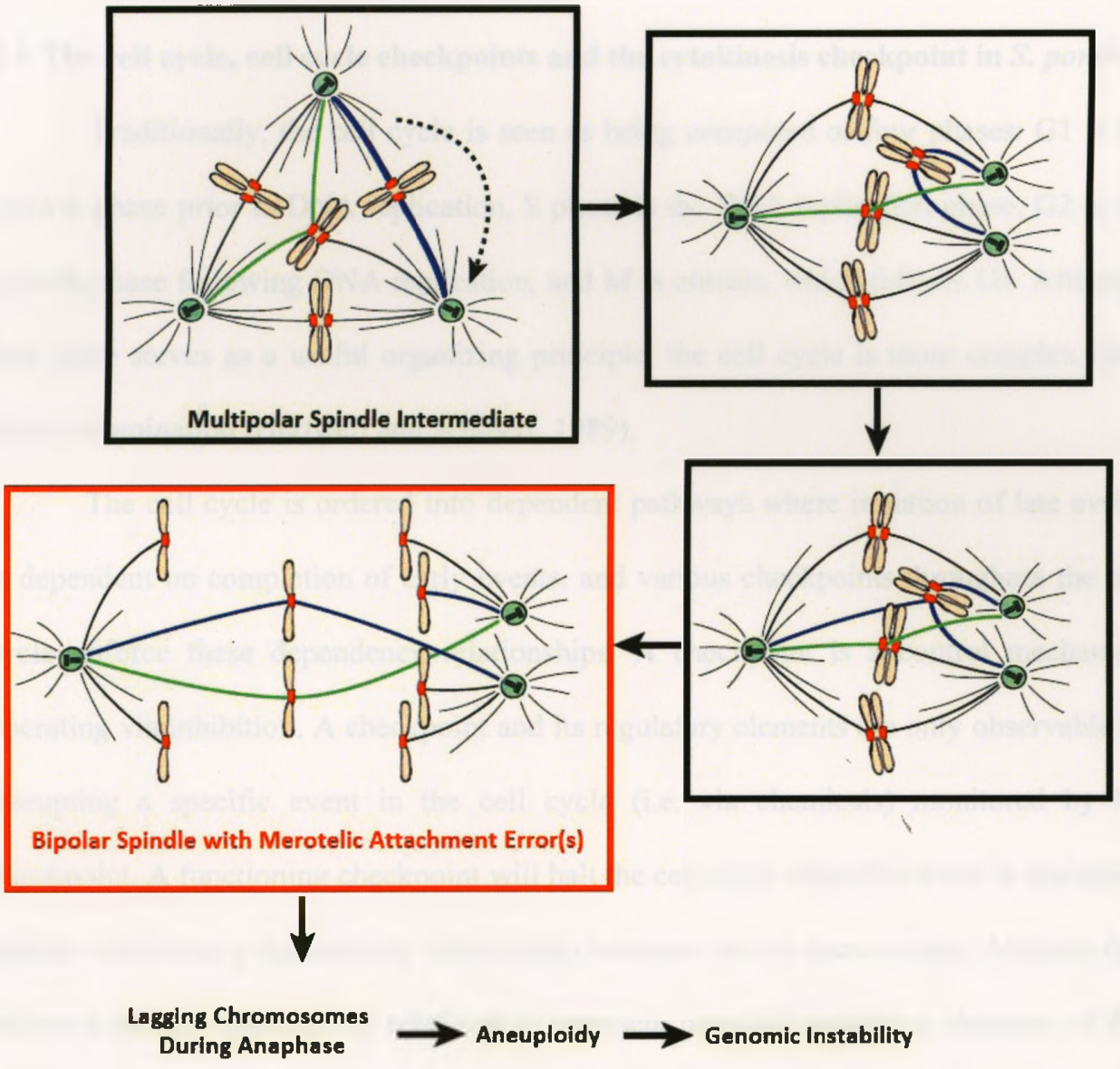
Multipolar Spindle Intermediate
Bipolar Spindle with Merotelic Attachment Error(s)
Lagging Chromosomes During Anaphase
Aneuploidy
Genomic Instability

creates the potential for genetic changes that can cause cancers to form and evolve into more dangerous forms.

1.6 The cell cycle, cell cycle checkpoints and the cytokinesis checkpoint in *S. pombe*

Traditionally, the cell cycle is seen as being composed of four phases: G1 is the growth phase prior to DNA replication, S phase is the DNA replication phase, G2 is the growth phase following DNA replication, and M is mitosis, which follows G2. Although this cycle serves as a useful organizing principle, the cell cycle is more complex upon closer examination (Hartwell and Weinert, 1989).

The cell cycle is ordered into dependent pathways where initiation of late events is dependent on completion of early events, and various checkpoints throughout the cell cycle enforce these dependency relationships. A checkpoint is a control mechanism operating via inhibition. A checkpoint and its regulatory elements are only observable by disrupting a specific event in the cell cycle (i.e. via chemicals) monitored by the checkpoint. A functioning checkpoint will halt the cell cycle when this event is disrupted, thereby enforcing a dependency relationship between two or more events. Mutants that relieve a specific dependency relationship represent potential regulatory elements of that checkpoint. Checkpoints are important, as elimination of checkpoints may result in cell death, infidelity in the distribution of chromosomes or other organelles, or increased susceptibility to environmental perturbations such as DNA damaging agents; Leland Hartwell and Paul Nurse are credited with the pioneering work that initially identified and characterized many checkpoints in both budding yeast and fission yeast (Hartwell and Weinert, 1989). However, there is another checkpoint of relevance to cytokinesis that

Figure 1.5 Treatment with low doses of Latrunculin A can be used as a tool to screen for mutants defective in the cytokinesis checkpoint response. Upon challenge with Latrunculin A, the majority of wild-type cells are able to successfully complete cytokinesis due to a Clp1p phosphatase mediated cell-cycle delay, and SIN hyperactivation (Mishra *et al.* 2005; Mishra *et al.* 2004). Mutants lacking Clp1p or components of the SIN are unable to maintain a functional contractile ring leading to cytokinesis failure (Karagiannis *et al.* 2005; Mishra *et al.* 2005, Mishra *et al.* 2004). Nuclear divisions continue in the absence of cell division resulting in lethality. The nuclei are depicted as black circles, actin patches and rings are shown in red. The blue dot represents the Cdc7 protein (spindle pole body localized Cdc7p is a cytological marker of active SIN signaling). Figure modified from Karagiannis *et al.* 2005.

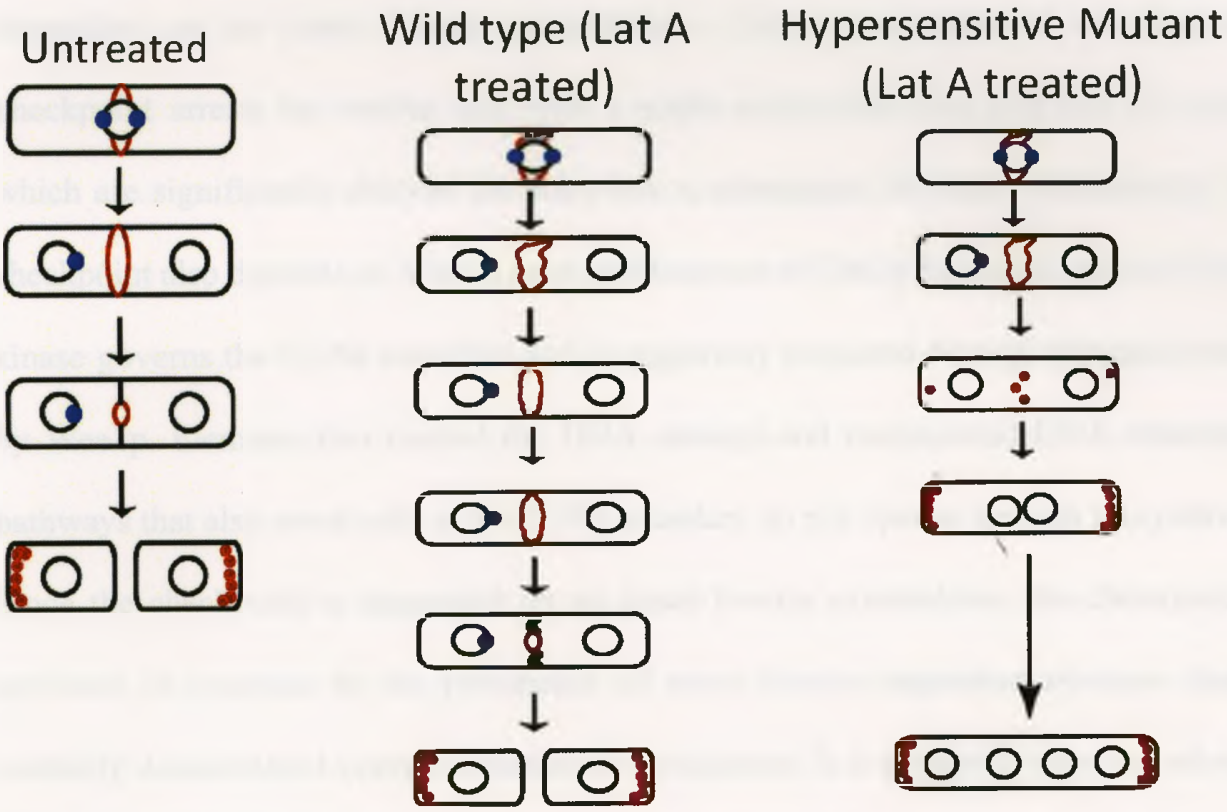
Untreated
Wild type (Lat A treated)
Hypersensitive Mutant (Lat A treated)

was not characterized in their early work, and this checkpoint monitors the G2/M transition in eukaryotic cells.

At the end of anaphase and following disassembly of the mitotic spindle, the actomyosin ring constricts. A study by Liu *et al.* revealed a G2/M boundary checkpoint in a temperature-sensitive mutant screen of *S. pombe* for new cytokinetic regulators. This 'cytokinesis-monitoring surveillance system' blocks the G2/M transition of each of the two daughter nuclei in a mother cell until cytokinesis is completed in the mother and is dependent on an intact F-actin cytoskeleton. Upon perturbation of the ring, this checkpoint arrests the mother cell with a stable actomyosin ring and two G2 nuclei, which are significantly delayed for entry into a subsequent M phase. Additionally, this checkpoint also depends on Wee1p mediated function of Cdc2p for mitotic arrest; Cdc2p-kinase governs the G2/M transition and is negatively regulated through phosphorylation by Wee1p. Elements that control the DNA damage and unreplicated DNA checkpoint pathways that also arrest cells at the G2/M boundary do not operate through this pathway. Since the checkpoint is dependent on an intact F-actin cytoskeleton, the checkpoint is activated in response to the persistence of some F-actin dependent structure that is normally disassembled upon completion of cytokinesis. It is presently unknown whether the actomyosin ring itself or some other structure depending on F-actin for its integrity is the source of the signal for the G2/M transition block. (Fig. 1.5) (Liu *et al.* 2000)

1.7 A genome-wide screen identifies four new regulators of the cytokinesis checkpoint in *S. pombe* with human orthologues

Discovery of the cytokinesis checkpoint prompted work to uncover new

regulators of this checkpoint. Since the checkpoint is active until ring constriction is complete, new regulators can be discovered in a mutant library by destabilizing the ring and looking for mutants that are unable to activate a G2/M arrest. A useful strategy is to disrupt the ring using a low dose of the drug Latrunculin A (LatA), a naturally occurring toxin produced by certain sponges. LatA disrupts the F-actin cytoskeleton by binding and impairing a region on the three-dimensional structure of the actin monomer, thereby sequestering the monomers in an assembly-incompetent complex. (Ayscough *et al.* 1997) At high doses, LatA will cause complete collapse of the F-actin cytoskeleton, however, at much lower doses, LatA will de-stabilize the ring, thereby preventing constriction. Under these conditions, cells with a functional checkpoint will halt the cell cycle while simultaneously stabilizing the ring by an as-of-yet unknown mechanism. Checkpoint-defective mutants however, will undergo cytokinetic failure due to disintegration of the ring before constriction is complete, along with repeated rounds of nuclear divisions, leading to inviable, multinucleate cells (Fig. 1.5).

Daniel McCollum of the University of Massachusetts Medical School had done a genome-wide LatA screen on the entire set of viable *S. pombe* gene deletion mutants, which is obtainable from the commercial supplier Bioneer (Mishra, McCollum, and Balasubramanian, unpublished). Strains inviable on media with a low dose of LatA represent putative new regulators of the checkpoint. This screen, in conjunction with follow up research by M.Sc. student Stefan Rentas, identified four ORFs of relevance to my M.Sc. project: SPAC22E12.11c (hereafter referred to as *lst1*), SPAC22E12.19 (hereafter referred to as *lst2*), SPCC1235.09 (hereafter referred to as *lst3*), and SPAC3G9.07c (hereafter referred to as *hos2*). My project aims to complete the

characterization of the Lst complex. Stefan's preliminary work on *lst1*, *lst2*, and *lst3* led to several conclusions. The fission yeast Lst1p, Lst2p, Lst3p and Hos2p proteins share sequence similarity to human MLL5, NCOR2, TBL1X and HDAC3 proteins, respectively. Lst1p, Lst2p and Lst3p form a nuclear-localized multi-protein complex that works in parallel to other regulators of the cytokinesis checkpoint, and each of the three Lst proteins is necessary for checkpoint function. Furthermore, the complex responds to LatA-induced checkpoint activation by increasing Lst1p, Lst2p and Lst3p expression levels 2-3 fold, and also responds by mounting a diagnostic transcriptional response for the fission yeast core environmental stress response (CESR) (Rentas, 2010).

Characterization of this complex extends beyond the realm of basic research into cancer research, since there is cross-species functional conservation of the complex and its role in faithful cytokinesis. HDAC3 and MLL5 are both candidate tumour-suppressor genes, often deleted in cancer cells. More convincingly however, RNAi-mediated knockdown of MLL5, TBL1X, and NCOR2 in HeLa cells increases rates of cytokinetic failure. Furthermore, these three proteins were shown to interact in nuclear extracts of HeLa cells and are proposed to form part of a larger chromatin-modifying histone de-acetylase complex that contains the histone de-acetylase, HDAC3. An orthologous complex (SET3C) has also been identified and characterized in budding yeast, which contains the budding yeast histone de-acetylase, Hos2 (orthologous to the fission yeast Hos2p histone de-acetylase and the mammalian HDAC3 histone de-acetylase). The budding yeast SET3C represses meiosis and cytokinesis specific genes, and is necessary for the proper transcriptional response to secretory stress. Taken together, these findings support the existence of an evolutionarily conserved chromatin-remodeling complex with

a role in promoting the faithful completion of cytokinesis. This complex is represented by the Lst complex in fission yeast, which is composed of *lst1, lst2, lst3*, and likely also contains the fission yeast histone de-acetylase *hos2*, although *hos2* has not been characterized in *S. pombe* in the context of the Lst complex and cytokinesis checkpoint functionuntil now(Cohen *et al.* 2008; Kittler *et al.* 2007; Pijnappel *et al.* 2001).

In light of the information just presented, I propose the following hypothesis:

The fission yeast *hos2* gene product interacts with and forms part of the Lst complex, which has an evolutionarily conserved role in promoting the faithful execution of cytokinesis.

The goal of this project is to test this hypothesis in order to develop a more detailed understanding of the Lst complex. In order to accomplish this, I have carried out the following experiments:

1. A phenotypic characterization of a *hos2Δ* gene deletion mutant will determine whether it displays the characteristic phenotype for cytokinesis failure under a low dose of LatA
2. A site-directed mutagenesis will be used to abolish the de-acetylase activity of *hos2* in wildtype *S. pombe*. Subsequently, a phenotypic characterization of this mutant will determine whether it displays the characteristic phenotype for cytokinesis failure under a low dose of LatA. This characterization will establish

whether checkpoint activation depends on the de-acetylase activity of Hos2p.

3. The subcellular localization of Hos2p will be determined by tagging the C-terminus of *hos2* with an in-frame GFP fluorophore tag, followed by fluorescence microscopy. A nuclear and cytoplasmic distribution is expected for Hos2p, since HDAC3 shows this particular distribution, owing to the presence of nuclear import and export tags in the HDAC3 sequence; if this distribution is observed for Hos2p, a time-course live-cell imaging experiment on the *hos2-GFP* strain under a low dose of LatA will determine whether the distribution pattern of Hos2p is checkpoint-responsive (Yang *et al.* 2002).
4. Co-immunoprecipitation experiments will be used to determine whether Hos2p forms a part of the Lst complex *in vivo*. To accomplish this, the C-terminus of *hos2* will be tagged with an in-frame Myc epitope tag, as well as an in-frame HA tag; these two strains will be used to generate six reciprocally double-tagged strains:

   *lst1/lst2/lst3*HA- *hos2*Myc

   *lst1/lst2/lst3*Myc- *hos2*HA

   Each of the six possible pairwise protein-protein interactions will be tested. Briefly, one tagged protein will be immunoprecipitated from a whole-cell protein extract, using a tag-specific antibody. Then, the putative Lst complex will be dissociated and denatured, followed by SDS-PAGE, followed by analysis via Western Blotting using an antibody specific for the tag on the other protein of interest.
5. Hos2p will be overexpressed at various dosages in wildtype cells, using the pREP

series of exosomal expression vectors in order to identify if there are phenotypes that result from Hos2p overexpression, and whether or not these phenotypes are dosage-dependent.

6. Since Lst1p, Lst2p and Lst3p expression levels increase in response to LatA exposure in conjunction with the CESR transcriptional response, it is likely that LatA is recognized as an environmental stressor. To test this idea and extend it, an analogous series of experiments will be carried out using various environmental stresses. A strain carrying an in-frame C-terminal HA epitope tag on *lst1* will be exposed to an environmental stressor for three hours; whole-cell protein extract made from the strain at 10 min., 1 hr. and 3 hr. following the treatment will be analyzed via Western blotting in parallel to a control treatment in order to quantify Lst1p expression and determine whether Lst1p is upregulated in response to environmental stress.

CHAPTER 2: MATERIALS AND METHODS

2.1 Strains, growth media, and culture conditions

All molecular cloning was performed using *Escherichia coli* strain XL1-Blue (*recA1 endA1 gyrA96 thi-1 hsdR17 supE44 relA1 lac* F' *proAB lacI*qZΔ*M15* Tn*10*). Cultures were grown in Luria-Bertani (LB) broth at 37°C with constant shaking at 200 rpm. XL1-Blue cells were rendered electrocompetent by culturing in 500 mL of LB broth to exponential phase (OD_{600}= 0.4) at 37° C with constant shaking at 200 rpm, washing three times with sterile, ice cold water, and resuspending in 1.5 mL of ice-cold 15% glycerol. Fifty microliter aliquots were stored in microfuge tubes at -80° C.

Schizosaccharomyces pombe strains used in the study (Table 2.1) were grown in yeast extract (YES) medium at 30° C with constant shaking at 200 rpm (Alfa 1993). In cases where selection was required, *S. pombe* cells were grown in Edinburgh minimal medium (EMM) containing the appropriate supplements (adenine, uracil, leucine or histidine at a concentration of 7.5 g/L) (Alfa 1993).

2.2 Molecular Techniques

Polymerase chain reactions amplifications were performed using High-Fidelity PCR Enzyme Mix (Fermentas Life Sciences) according to the supplier's recommendations. Primers used in this study (Table 2.2) were designed with the aid of the open source software program, Primer3 (http://www.bioinformatics.nl/cgi-bin/primer3plus/primer3plus.cgi) and purchased from Integrated DNA Technologies. Purified wildtype *S. pombe* genomic DNA (Alfa 1993) was used as the template in PCR

Table 2.1 *S. pombe* and *E. coli* strains used in this study.

Strain	Relevant Genotype	Source
CG1	*E.coli XL1-Blue pJK210 hos2-GFP*	This study
CG2	*E.coli XL1-Blue pREP1 hos2*	This study
CG3	*E.coli XL1-Blue pREP41 hos2*	This study
CG4	*E.coli XL1-Blue pREP81 hos2*	This study
CG5	*E.coli XL1-Blue pJK210 hos2-myc*	This study
CG6	*E.coli XL1-Blue pJK210 hos2-HA*	This study
CG10	*E.coli XL1-Blue pJK210 hos2Y321H-HA*	This study
SCG1	*ura4-D18 leu1-32 ade6-210 his7-366 h⁻ (pREP1-hos2)*	This study
SCG2	*ura4-D18 leu1-32 ade6-210 his7-366 h⁻(pREP41-hos2)*	This study
SCG3	*ura4-D18 leu1-32 ade6-210 his7-366 h⁻ (pREP81-hos2)*	This study
JK561	*hos2-GFP::ura4⁺ ura4-D18 leu1-32 ade6-210 his7-366 h⁻*	This study
SCG5	*hos2-myc::ura4⁺ ura4-D18 leu1-32 ade6-210 his7-366 h⁻*	This study
SCG6	*hos2-HA::ura4⁺ ura4-D18 leu1-32 ade6-210 his7-366 h⁻*	This study
SCG9	*lst1-myc::ura4⁺ hos2-HA::ura4⁺ ura4-D18*	This study
SCG10	*lst1-HA::ura4⁺ hos2-myc::ura4⁺ ura4-D18*	This study
SCG11	*lst2-myc::ura4⁺ hos2-HA::ura4⁺ ura4-D18*	This study
SCG12	*lst2-HA::ura4⁺ hos2-myc::ura4⁺ ura4-D18*	This study
SCG13	*lst3-myc::ura4⁺ hos2-HA::ura4⁺ ura4-D18*	This study
SCG14	*lst3-HA::ura4⁺ hos2-myc::ura4⁺ ura4-D18*	This study
SR5	*lst1-HA::ura4⁺ ura4-D18 h⁺*	JK collection
SR6	*lst1-myc::ura4⁺ ura4-D18 h⁺*	JK collection
SR10	*lst3-HA::ura4⁺ ura4-D18 h⁺*	JK collection
SR11	*lst3-myc::ura4⁺ ura4-D18 h⁺*	JK collection
SR15	*lst2-HA::ura4⁺ ura4-D18 h⁺*	JK collection
SR16	*lst2-myc::ura4⁺ ura4-D18 h⁺*	JK collection
SR20	*lst1::KanMX ura4-D18 leu-32 ade6-216 h⁺*	JK collection
JK484	*ura4-D18 leu1-32 ade6-210 his7-366 h⁻*	JK collection
JK468	*hos2::KanMX ura4-D18 leu-32 ade6-216 h⁺*	JK collection
JK 402	*E. coli XL1-Blue*	JK collection
MBY624	*rlc1GFP::ura4⁺ura4-D18*	JKcollection
JK659	*rlc1GFP::ura4⁺ hos2::KanMX ura4-D18*	This study
JK648	*hos2Y321H::ura4⁺ ura4-D18*	This study
JK670	*leu1-32 (pREP1)*	JK collection

Table 2.2 Primers used in this study.

Oligo	Sequence	Description
CPN1	5'-CGTCTGTGAGGGGAGCGTTT-3'	Reverse, verification of upstream junction of Bioneer *hos2* gene deletion
CPN10	5'-GATGTGAGAACTGTATCCTAGCAAG-3'	Reverse, verification of upstream junction of Bioneer *hos2* gene deletion
CPC1	5'-TGATTTTGATGACGAGCGTAAT-3'	Forward, verification of downstream junction of Bioneer *hos2* gene deletion
CPC3	5'-GGCTGGCCTGTTGAACAAGTCTGGA-3'	Forward, verification of downstream junction of Bioneer *hos2* gene deletion
JK105	5'-ATCGGGTTTAGCGACCTTTT-3'	Forward, region upstream of *hos2*
JK106	5'-AGCCCTGCAGTTCGTTTAGA-3'	Reverse, region downstream of *hos2*
oJK136	5'-GGGGGGAATTCTGAACGAATTTTTCGCACCAGAT-3'	Forward, *hos2GFP* and *hos2HA* c-terminal tagging
oJK137	5'-GGGGGCCCGGGGCCTCGAACGCGAACATC-3'	Reverse, *hos2GFP*, *hos2HA* and *hos2Myc* c-terminal tagging, *hos2Y321H* site-mutation (primer 4)
oJK138	5'-GGGGGATTAATATGGATACTCCTGAGACATCCACAC-3'	Forward, *hos2* over-expression from pREP vectors
oJK139	5'-GGGGGGGATCCTCAGCCTCGAACGCGAAC-3'	Reverse, *hos2* over-expression from pREP vectors
OME10	5'-TGGGACAACTCCAGTGAAAA-3'	Reverse, verification of *hos2GFP* construct integration
oJK142	5'-GCGTGTTCAATCTGAGCATC-3'	Forward, verification of *hos2GFP, hos2HA* and *hos2Myc* construct integration
oJK143	5'-GGGGGGGTACCTGAACGAATTTTTCGCACCAGAT-3'	Forward, *hos2Myc* c-terminal tagging
oRS17	5'GAGATTAGCTTTTGTTCACCG3'	Reverse, verification of *hos2Myc* construct integration
oJK153	5'-GGGGGGAATTCTGACGTGGTGAGGCTAGTGGATTC-3'	Forward, *hos2Y321H* site-mutation (primer 1), confirmation of base-pair substitution in *hos2Y321H* integrant

oJK154	5'-GAGGTGGTGGTCATACTCTTAGAAA-3'	Forward, *hos2Y321H* site-mutation (primer 2)
oJK155	5'-TTTCTAAGAGTATGACCACCACCTC-3'	**Reverse, *hos2Y321H* site-mutation (primer 3)**
pUC/M13 reverse	5'-TCACACAGGAAACAGCTATGAC-3'	Reverse, confirmation of base-pair substitution in *hos2Y321H* integrant
oJK158	5'-ATGCTTCTCGGAAGTTAGTG-3'	**Forward, verification of *hos2Y321H* construct integration, amplification of *hos2Y321H* construct for post-integration sequencing**
oJK159	5'-GCCTACATACCTCGCTCTGC-3'	Reverse, verification of hos2Y321H construct integration, amplification of *hos2Y321H* construct for post-integration sequencing
oRS16	5'-CGCATAGTCAGGAACATCGT-3'	**Reverse, verification of *hos2HA* construct integration**

amplifications used to generate amplicons for the purposes of molecular cloning.

Colony PCR was performed to confirm genomic integration of gene deletion cassettes and carboxy-terminal epitope tagging constructs. Briefly, template DNA was obtained by incubating a loopful of the desired yeast colony with 10 µL of 0.05 units/µL Zymolyase in PBS pH 7.4 at 36° C for 15 min (Forsburg and Rhind 2006). Five microliters of the spheroplasted yeast cells were then used as template for the colony PCR. All colony PCR were performed using Taq DNA polymerase (Fermentas Life Sciences) according to the supplier's recommendations.

All restriction enzymes used in molecular cloning experiments were purchased from Fermentas Life Sciences and used according to the supplier's recommendations. Ligation reactions were performed using the Rapid DNA Ligation Kit (Fermentas Life Sciences) according to the manufacturer's instructions. The resulting ligation products were introduced into *E. coli* strain, XL1-Blue, by electrotransformation (Alfa 1993). After electrotransformation cells were spread on LB agar plates containing ampicillin at a concentration of 100 µg/ml and incubated overnight at 36° C. Single, isolated colonies were picked and inoculated in liquid LB medium containing 100 µg/ml ampicillin and incubated overnight at 36° C with constant shaking at 200 rpm. Plasmid DNA was purified using the GeneJET Plasmid Miniprep Kit (Fermentas Life Sciences).

All sequencing was performed using the Robarts Sequencing Facility (http://www.robarts.ca). Plasmid DNA was prepared for sequencing according to Robart's Sequencing Facility guidelines (http://www.robarts.ca/sample-preperation). Sequencing results were analyzed using GENtle software (University of Cologne, Version 1.9.4).

2.3 Genetic techniques

Double mutant strains of the desired genotype were constructed through mating the individual single mutants and subsequently analyzing the meiotic products through tetrad analysis (Alfa 1993).

2.4 Verification of Bioneer gene deletion mutants

Strains bearing gene deletions of *lst1* and *hos2* were purchased from Bioneer Corporation (http://pombe.bioneer.co.kr/). These strains have had the open reading frame of interest replaced with a KanMX selectable marker conferring resistance to the antibiotic G418 (Kim *et al.* 2010). Colony PCR verified the genotype of the *hos2*Δ strain (Figure 2.1);a colony PCR to confirm the genotype of the *lst1*Δ strain was done by Stefan previously.

2.5 Generation of strains expressing carboxy-terminal epitope tagged Hos2p fusion protein

S. pombe strains expressing carboxy-terminal epitope tagged fusion protein were constructed using a PCR-based cloning strategy. Briefly, a carboxy-terminal fragment of the gene of interest was PCR-amplified (see Table 2.2) from wildtype *S. pombe* genomic DNA and cloned in frame to DNA sequences encoding the epitope of interest (GFP, HA, or Myc) in the pJK210 series of integrative vectors (pJK210-GFP, pJK210-HA, or pJK210-Myc). Molecular cloning of the desired fragments was confirmed by restriction digestion and DNA sequencing. Plasmid clones containing the desired fragments were then transformed into *S. pombe* strain JK484 using the lithium acetate method (Forsburg

Figure 2.1 Strategy for Verification of the Bioneer *hos2* deletion mutant. The Bioneer gene deletion mutant has the *hos2* ORF replaced with a KanMX selectable marker conferring resistance to the antibiotic G418 (Kim *et al.* 2010). Primers JK105 and JK106 are specific to the region upstream and downstream of the *hos2* ORF, respectively. Primers CPN1, CPN10, CPC1 and CPC3 are specific to the KanMX module. Four PCR reactions are performed. The red and blue arrows indicate primer pairs used in individual PCR reactions to generate an amplicon (indicated below the schematic in red or blue). Generation of all four amplicons provides evidence for deletion of the *hos2* ORF with the KanMX deletion cassette. Figure 2.1 was adapted from (http://pombe.bioneer.co.kr/technic_infomation/Verification.jsp).

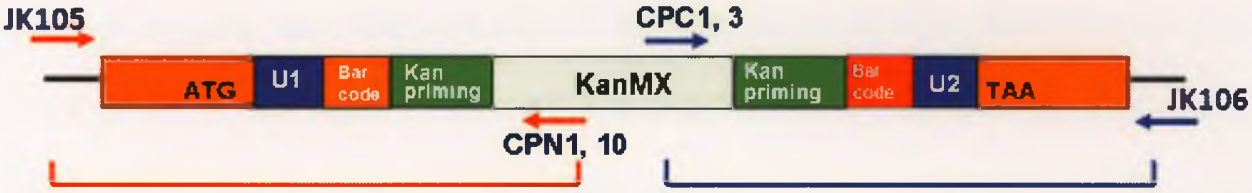
JK105
CPC1, 3
ATG
U1
Bar code
Kan priming
KanMX
Kan priming
Bar code
U2
TAA
JK106
CPN1, 10

Figure 2.2 Schematic describing construction of the *hos2*-GFP integrant strain. The vector containing the cloned *hos2* C-terminal fragment (see Materials and Methods) was transformed into wildtype *S. pombe* strain JK484. Transformation of the circular vector into *S. pombe* was followed by the selection of *ura4*$^+$transformants. Individual *ura4*$^+$colonies were screened by colony PCR to identify strains that integrate the vector into the genome via homologous recombination. To confirm integration at the *hos2* locus, colony PCR was performed with one primer specific to a region upstream of the carboxy-terminal fragment used in cloning and a second primer was specific to the GFP gene. Carboxy-terminal HA and Myc epitope tagging was performed using an analogous strategy.

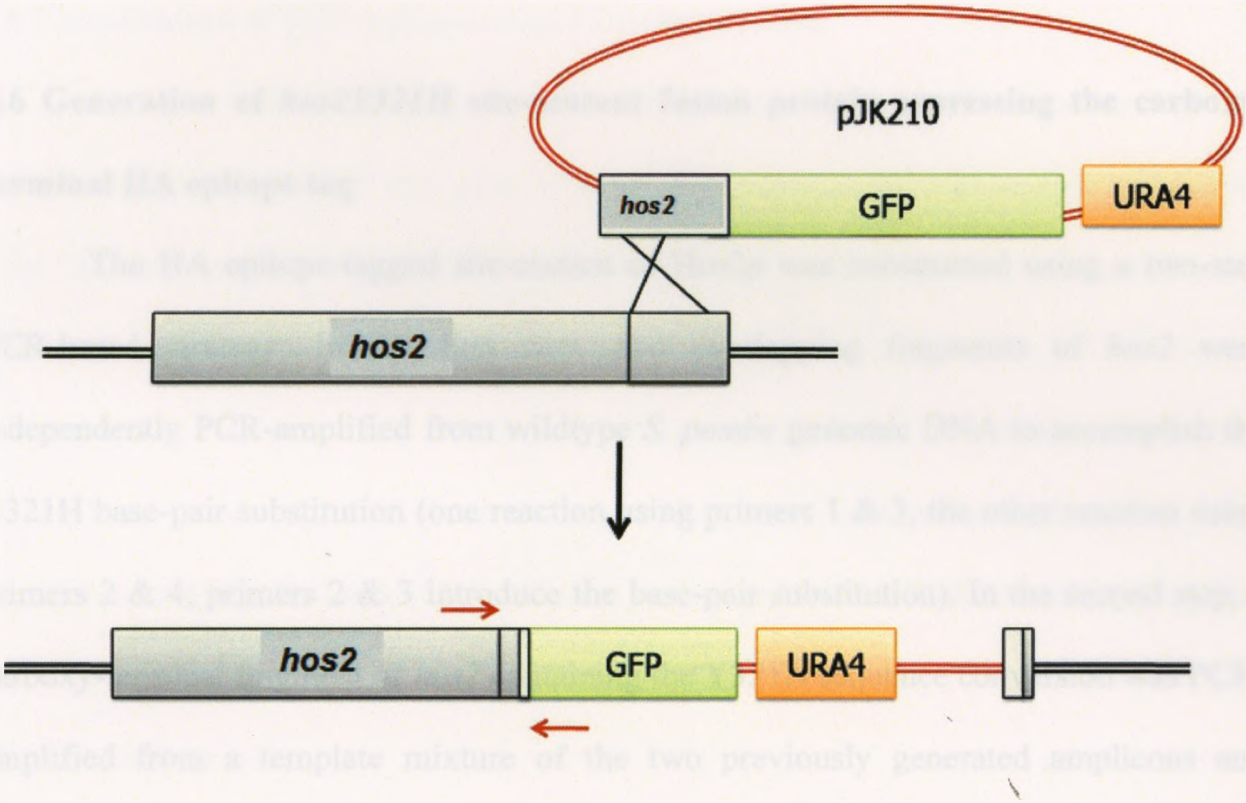
pJK210
hos2
GFP
URA4
hos2
hos2
GFP
URA4

and Rhind 2006). The *ura4*$^+$integrants were selected for by growth on EMM lacking uracil. Cells having integrated the construct at the desired locus by homologous recombination were identified by performing colony PCR on individual *ura4*$^+$transformants (Figure 2.2).

2.6 Generation of *hos2Y321H* site-mutant fusion protein expressing the carboxy-terminal HA epitope tag

The HA epitope-tagged site-mutant of Hos2p was constructed using a two-step PCR-based strategy. In the first step, two overlapping fragments of *hos2* were independently PCR-amplified from wildtype *S. pombe* genomic DNA to accomplish the Y321H base-pair substitution (one reaction using primers 1 & 3, the other reaction using primers 2 & 4; primers 2 & 3 introduce the base-pair substitution). In the second step, a carboxy-terminal fragment of *hos2* containing the Y321H sequence conversion was PCR-amplified from a template mixture of the two previously generated amplicons and primers 1 & 4 and cloned in-frame to the pJK210-HA vector, as described in Section 2.5 (Fig. 2.3). This construct was then used to create the *S. pombe hos2Y321H* integrant (see Section 2.5), followed by post-integration sequencing to ensure that recombination occurred upstream of the substituted residue.

2.7 Latrunculin A treatment

S. pombe cells were grown to early log phase (OD_{600} = 0.15-0.2) in YES, at 30° C with shaking (200 rpm), and treated with a low dose (0.5 μM) of Latrunculin A (LatA) dissolved in DMSO (Karagiannis *et al.* 2005; Mishra *et al.* 2004). LatA-treated cells were

grown at 30° C with shaking at 200 rpm for 5 hrs. LatA was purchased from Enzo Life Sciences International Inc. (Plymouth Meeting, PA). The cells were subsequently fixed, stained and analyzed with fluorescence microscopy (see Section 2.13).

2.8 Visualization of GFP epitope-tagged fusion proteins

S. pombe cells expressing the GFP epitope-tagged protein of interest were grown to mid- log phase (OD_{600} = 0.4) prior to acquiring images and videos.Images and videos were taken using a Leica DMI 6000B microscope with a BD CARV II Confocal Imager fitted with a GFP filter (BD Biosciences, San Jose, CA) and a Quantem: 512SC camera (Photometrics, Tucson, AZ). During the filming of videos, *S. pombe* cells were immobilized in one plane of focus while growing under continuous perfusion of fresh growth media using the Onix™ Microfluidic Perfusion Platform(Cellasic corp.) (Fig. 2.4).

2.9 Protein Extraction

Cells were grown to log phase (OD_{600} = 0.8 or lower), collected by centrifugation and resuspended in STOP buffer (10 mM Tris-HCl pH 8.0, 150 mM NaCl, 50 mM NaF, 10 mM EDTA and 1 mM NaN_3). Cell pellets were snap frozen on dry ice and stored at -80° C prior to cell lysis and protein extraction. Cells were lysed by vortexing the cell pellets with acid-washed glass beads (425-600 μm) in extraction buffer (1% IGEPAL CA630 (tert-Octylphenoxy polyethanol), 150 mM NaCl, 50 mM Tris-HCl pH 8.0, 2 mM EDTA, 1 mM PMSF (phenylmethanesulphonylfluoride), 2 mM Benzamidine, 50 mM NaF, 0.1 mM Na_3VO_4, 50 mM B-glycerophosphate, 15 mM p-nitrophenyl phosphate, ¼ Tablet Sigma Protease Inhibitors), using a Mini-beadbeater 16 Cell Disrupter (Biospec,

Figure 2.3 Schematic describing the *hos2Y321H* basepair conversion in the pJK210 *hos2Y321H*-HA vector construct. Primers 1 and 3 (see Table 2.2) were used to amplify an upstream region of a C-terminal fragment of *hos2.* Primers 2 and 4 (see Table 2.2) were used to amplify an overlapping, downstream region of the same C-terminal fragment of *hos2.* The two overlapping amplicons were subsequently used as template to amplify the entire C-terminal fragment of *hos2* with the *Y321H* basepair substitution (red), which was introduced by primers 2 and 3. This *hos2Y321H* construct was cloned into the pJK210-HA vector, which was subsequently used to create the site-mutant as described in Figure 2.2.

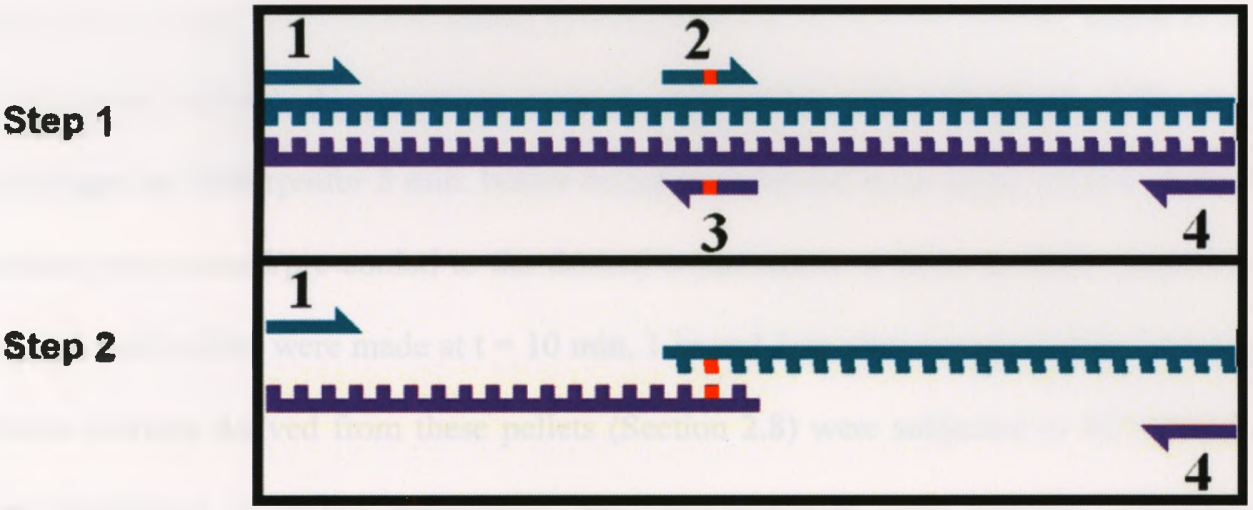
Step 1
1
2
3
4
Step 2
1
4

Bartlesville, OK). Protein quantification was performed using the Bradford Assay (Stoscheck, 1990).

2.10 Analysis of Lst1p protein levels following stress exposure

A strain bearing the HA-epitope tagged Lst1p fusion protein (Table 2.1) was grown to early log phase (OD_{600} = 0.04), then split into two cultures (one experimental, one control).Methyl methanesulfonate, hydroxyurea and H_2O_2 were directly added to the experimental culture. To introduce sorbitol, heat shock and cold shock, cells were centrifuged at 3000 rpmfor 5 min. before being resuspended in an equal volume of fresh medium pre-warmed/pre-cooled to the desired temperature, or fresh medium containing sorbitol. Cell pellets were made at t = 10 min, 1 hr and 3 hr after introducing the stressor. Protein extracts derived from these pellets (Section 2.8) were subjected to SDS-PAGE, then transferred to PVDF membranes and immunoblotted with anti-HA 1°antibody (HA.11; Sigma) at a 1:2000 dilution. As a loading control, anti-tubulin (B14; Sigma) was used at a 1:2000 dilution. Peroxidase conjugated anti-mouse IgG (Sigma), 1:10000, was used as 2°antibody for both HA and tubulin blotted membranes.

2.11 Co-immunoprecipitation experiments

Cell extracts were obtained from the indicated early-log phase (OD_{600}= 0.1-0.15) epitope tagged strains as described in Section 2.8. Immunoprecipitations were performed using Protein G Dynabeads® (Invitrogen) according to the manufacturer's protocol. Briefly, immunoprecipitations (IP) were performed by incubating anti-HA antibodies (HA.11; Sigma) or anti-Myc antibodies (9E10; Sigma) with the Protein G Dynabeads

Figure 2.4 Brief Description of the Onix™ Microfluidic Perfusion Platform. (A) Microfluidic plates of the Onix™ Microfluidic Perfusion Platform. Cells grow with continuous perfusion in the growth medium of interest. Multiple in-flow outlets for each growth chamber allow for rapid media switching. One out-flow outlet for each growth chamber allows for continuous renewal of medium through the in-flow outlets. **(B) Loading of cells into the Onix™ Microfluidic plates.** Cells are driven between a rigid glass floor and elastic ceiling via a pressure gradient, which raises the elastic ceiling to allow cells to enter between the floor and plate uninhibited. Upon release of the pressure gradient, the elastic ceiling drops and holds the cells stably in a fixed location. **(C) Basic elements of the Onix™ Microfluidic Perfusion Platform.** Images and videos were generated using a confocal microscope with the microfluidic plate placed on the viewing platform. Growth conditions were manipulated as desired using the ONIX Control System, which itself was controlled with ONIX software on a separate computer. Fig. 2.4 A, B and C are adapted from (http://www.cellasic.com/).

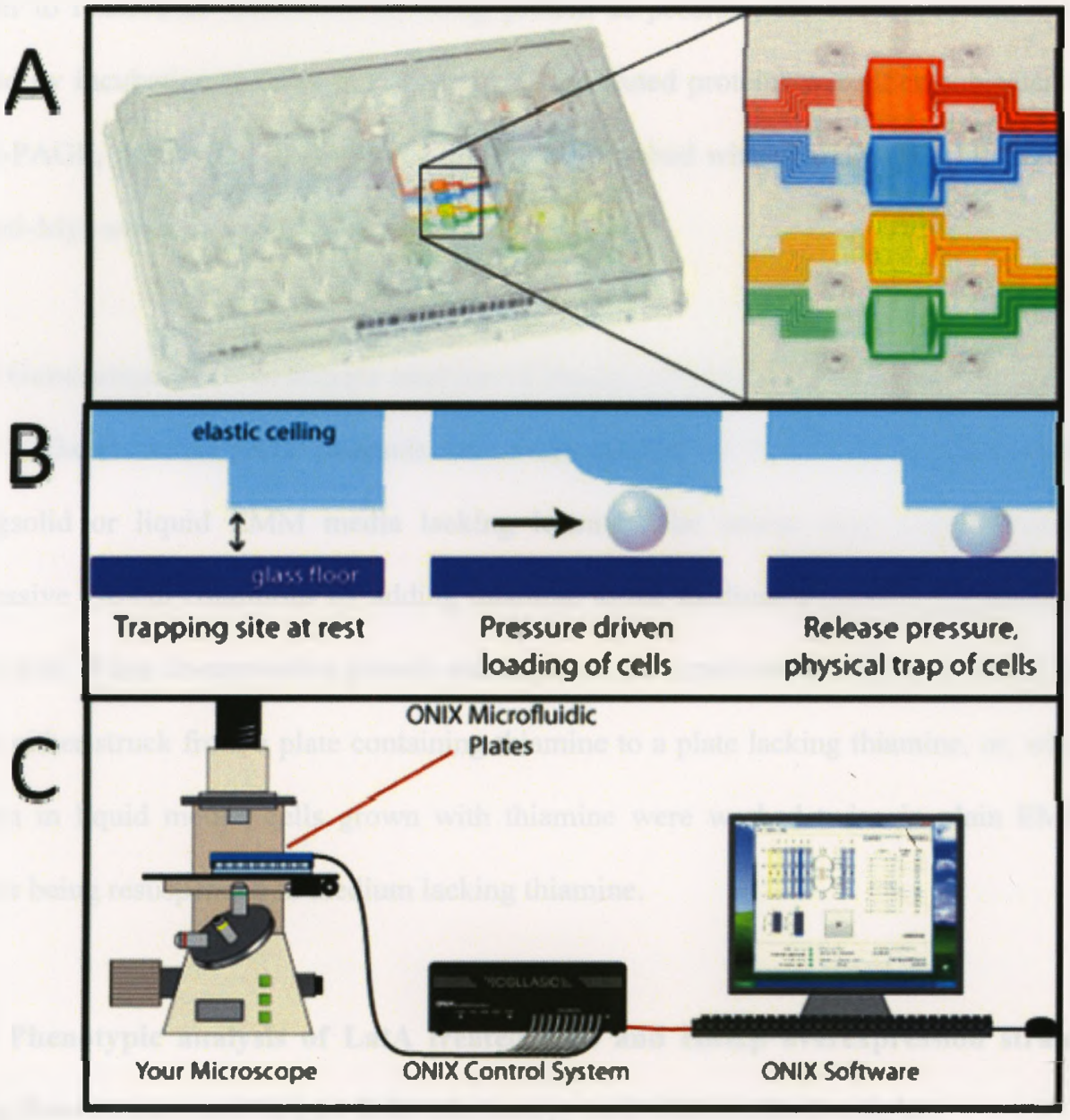
A
B
elastic ceiling
glass floor
Trapping site at rest
Pressure driven loading of cells
Release pressure, physical trap of cells
C
ONIX Microfluidic Plates
Your Microscope
ONIX Control System
ONIX Software

using extraction buffer (Section 2.8) as the wash solution. Cell extracts were then added to the antibody-bound bead slurry. After incubation and repeated washing with extraction buffer to remove as much contaminating protein as possible, the bound proteins were eluted by incubation at 96° C for 5 minutes. The eluted proteins were then subjected to SDS-PAGE, transferred to PVDF membranes and probed with anti-HA (HA.11; Sigma) or anti-Myc antibodies (9E10; Sigma).

2.12 Generation and Phenotypic analysis of Hos2p overexpression strains

The exosomal pREP plasmids were maintained in the cells by growing the strains usingsolid or liquid EMM media lacking leucine. The strains were cultured under repressive growth conditions by adding thiamine to the medium at a final concentration of 10 μM. When de-repressive growth was required for experimental analyses, the strains were either struck from a plate containing thiamine to a plate lacking thiamine, or, when grown in liquid media, cells grown with thiamine were washed twice in plain EMM before being resuspended in medium lacking thiamine.

2.13 Phenotypic analysis of LatA treated cells and Hos2p overexpression strains using fluorescence and bright-field microscopy and white reflective light

LatA treated cells and Hos2p overexpression cells were fixed in ethanol (Forsburg and Rhind 2006) and then washed once with a solution of either 1% (v/v) triton-X 100 (for LatA treated cells) or 10% (v/v) triton-X 100 (for Hos2p overexpression strains) in phosphate buffered saline pH 7.4 (PBS). After two washes in PBS pH 7.4, cells were then resuspended in a solution of 15% glycerol (v/v) in PBS pH 7.4. Cells were then stained

with 4', 6- diamidino-2-phenylindole (DAPI) at a concentration of 0.02 μg/μL, and aniline blue at a concentration of 1 μg/μL. Images were taken using a Zeiss Axioskop 2 fluorescence microscope fitted with a DAPI filter, Scion CFW Monochrome CCD Firewire Camera (Scion Corporation, Frederick, MD), and ImageJ 1.41 software (National Institutes of Health). Bright-field, magnified images of Hos2p overexpression strain colonies on solid media plates were taken using the same microscope. Unmagnified pictures under white, reflective light of Hos2p overexpression strains on solid media plates were taken using a Flurochem SP CCD (Alpha Innotech).

CHAPTER 3: RESULTS

3.1 The fission yeast Hos2p protein is orthologous to the human HDAC3 protein

A mutant screen was performed on the commercially available genome-wide set of viable *S. pombe* deletion mutants (http://pombe.bioneer.co.kr). This screen was done using a low dose (0.3-0.5 μM) of Latrunculin A (LatA) in order to identify novel regulators of the cytokinesis checkpoint. One of the strains sensitive to LatA bore a deletion in the annotated open reading frame (ORF) SPAC22E12.11c (Wood *et al.* 2002), a SET [su(var)3-9, enhancer-of-zeste and trithorax] domain containing transcription factor, later named *lst1* (latrunculin sensitive transcription factor). Bioinformatic analyses by Stefan Rentas revealed that *lst1* is orthologous to the mammalian *MLL5* (unpublished), and that MLL5 forms part of a larger histone de-acetylase complex (HDAC3-NCOR2/SMRT) implicated in faithful cytokinesis; furthermore, an orthologous complex also exists in budding yeast(Kittler *et al.* 2007; Pijnappel *et al.* 2001). Through experimental analyses, Stefan demonstrated that an orthologous complex containing Lst1p also exists in fission yeast, although the fission yeast histone de-acetylase has yet to be analyzed with respect to its role as part of this complex (Rentas, 2010).

A BLAST search using the HDAC3 amino acid sequence was performed against the *S. pombe* protein database at the *S. pombe* GeneDB (http://old.genedb.org/genedb/pombe/index.jsp), which identified the protein encoded by ORF SPAC3G9.07c as a likely orthologue for HDAC3 (E value of 5e-138) (Fig. 3.1). This ORF encodes a histone de-acetylase (*hos2*), initially characterized by Olsson *et al.* in 1998. A phylogenetic tree was also constructed (

CHAPTER 3: RESULTS

3.1 The fission yeast Hos2p protein is orthologous to the human HDAC3 protein

A mutant screen was performed on the commercially available genome-wide set of viable *S. pombe* deletion mutants (http://pombe.bioneer.co.kr). This screen was done using a low dose (0.3-0.5 μM) of Latrunculin A (LatA) in order to identify novel regulators of the cytokinesis checkpoint. One of the strains sensitive to LatA bore a deletion in the annotated open reading frame (ORF) SPAC22E12.11c (Wood *et al.* 2002), a SET [su(var)3-9, enhancer-of-zeste and trithorax] domain containing transcription factor, later named *lst1* (latrunculin sensitive transcription factor). Bioinformatic analyses by Stefan Rentas revealed that *lst1* is orthologous to the mammalian *MLL5* (unpublished), and that MLL5 forms part of a larger histone de-acetylase complex (HDAC3-NCOR2/SMRT) implicated in faithful cytokinesis; furthermore, an orthologous complex also exists in budding yeast(Kittler *et al.* 2007; Pijnappel *et al.* 2001). Through experimental analyses, Stefan demonstrated that an orthologous complex containing Lst1p also exists in fission yeast, although the fission yeast histone de-acetylase has yet to be analyzed with respect to its role as part of this complex (Rentas, 2010).

A BLAST search using the HDAC3 amino acid sequence was performed against the *S. pombe* protein database at the *S. pombe* GeneDB (http://old.genedb.org/genedb/pombe/index.jsp), which identified the protein encoded by ORF SPAC3G9.07c as a likely orthologue for HDAC3 (E value of 5e-138) (Fig. 3.1). This ORF encodes a histone de-acetylase (*hos2*), initially characterized by Olsson *et al.* in 1998. A phylogenetic tree was also constructed (

CHAPTER 3: RESULTS

3.1 The fission yeast Hos2p protein is orthologous to the human HDAC3 protein

A mutant screen was performed on the commercially available genome-wide set of viable *S. pombe* deletion mutants (http://pombe.bioneer.co.kr). This screen was done using a low dose (0.3-0.5 μM) of Latrunculin A (LatA) in order to identify novel regulators of the cytokinesis checkpoint. One of the strains sensitive to LatA bore a deletion in the annotated open reading frame (ORF) SPAC22E12.11c (Wood *et al.* 2002), a SET [su(var)3-9, enhancer-of-zeste and trithorax] domain containing transcription factor, later named *lst1* (latrunculin sensitive transcription factor). Bioinformatic analyses by Stefan Rentas revealed that *lst1* is orthologous to the mammalian *MLL5* (unpublished), and that MLL5 forms part of a larger histone de-acetylase complex (HDAC3-NCOR2/SMRT) implicated in faithful cytokinesis; furthermore, an orthologous complex also exists in budding yeast(Kittler *et al.* 2007; Pijnappel *et al.* 2001). Through experimental analyses, Stefan demonstrated that an orthologous complex containing Lst1p also exists in fission yeast, although the fission yeast histone de-acetylase has yet to be analyzed with respect to its role as part of this complex (Rentas, 2010).

A BLAST search using the HDAC3 amino acid sequence was performed against the *S. pombe* protein database at the *S. pombe* GeneDB (http://old.genedb.org/genedb/pombe/index.jsp), which identified the protein encoded by ORF SPAC3G9.07c as a likely orthologue for HDAC3 (E value of 5e-138) (Fig. 3.1). This ORF encodes a histone de-acetylase (*hos2*), initially characterized by Olsson *et al.* in 1998. A phylogenetic tree was also constructed (

CHAPTER 3: RESULTS

3.1 The fission yeast Hos2p protein is orthologous to the human HDAC3 protein

A mutant screen was performed on the commercially available genome-wide set of viable *S. pombe* deletion mutants (http://pombe.bioneer.co.kr). This screen was done using a low dose (0.3-0.5 μM) of Latrunculin A (LatA) in order to identify novel regulators of the cytokinesis checkpoint. One of the strains sensitive to LatA bore a deletion in the annotated open reading frame (ORF) SPAC22E12.11c (Wood *et al.* 2002), a SET [su(var)3-9, enhancer-of-zeste and trithorax] domain containing transcription factor, later named *lst1* (latrunculin sensitive transcription factor). Bioinformatic analyses by Stefan Rentas revealed that *lst1* is orthologous to the mammalian *MLL5* (unpublished), and that MLL5 forms part of a larger histone de-acetylase complex (HDAC3-NCOR2/SMRT) implicated in faithful cytokinesis; furthermore, an orthologous complex also exists in budding yeast(Kittler *et al.* 2007; Pijnappel *et al.* 2001). Through experimental analyses, Stefan demonstrated that an orthologous complex containing Lst1p also exists in fission yeast, although the fission yeast histone de-acetylase has yet to be analyzed with respect to its role as part of this complex (Rentas, 2010).

A BLAST search using the HDAC3 amino acid sequence was performed against the *S. pombe* protein database at the *S. pombe* GeneDB (http://old.genedb.org/genedb/pombe/index.jsp), which identified the protein encoded by ORF SPAC3G9.07c as a likely orthologue for HDAC3 (E value of 5e-138) (Fig. 3.1). This ORF encodes a histone de-acetylase (*hos2*), initially characterized by Olsson *et al.* in 1998. A phylogenetic tree was also constructed (

Figure 3.1 ClustalW alignment of Hos2p and its predicted orthologue HDAC3 (isoform 1). Sequences were downloaded from the *S. pombe* Gene Database (http://old.genedb.org/genedb/pombe) or UniProtKB (http://www.uniprot.org). "*" denotes amino acid identity, ":" denotes a conserved substitution and "." denotes a semi-conserved substitution. There is 51.1% identity between the HDAC3 and Hos2p amino acid sequence.

```
Hos2p    MDTPETSTPYEQVEKGSFFSFRPQKKRVTYHLDEQVGNYHYGDKHPMKPHRITITNHLVM 60
HDAC3    ----------------------MAKTVAYFYDPDVGNFHYGAGHPMKPHRLALTHSLVL 37
                               * *:*. * :***:***  *******:::*: **:

Hos2p    GYGLHNKMSVFSPRMATFGEMSEFHREDYLDFLKRVTPDNAEQFADKFQQFNIGDDCPVF 120
HDAC3    HYGLYKKMIVFKPYQASQHDMCRFHSEDYIDFLQRVSPTNMQGFTKSLNAFNVGDDCPVF 97
          ***::** **.*  *:  :*..** ***:***:**:* * : *:..:: **:*******

Hos2p    DGTYEFSQRSAGASLDASRKLVQGQTDIAINWSGGLHHAKRGEASGFCYVNDIVLAILNM 180
HDAC3    PGLFEFCSRYTGASLQGATQLNNKICDIAINWAGGLHHAKKFEASGFCYVNDIVIGILEL 157
          * :**..* :****:.: :* :   ******:*******: ************:.**::

Hos2p    LRFFPRVLYIDIDIHHGDGVQQAFYESDRVLTVSFHKYNGDFFPATGNFDENGVKGGKYF 240
HDAC3    LKYHPRVLYIDIDIHHGDGVQEAFYLTDRVMTVSFHKYGNYFFPGTGDMYEVGAESGRYY 217
         *::.******************:*** :***:*******.. ***.**:: * *.:.*:*:

Hos2p    ALNVPLEDGIGDEQYTSLFKSIIEPTINTFQPSAIVLQCGADSLGYDRLGVFNLSIHAHG 300
HDAC3    CLNVPLRDGIDDQSYKHLFQPVINQVVDFYQPTCIVLQCGADSLGCDRLGCFNLSIRGHG 277
         .*****.***.*:.*. **:.:*: .:: :**:.********** **** *****:.**

Hos2p    ECVRFTRSFNIPMLVVGGGGYTLRNVARAWCYETSICVNEQIPSELPRETLYYEFFAPDY 360
HDAC3    ECVEYVKSFNIPLLVLGGGGYTVRNVARCWTYETSLLVEEAISEELP-YSEYFEYFAPDF 336
         ***.:.:*****:**:******:*****.* ****: *:* *..***  : *:*:****:

Hos2p    TLHPRLTTKIENKNTPKALEDLRIRALEQLRYLGGAPSVQMQQIPPDL-----TGHLEEE 415
HDAC3    TLHPDVSTRIENQNSRQYLDQIRQTIFENLKMLNHAPSVQIHDVPADLLTYDRTDEADAE 396
         **** ::*:***:*: : *:::*   :*:*: *. *****::::*.**     *.. : *

Hos2p    DERLNDEY---------------LDKAVDVRVRG 434
HDAC3    ERGPEENYSRPEAPNEFYDGDHDNDKESDVEI-- 428
         :.  :::*                **  **.:
```

Figure 3.2 TreeFam Orthologue Tree showed evolutionary conservation of HDAC3.

Treefam ortholog tree (TF106172) of various eukaryotic species showed that human HDAC3 and fission yeast Hos2p are orthologues of one another (http://www.treefam.org/). Red nodes stand for gene duplications and blue for speciations or undefined nodes. The green numbers denote the bootstrap values. Red arrows indicate *S. pombehos2* and *H. sapiensHDAC3*.

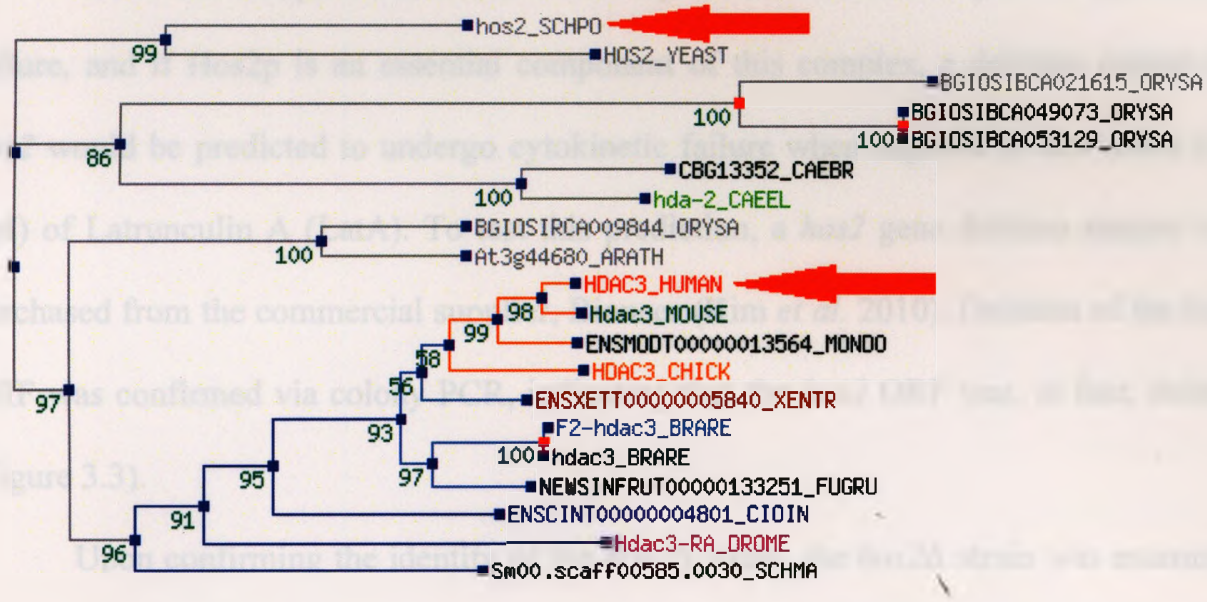
hos2_SCHPO
99
HOS2_YEAST
BGIOSIBCA021615_ORYSA
100
BGIOSIBCA049073_ORYSA
100
BGIOSIBCA053129_ORYSA
86
CBG13352_CAEBR
100
hda-2_CAEEL
BGIOSIRCA009844_ORYSA
100
At3g44680_ARATH
HDAC3_HUMAN
98
Hdac3_MOUSE
99
ENSMODT00000013564_MONDO
58
HDAC3_CHICK
56
ENSXETT00000005840_XENTR
97
93
F2-hdac3_BRARE
100
hdac3_BRARE
95
97
NEWSINFRUT00000133251_FUGRU
91
ENSCINT00000004801_CIOIN
96
Hdac3-RA_DROME
Sm00.scaff00585.0030_SCHMA

http://www.treefam.org/), showing that Hos2p shows cross-species sequence conservation (Fig. 3.2).

3.2 A *hos2* gene deletion mutant displayed the characteristic *S. pombe* phenotype for cytokinesis failure upon perturbation of the contractile actomyosin ring by Latrunculin A

If the Lst complex has a role in checkpoint surveillance to prevent cytokinetic failure, and if Hos2p is an essential component of this complex, a deletion mutant for *hos2* would be predicted to undergo cytokinetic failure when exposed to low doses (0.5 μM) of Latrunculin A (LatA). To test this prediction, a *hos2* gene deletion mutant was purchased from the commercial supplier, Bioneer (Kim *et al.* 2010). Deletion of the *hos2* ORF was confirmed via colony PCR, indicating that the *hos2* ORF was, in fact, deleted (Figure 3.3).

Upon confirming the identity of the *hos2*Δ strain, the *hos2*Δ strain was examined microscopically to determine whether the *hos2*Δ strain displayed the characteristic phenotype of cytokinesis failure present in checkpoint defective cells under LatA treatment (again, wildtype and *lst1*Δ cells were used as controls). The *hos2*Δ strain was grown in liquid YES with either 0.5 μM LatA or DMSO (solvent control) for 5 hours. Subsequently, the cells were fixed and stained with DAPI and aniline blue to visualize the nucleus and cell wall/septum, respectively (Balasubramanian *et al.* 1998). Most of the *hos2*Δ and *lst1*Δ cells underwent cytokinesis failure upon LatA exposure, whereas most wildtype cells completed cytokinesis successfully under identical conditions. Cells were scored into several phenotypic classes for the analysis; cytokinesis failures are

Figure 3.3 Verification of the integration of the *hos2* gene deletion cassette by colony PCR. Labels below each lane indicate the primer pair used to confirm the upstream and downstream junctions of integration. Labels above the image indicate the strain tested. PCR amplicons were separated via agarose gel electrophoresis and visualized by staining with ethidium bromide and exposing to UV light.

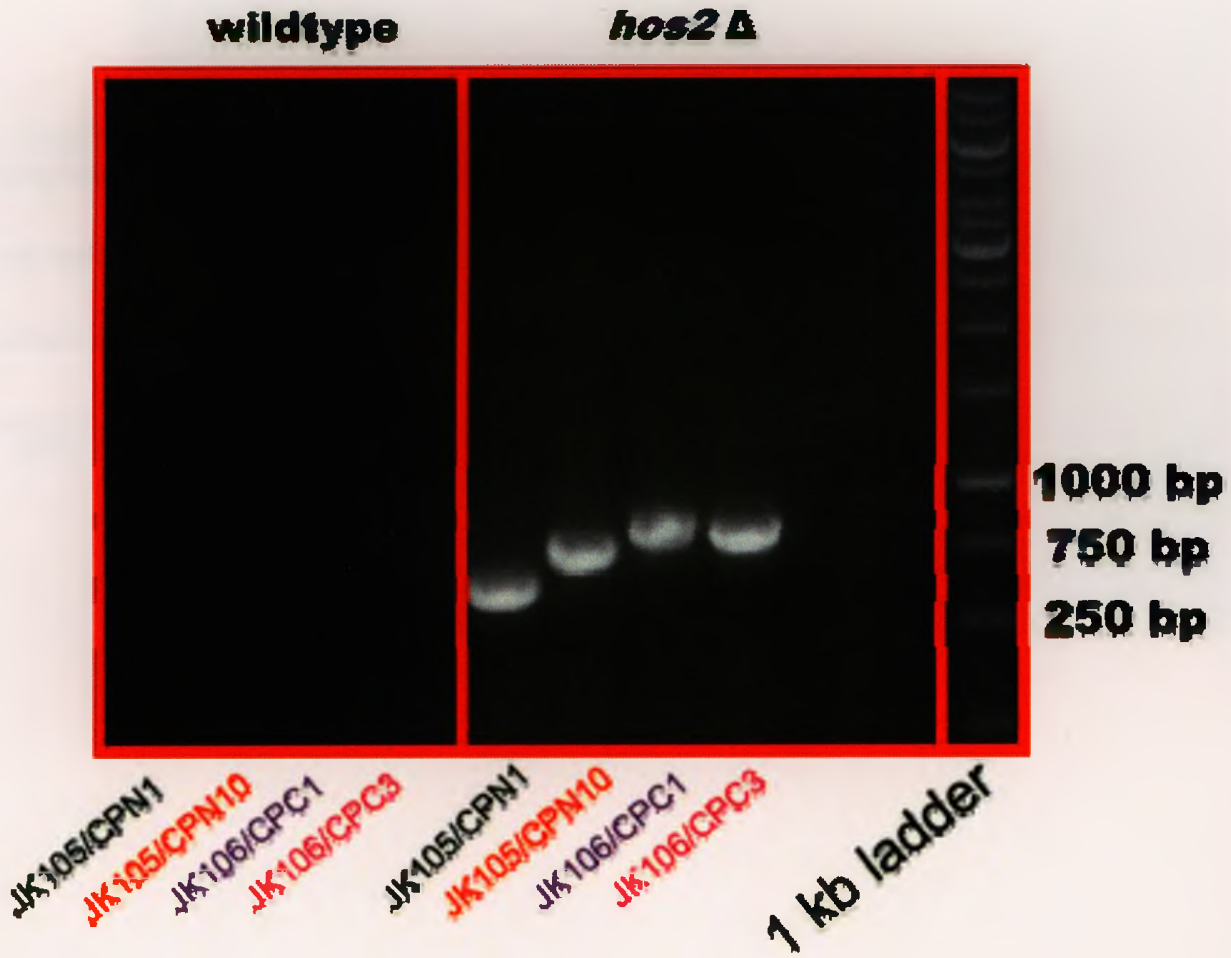
wildtype
hos2 Δ
1000 bp
750 bp
250 bp
JK105/CPN1
JK105/CPN10
JK106/CPC1
JK106/CPC3
JK105/CPN1
JK105/CPN10
JK106/CPC1
JK106/CPC3
1 kb ladder

Figure 3.4 A *hos2*Δ gene deletion mutant displayed loss of cytokinesis checkpoint activity upon treatment with LatA. Cells of the indicated genotypes were grown up to mid-log phase in YES, then treated with either 0.5 μM LatA or DMSO (solvent control) for 5 hr. Cells were then fixed in ethanol and visualized under fluorescence microscopy after being stained with DAPI and aniline blue.

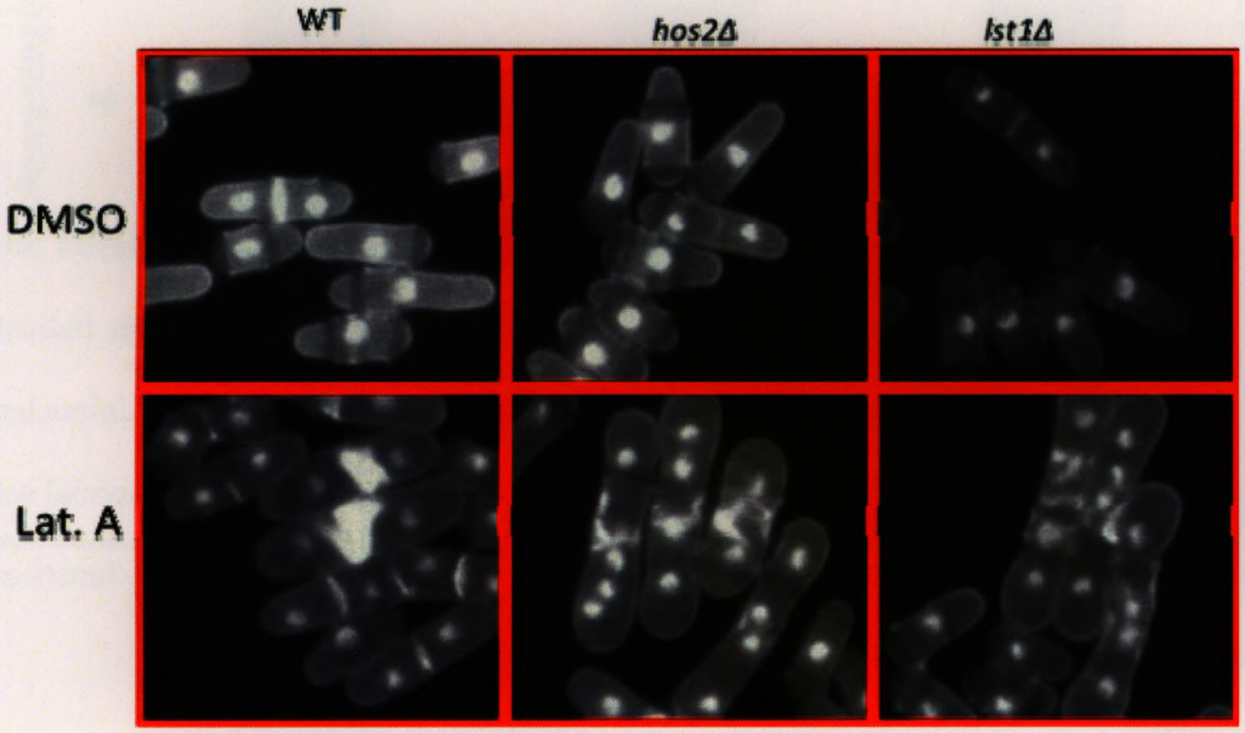
WT
hos2Δ
lst1Δ
DMSO
Lat. A

Figure 3.5 Upon LatA exposure,*hos2*Δ gene deletion mutant cells displayed more cytokinesis failure events than wildtype cells.Five hundred cells of each indicated genotype were scored and grouped into several phenotypic classes. Uninucleate, binucleate (no septum), and binucleate (septum functional) classes represent normal cells. Binucleate (septum non-functional), trinucleate and tetranucleate (septum non-functional) classes represented cells that underwent cytokinesis failure.

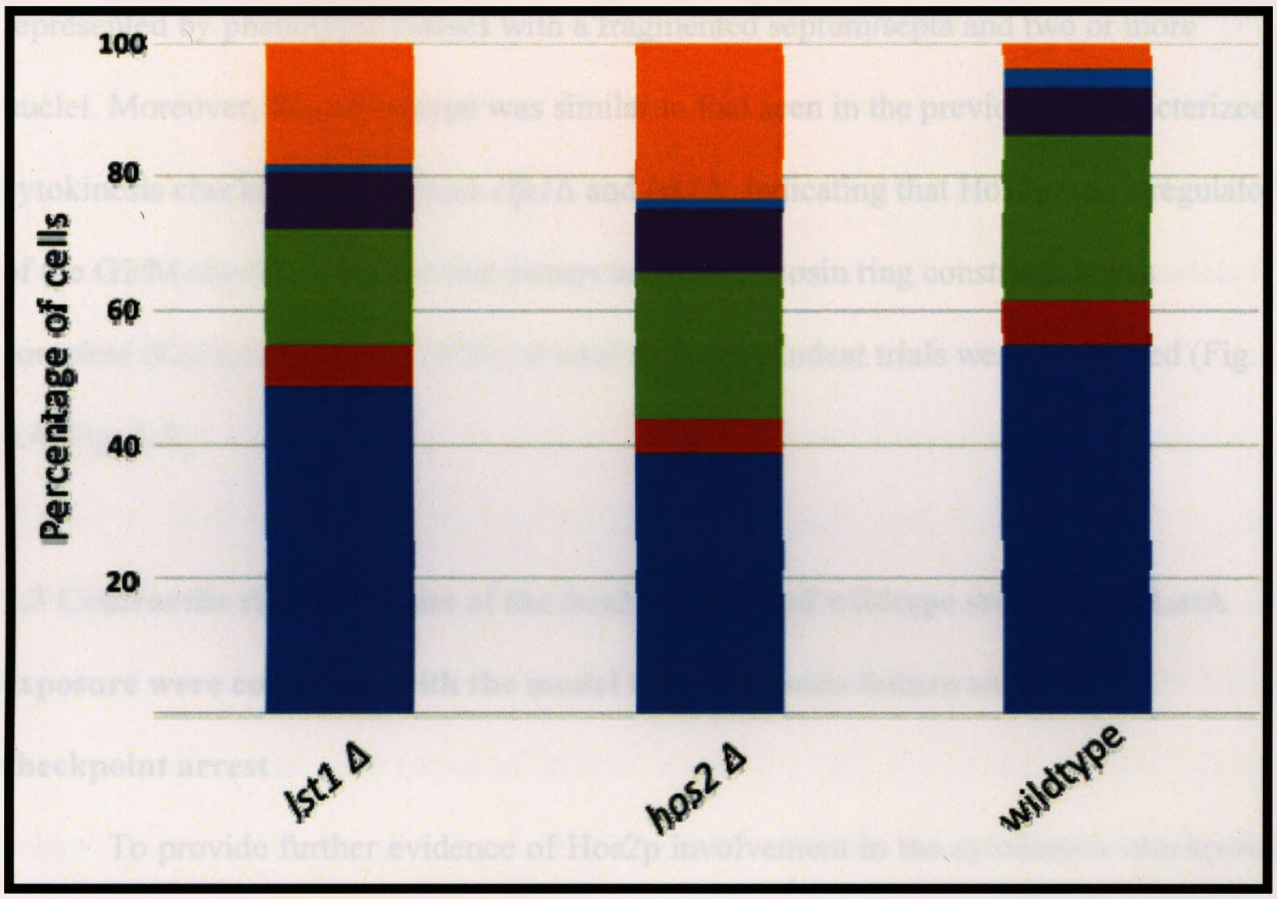
100
80
60
40
20
Percentage of cells
lst1 Δ
hos2 Δ
wildtype
Tetranucleate (septum non-functional)
Trinucleate
Binucleate (septum non-functional)
Binucleate (septum functional)
Binucleate (no septum)
Uninucleate

represented by phenotypic classes with a fragmented septum/septa and two or more nuclei. Moreover, this phenotype was similar to that seen in the previously characterized cytokinesis checkpoint regulators *clp1*Δ and *lsk1*Δ, indicating that Hos2p was a regulator of the G2/M checkpoint arrest that occurs until actomyosin ring constriction was complete (Karagiannis *et al.* 2005). A total of 3 independent trials were performed (Fig. 3.4, Fig. 3.5).

3.3 Contractile ring dynamics of the *hos2*Δ strain and wildtype strain upon LatA exposure were consistent with the model for cytokinesis failure and G2/M checkpoint arrest

To provide further evidence of Hos2p involvement in the cytokinesis checkpoint, ring dynamics were visualized via live cell imaging, which was used in conjunction with a GFP-tagging strategy. Visualization of the actomyosin ring was done via fusion of the *rlc1* gene (myosin regulatory light chain 1) with a GFP tagfrom its native promoter and integrated at its native genetic locus (Le Goff *et al.* 2000). This strain was subsequently crossed with the *hos2*Δ strain, in order to create the *rlc1*GFP-*hos2*Δ strain.

The *rlc1*GFP strain was used to observe wildtype actomyosin ring and checkpoint dynamics, whereas the *rlc1*GFP-*hos2*Δ strain was used to observe the actomyosin ring and checkpoint deficiency dynamics of the *hos2*Δ strain. Both strains were grown in YES with either 0.5 μM Lat. A or DMSO (solvent control) for 1 hour or less under continuous perfusion, while a time-lapse video was generated using the ONIX™ Microfluidic Perfusion System (http://www.cellasic.com/). A total of 3 independent trials were performed for each of the four videos.

The videos obtained for the *rlc1*GFP + DMSO treatment (Supplementary Disc, vid. 3.1) and the *rlc1*GFP-*hos2Δ* + DMSO treatment (Supplementary Disc, vid. 3.2) showed normal cytokinesis, with the ring successfully cleaving the mother cell in both treatments. The videos obtained with LatA also conformed to the established models for the G2/M checkpoint arrest and cytokinesis failure, as *rlc1*GFP + LatA cells (Supplementary Disc, vid. 3.3) undergo a G2/M arrest while maintaining the integrity of the actomyosin ring (which does not constrict noticeably), and *rlc1GFP-hos2Δ* + LatA cells (Supplementary Disc, vid. 3.4) initiated ring constriction upon assembly of the ring, which disintegrates before cytokinesis is complete, thus resulting in cytokinesis failure.An additional observation of interest is that the ring of *rlc1*GFP-*hos2Δ* + DMSO constricts at a noticeably slower rate than *rlc1GFP* + DMSO, even though cytokinesis is otherwise normal. The cause and significance of this observation is currently unknown.

3.4 Hos2p localized to the nucleus and cytoplasm and becomes shuttled into the nucleus upon LatA exposure

If the Lst complex is necessary for functioning of the cytokinesis checkpoint, and if Hos2p is an essential member of the complex, it will co-localize with Lst1p, Lst2p and Lst3p to the nucleus. To test this prediction, a strain was created that expressed a C-terminally GFP-tagged allele of Hos2p from its native promoter and integrated at its native genetic locus. Under normal logarithmic growth conditions, Hos2p was found to localize to both the nucleus and cytoplasm, consistent with the hypothesis that it forms part of the Lst complex, which has a role in chromatin modification (Fig. 3.6).

Figure 3.6 Hos2p localized to both the nucleus and the cytoplasm. Cells bearing a C-terminal GFP fluorophore tag on Hos2p were grown in YES to mid-log phase. The GFP signal was visualized by fluorescence microscopy as described in the Materials and Methods.

Figure 3.7 Hos2p shuttles into the nucleus in response to LatA induced checkpoint activation. The aforementioned *hos2*GFP strain was grown to mid-log phase in YES, then treated with either 0.5 μM LatA or DMSO (solvent control). Cells were visualized under fluorescence microscopy as described in Materials and Methods.

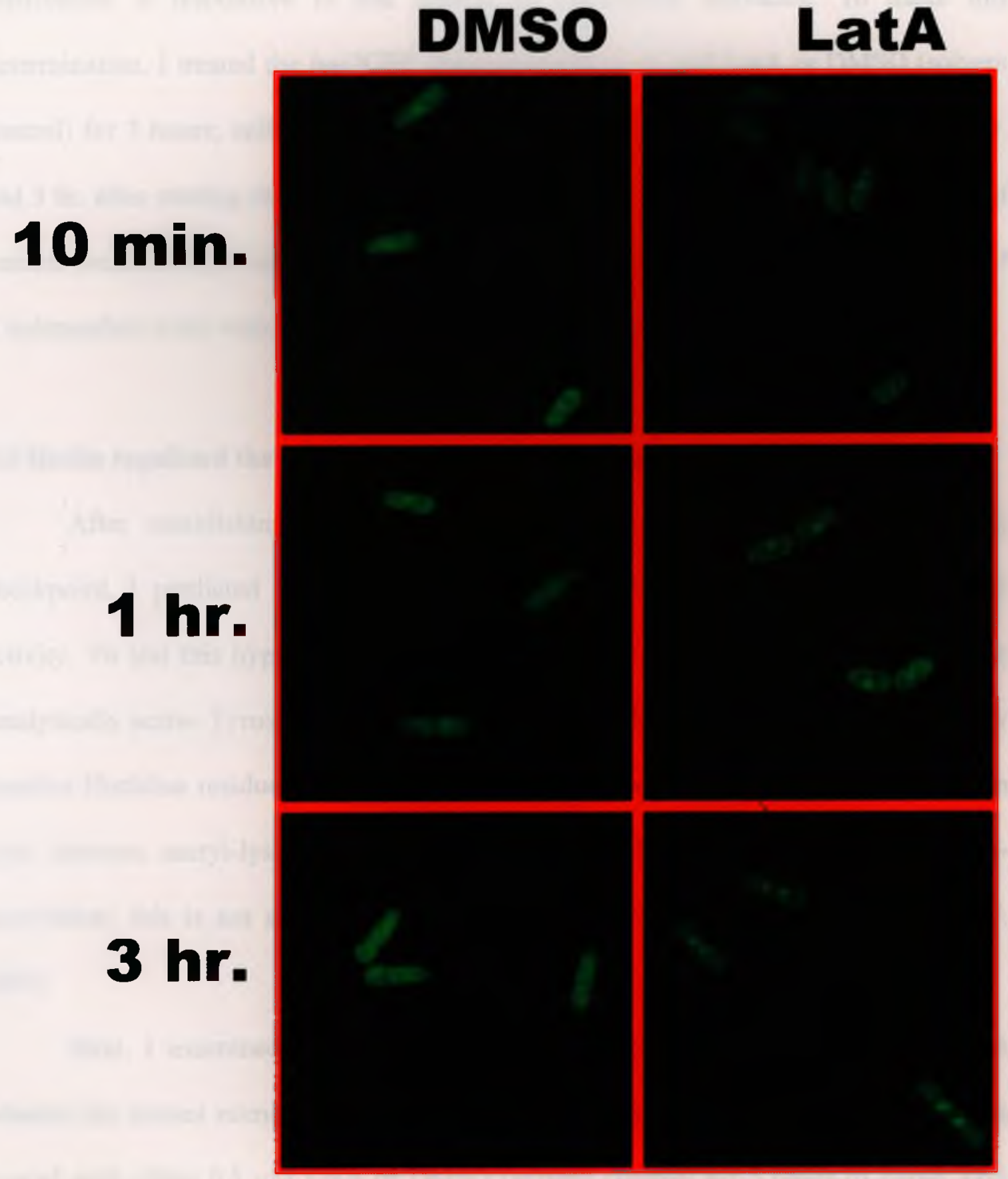
DMSO
LatA
10 min.
1 hr.
3 hr.

As Hos2p is both nuclear and cytoplasmic, I wanted to determine whether the distribution is responsive to and altered by checkpoint activation. To make this determination, I treated the *hos2*GFP strain with either 0.5 μM LatA or DMSO (solvent control) for 3 hours; cells were viewed using fluorescence microscopy at 10 min., 1 hr. and 3 hr. after starting the treatment. Strikingly, Hos2p clearly shows increased levels of nuclear localization in response to checkpoint activation relative to the control.A total of 3 independent trials were performed for this experiment (Fig. 3.7).

3.5 Hos2p regulated the cytokinesis checkpoint through its de-acetylase activity

After establishing that Hos2p was essential for a functioning cytokinesis checkpoint, I predicted that Hos2p regulates the checkpoint through its de-acetylase activity. To test this hypothesis, I performed a site-directed mutagenesis to replace the catalytically active Tyrosine residue in the catalytic pocket of Hos2p with a catalytically inactive Histidine residue. This Tyrosine residue catalyzes stabilization of the transition state between acetyl-lysine and lysine, thereby allowing for catalysis of lysine de-acetylation; this is not chemically possible through a Histidine residue. (Lahm *et al.* 2007)

Next, I examined the *hos2* site-directed mutant microscopically to determine whether the mutant mimics the *hos2*Δ phenotype for cytokinesis failure; the mutant was treated with either 0.5 μM LatA or DMSO (solvent control) for 5 hours in liquid YES (wildtype and *hos2*Δ cells were used as a resistant and sensitive control, respectively). Subsequently, the cells were fixed and stained with DAPI and aniline blue to visualize the nucleus and cell wall/septum, respectively (Balasubramanian *et al.* 1998). Most of the

Figure 3.8 A *hos2* site-directed mutant displayed loss of cytokinesis checkpoint activity upon treatment with LatA. Cells of the indicated genotypes were grown up to mid-log phase in YES, then treated with either 0.5 μM LatA or DMSO (solvent control) for 5 hr. Cells were then fixed in ethanol and visualized under fluorescence microscopy after being stained with DAPI and aniline blue.

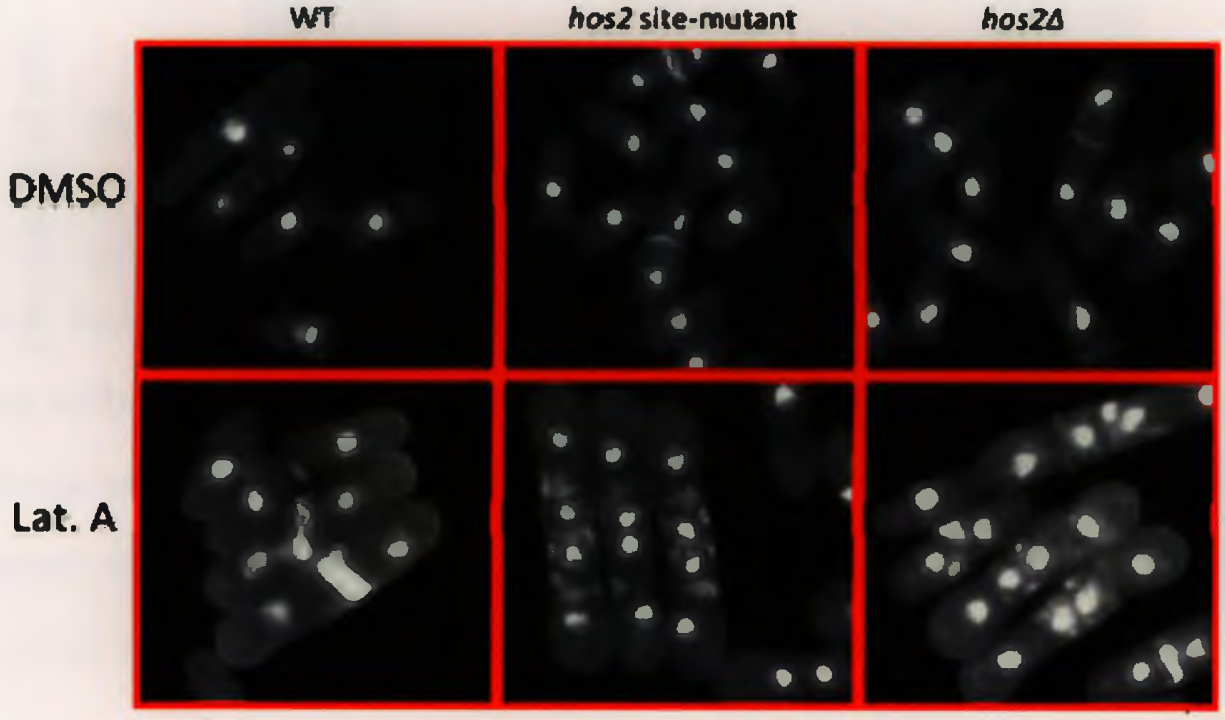
WT
hos2 site-mutant
hos2Δ
DMSO
Lat. A

Figure 3.9 Upon LatA exposure,*hos2* site-directed mutant cells displayed more cytokinesis failure events than wildtype cells.500 cells of each indicated genotype were scored and grouped into several phenotypic classes. Uninucleate, binucleate (no septum), and binucleate (septum functional) classes represent normal cells. Binucleate (septum non-functional), trinucleate and tetranucleate (septum non-functional) classes represent cells that underwent cytokinesis failure.

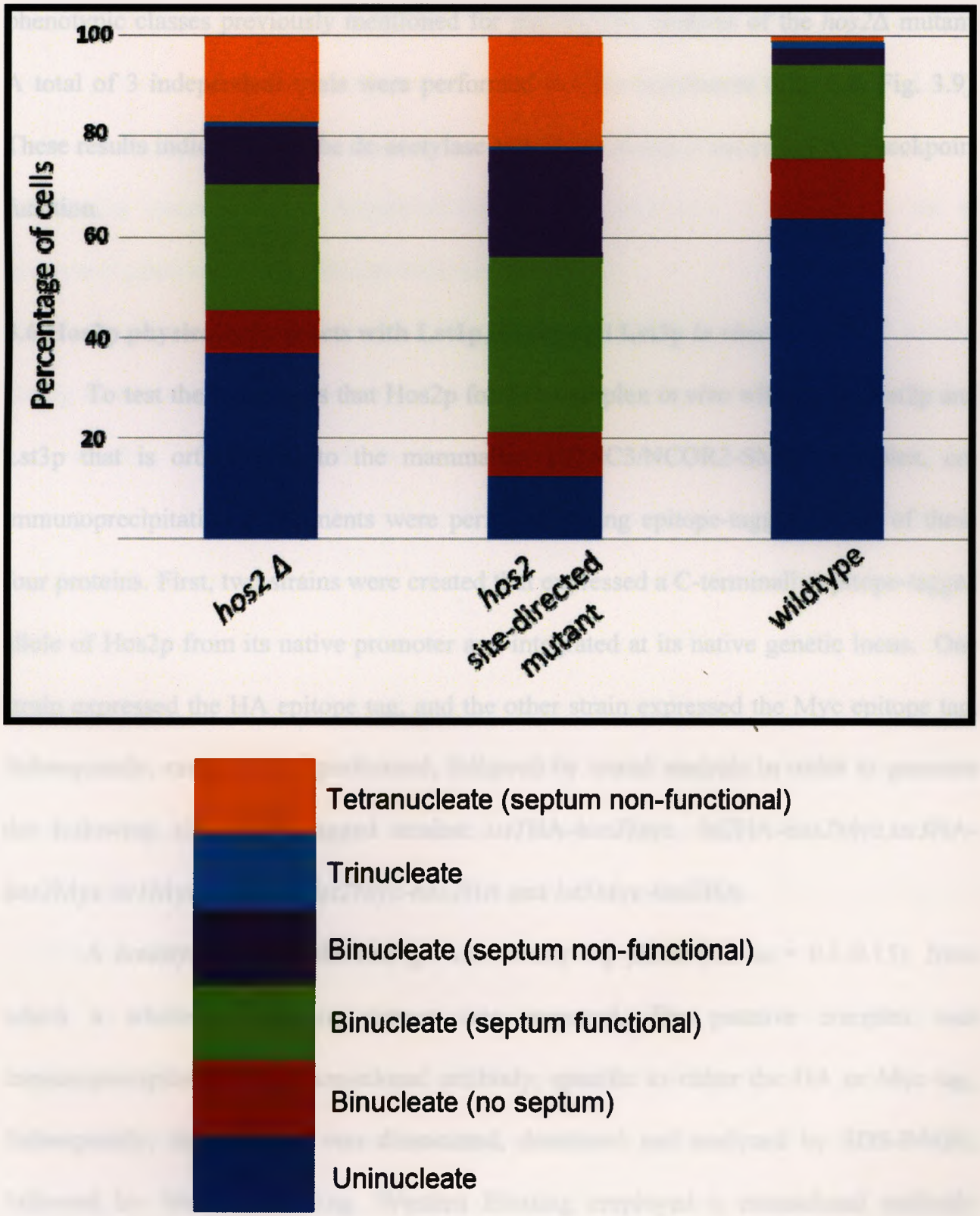
100
80
60
40
20
Percentage of cells
hos2 Δ
hos2 site-directed mutant
wildtype
Tetranucleate (septum non-functional)
Trinucleate
Binucleate (septum non-functional)
Binucleate (septum functional)
Binucleate (no septum)
Uninucleate

*hos2*Δ and site-directed mutant cells displayed cytokinesis failure upon LatA treatment, whereas most wildtype cells completed cytokinesis successfully. Cells were scored into phenotypic classes previously mentioned for microscopic analysis of the *hos2*Δ mutant. A total of 3 independent trials were performed for this experiment (Fig. 3.8, Fig. 3.9). These results indicated that the de-acetylase activity of Hos2p is necessary for checkpoint function.

3.6 Hos2p physically interacts with Lst1p, Lst2p and Lst3p *in vivo*

To test the hypothesis that Hos2p forms a complex *in vivo* with Lst1p, Lst2p and Lst3p that is orthologous to the mammalian HDAC3/NCOR2-SMRT complex, co-immunoprecipitation experiments were performed using epitope-tagged alleles of these four proteins. First, two strains were created that expressed a C-terminally epitope-tagged allele of Hos2p from its native promoter and integrated at its native genetic locus. One strain expressed the HA epitope tag, and the other strain expressed the Myc epitope tag. Subsequently, crosses were performed, followed by tetrad analysis in order to generate the following six doubly-tagged strains: *lst1*HA-*hos2*Myc, *lst2*HA-*hos2*Myc,*lst3*HA-*hos2*Myc *lst1*Myc-*hos2*HA, *lst2*Myc-*hos2*HA and *lst3*Myc-*hos2*HA.

A doubly-tagged strain was grown to early-log phase (OD_{600} = 0.1-0.15), from which a whole-cell protein extract was prepared. The putative complex was immunoprecipitated via a monoclonal antibody, specific to either the HA or Myc tag. Subsequently, the complex was dissociated, denatured and analyzed by SDS-PAGE, followed by Western Blotting. Western Blotting employed a monoclonal antibody specific to the HA tag (for anti-Myc immunoprecipitates) or Myc tag (for anti-HA

immunoprecipitates). Hos2p was detected in immunoprecipitates of Lst1p, Lst2p and Lt3p; a reciprocal co-immunoprecipitation was carried out for each of the three protein-pair combinations, each of which also indicated an interaction (Fig. 3.10). Together, these results provided compelling evidence of a physical interaction between Lst1p, Lst2p, Lst3p and Hos2p.

3.7 Hos2p overexpression impaired growth and generates a pleiotropic set of abnormal phenotypes in a dosage-dependent manner

To date, no one has determined the effects of Hos2p overexpression in *S. pombe.* Doing so and studying the phenotypic consequences will help develop a more complete understanding of Hos2p and its functions. To determine the effects of Hos2p overexpression, I cloned *hos2* into the pREP series of exosomal expression vectors and transformed the vector constructs into wildtype *S. pombe*; the pREP vector series transcribe a gene cloned downstream of the promoter. Different pREP vectors use different allelic variations of the thiamine-repressible *nmt1*$^{+}$promoter, which modifies expression levels downstream of the promoter;*hos2* was cloned into pREP1 (high level overexpressor), pREP41 (moderate level overexpressor) and pREP81 (low level overexpressor), and empty pREP1 was transformed into wildtype cells as a negative control, for a total of four strains in this experiment.

To determine the consequences of Hos2p over-expression on growth, I performed 3 independent trials of a plate assay on EMM selectable media plates with supplements. The strains were initially struck on repressive media and incubated for 24 hours to obtain actively growing inoculant. This inoculant was used for two parallel treatments: one with repression, and one without. The inoculant was struck onto the appropriate plate, and

Figure 3.10 Hos2p physically interacts with Lst1p, Lst2p and Lst3p *in vivo*. Protein extracts derived from cells expressing the indicated epitope-tagged fusion proteins were immunoprecipitated with a Myc-specific or HA-specific 1° antibody as described in the Materials and Methods. After washing, dissociation and denaturation, the immune complexes were subjected to SDS-PAGE, transferred to PVDF membranes, and blotted with HA-specific (for anti-Myc immunoprecipitates) or Myc-specific (for anti-HA immunoprecipitates) 1° antibody.

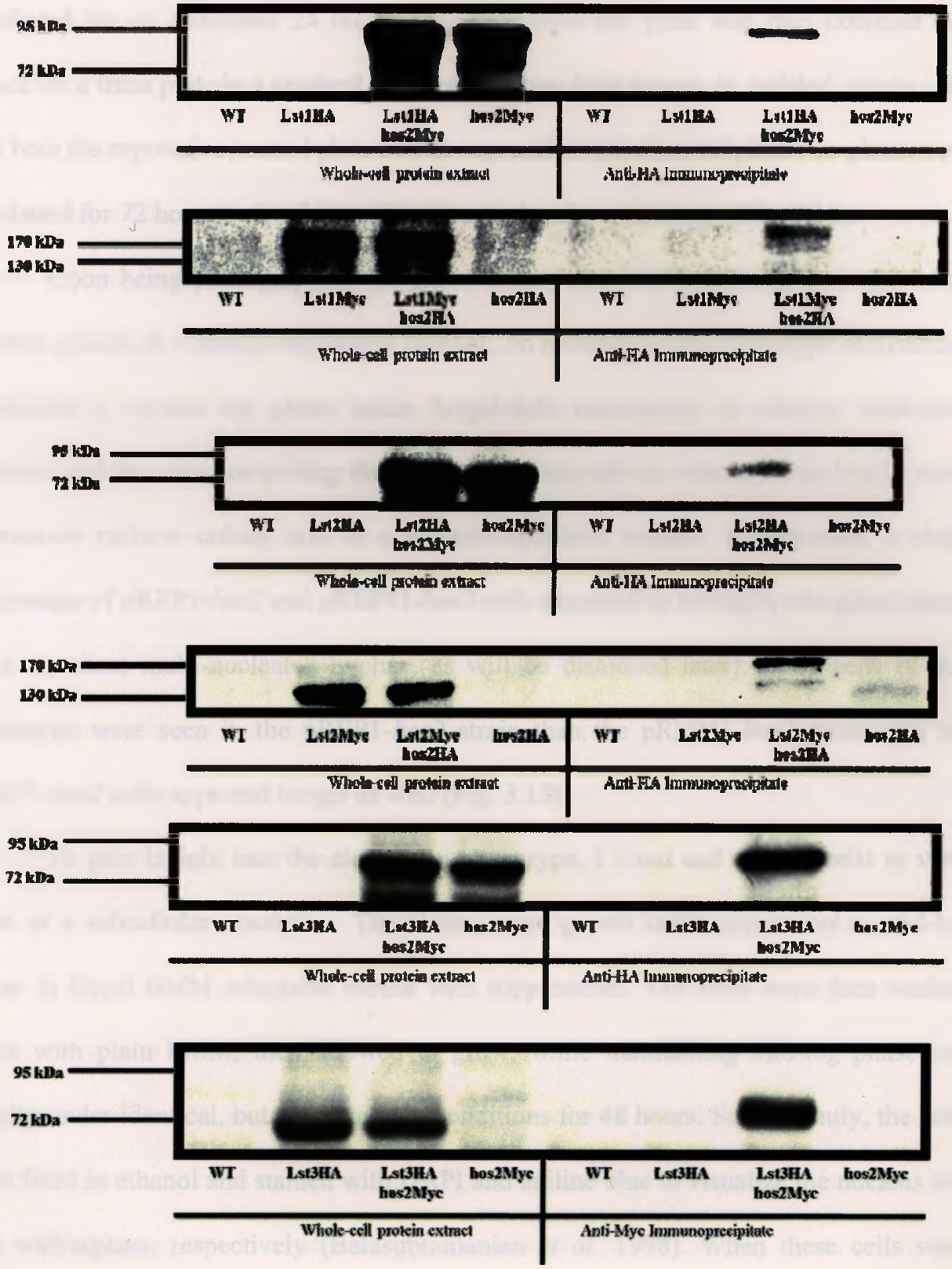
95 kDa
72 kDa
WT
Lst1HA
Lst1HA hos2Myc
hos2Myc
WT
Lst1HA
Lst1HA hos2Myc
hos2Myc
Whole-cell protein extract
Anti-HA Immunoprecipitate
170 kDa
130 kDa
WT
Lst1Myc
Lst1Myc hos2HA
hos2HA
WT
Lst1Myc
Lst1Myc hos2HA
hos2HA
Whole-cell protein extract
Anti-HA Immunoprecipitate
95 kDa
72 kDa
WT
Lst2HA
Lst2HA hos2Myc
hos2Myc
WT
Lst2HA
Lst2HA hos2Myc
hos2Myc
Whole-cell protein extract
Anti-HA Immunoprecipitate
170 kDa
130 kDa
WT
Lst2Myc
Lst2Myc hos2HA
hos2HA
WT
Lst2Myc
Lst2Myc hos2HA
hos2HA
Whole-cell protein extract
Anti-HA Immunoprecipitate
95 kDa
72 kDa
WT
Lst3HA
Lst3HA hos2Myc
hos2Myc
WT
Lst3HA
Lst3HA hos2Myc
hos2Myc
Whole-cell protein extract
Anti-HA Immunoprecipitate
95 kDa
72 kDa
WT
Lst3HA
Lst3HA hos2Myc
hos2Myc
WT
Lst3HA
Lst3HA hos2Myc
hos2Myc
Whole-cell protein extract
Anti-Myc Immunoprecipitate

incubated for an additional 24 hours. Inoculant from this plate was then obtained and struck on a fresh plate in a gradient progressing from high density to isolated, single cells and both the repressive control plate and de-repressive experimental plate two plates were incubated for 72 hours before being photographed under white light (Fig. 3.11).

Upon being photographed, the plates clearly showed that Hos2p overexpression inhibits growth in a dosage-dependent manner. To investigate this phenotype at a cellular resolution, I viewed the plates under bright-field microscopy to observe individual colonies and the cells comprising these colonies. I was able to conclude that Hos2p over-expression reduces colony size in a dosage-dependent manner. Furthermore, a small percentage of pREP1-*hos2* and pREP41-*hos2* cells appeared to be highly elongated (these cells represent multi-nucleated hyphae, as will be discussed later); more cells of this phenotype were seen in the pREP1-*hos2* strain than the pREP41-*hos2* strain and the pREP1-*hos2* cells appeared longer as well (Fig. 3.12).

To gain insight into the elongation phenotype, I fixed and stained cells to view them at a subcellular resolution. The strains were grown under repression to mid-log phase in liquid EMM selectable media with supplements. The cells were then washed twice with plain EMM, then allowed to grow, while maintaining mid-log phase cell density under identical, but de-repressive conditions for 48 hours. Subsequently, the cells were fixed in ethanol and stained with DAPI and aniline blue to visualize the nucleus and cell wall/septum, respectively (Balasubramanian *et al.* 1998). When these cells were observed using fluorescence microscopy, I noted that the highly elongated cells previously observed were actually multi-nucleated (and oftentimes branched) hyphae

with a unique set of hyphal phenotypes, and additionally, a set of phenotypes was present in both hyphae and non-hyphal cells (Fig. 3.13).

Hyphal phenotypes included a variety of defects representing abnormalities in septum formation and/or cell division. These include a failure of the septum plane to bisect the long axis of the cell at a perpendicular angle, failure for cells to separate via cytokinesis at the plane of septum deposition, multiple septa forming between two independent nuclei, abnormally shaped septa and abnormally thick septa (Fig. 3.13).

Phenotypes present that were not unique to hyphae and present in both hyphae and non-hyphal cells included the formation of cell wall deposits and spherical morphology; these phenotypes tended to co-occur, indicating that they were both related to each other.Also, these phenotypes were present in all three overexpressor strains. Furthermore, non-hyphal cells and individual compartments of hyphae showed an increase in length, a phenotype that did not occur in pREP81-*hos2*. These three phenotypes all appeared to be dose-dependent (Fig. 3.13).

Quantitative evidence showing dose-dependence of the hyphal phenotypes was generated by making a frequency distribution for cell length in the three overexpressor strains relative to the empty pREP1 control strain, and both non-hyphal cells and hyphae were measured in the analysis. All strains show a normal distribution, but pREP1-*hos2* and pREP41-*hos2* have a tail at the right end of the distribution, showing a percentage of cells with abnormal and variable length; these represent hyphae (Fig. 3.14, Fig. 3.15). Also, pREP81-*hos2* cells are not noticeably different from the control (Fig. 3.16). The number and length of hyphae is seen from these distributions to be greater in pREP1-*hos2*

Figure 3.11 Hos2p over-expression inhibited growth in a dosage-dependent manner. Cells of the indicated genotypes were grown with repression on EMM selectable media with supplements for 24 hours, allowed to de-repress for 24 hours on EMM selectable media plates with supplements for 24 hours, then re-streaked out to single colonies on de-repressive EMM selectable media plates with supplements. A repressed control plate was grown in parallel. After 72 hours of growth, the gradient plates were photographed. Hos2p overexpression impairs growth in a dosage-dependent manner.

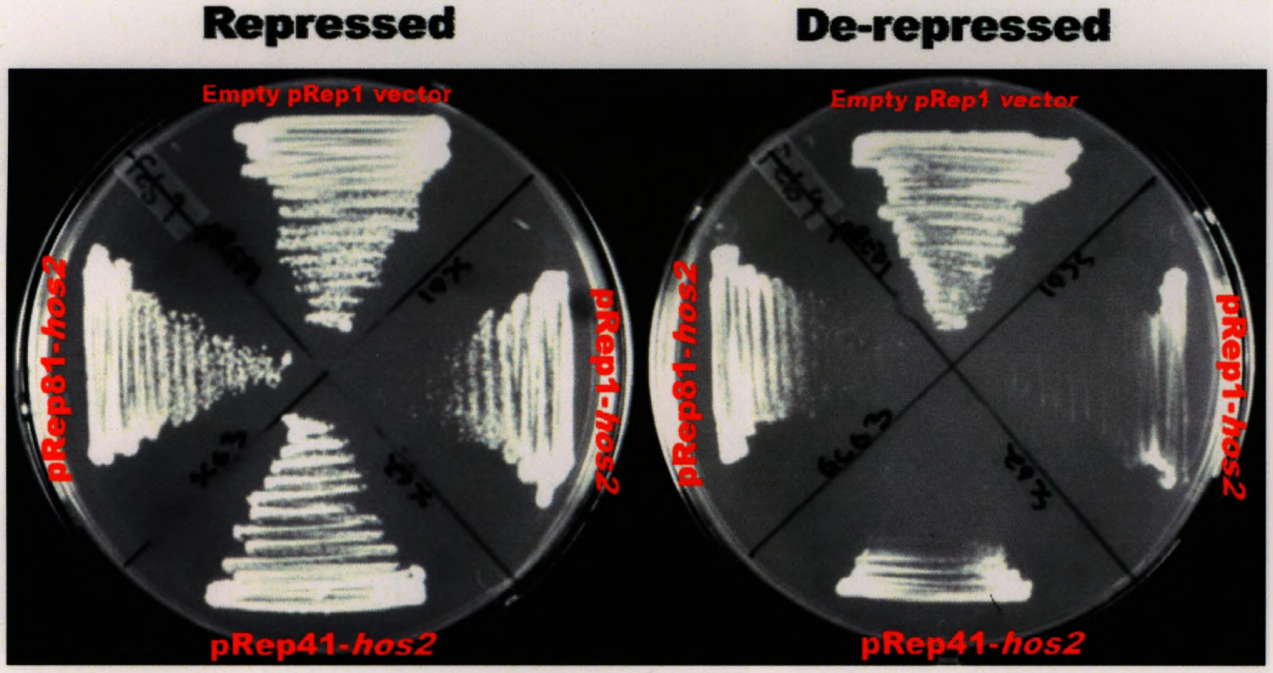
Repressed
De-repressed
Empty pRep1 vector
pRep81-hos2
pRep1-hos2
pRep41-hos2
Empty pRep1 vector
pRep81-hos2
pRep1-hos2
pRep41-hos2

Figure 3.12 Hos2p overexpression impaired colony formation and caused highly elongated cells to appear above a threshold level of Hos2p overexpression. A representative colony of each strain on the plates from the previous figure were photographed using bright-field microscopy at 40X magnification. pREP1-*hos2* and pREP41-*hos2* colonies contained highly elongated cells; more of these cells were present in pREP1-*hos2* than pREP41-*hos2*.

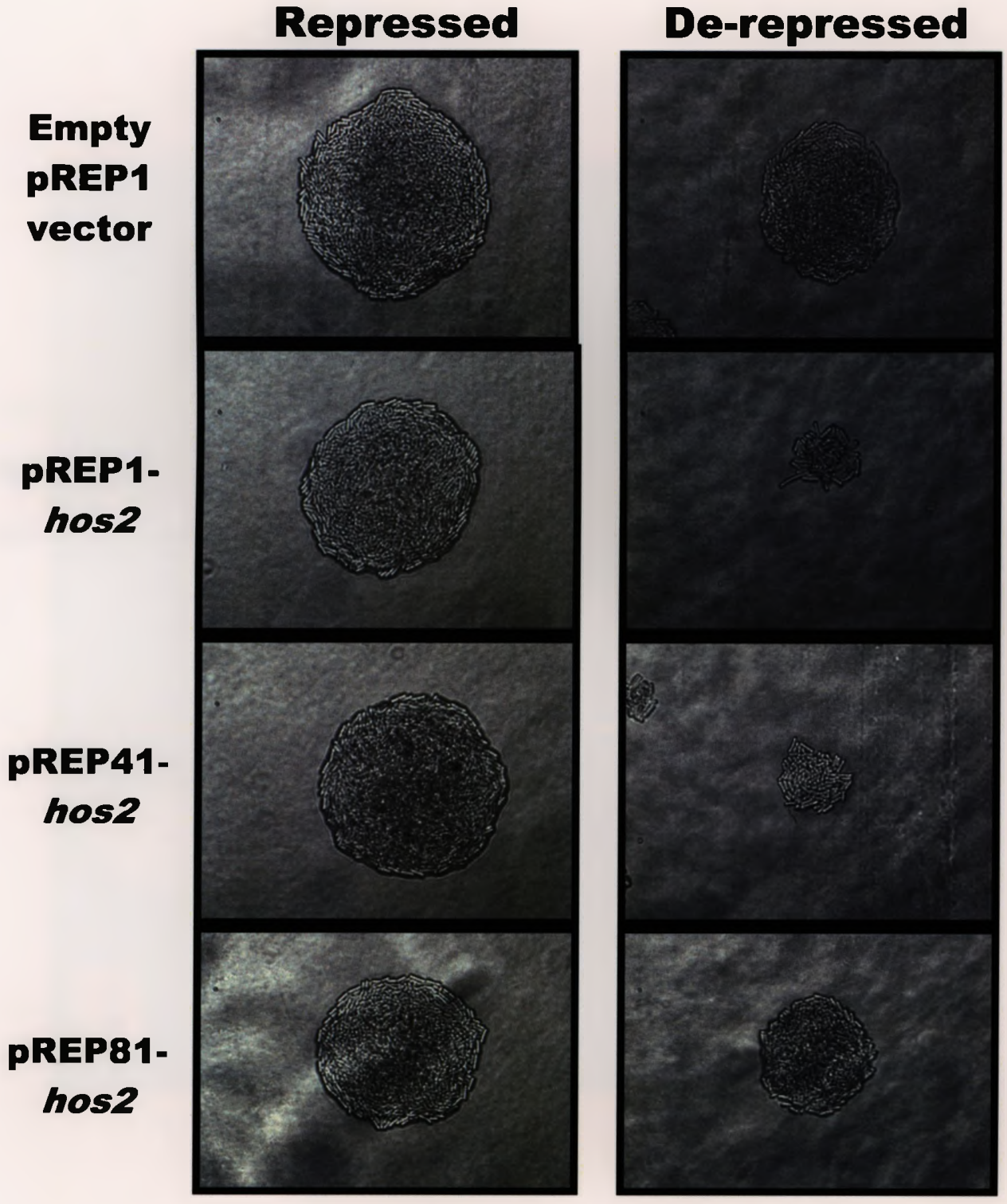
Repressed
De-repressed
Empty pREP1 vector
pREP1-hos2
pREP41-hos2
pREP81-hos2

Figure 3.13 Hos2p over-expression produced a pleiotropic set of phenotypes in a dosage-dependent manner. **(A)** Hypha displaying all of the associated phenotypes. **(B)** Three abnormally spherical cells with abnormal deposits of cell wall material. **(C)** One abnormally long cell and one abnormally spherical cell.

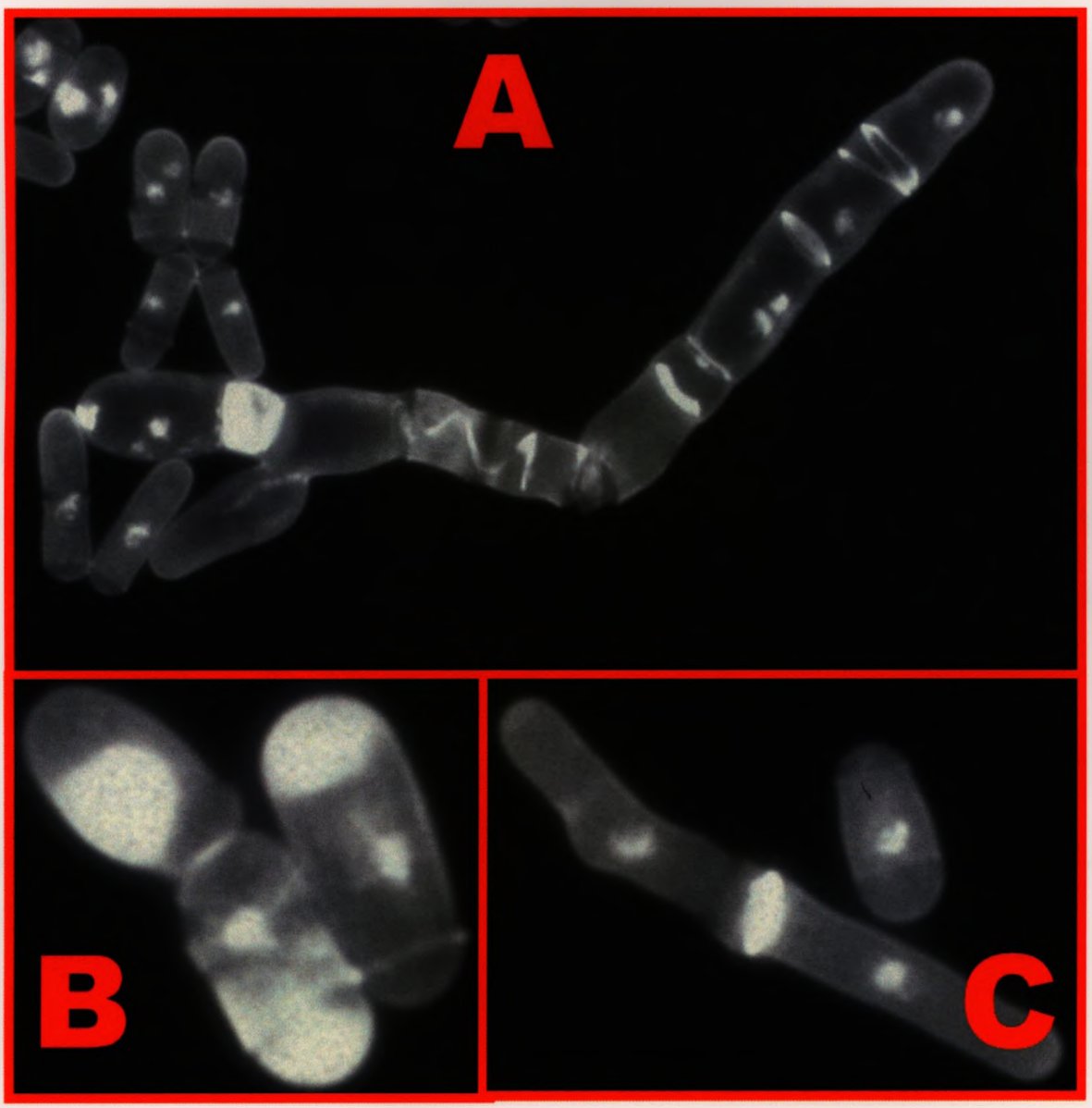
A
B
C

Figure 3.14 Frequency distribution of cell length for pREP1-*hos2* strain relative to the empty pREP1 vector control strain under de-repressive conditions. pREP1-*hos2* cells are longer overall than the control strain; a small subset of cells are highly elongated hyphae with variable length. A total of 500 cells for each strain were measured.

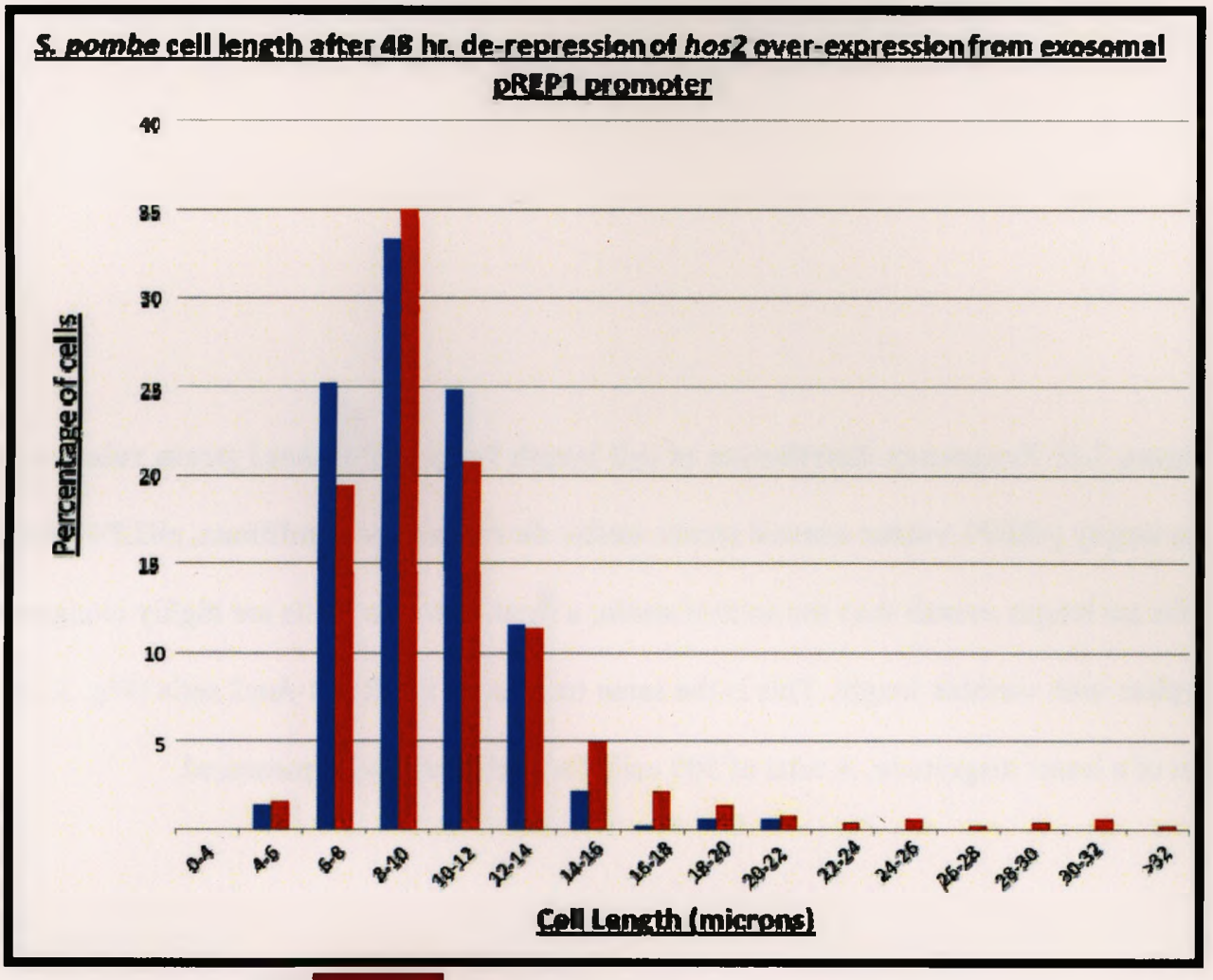
S. pombe cell length after 48 hr. de-repression of hos2 over-expression from exosomal pREP1 promoter
Percentage of cells
40
35
30
25
20
15
10
5
0-4
4-6
6-8
8-10
10-12
12-14
14-16
16-18
18-20
20-22
22-24
24-26
26-28
28-30
30-32
>32
Cell Length (microns)
pREP1-hos2
empty pREP1 vector control

Figure 3.15 Frequency distribution of cell length for pREP41-*hos2* strain relative to the empty pREP1 vector control strain under de-repressive conditions. pREP41-*hos2* cells are longer overall than the control strain; a small subset of cells are highly elongated hyphae with variable length. This is the same trend seen in pREP1-*hos2* cells (Fig. 3.14), but of a lesser magnitude. A total of 500 cells for each strain were measured.

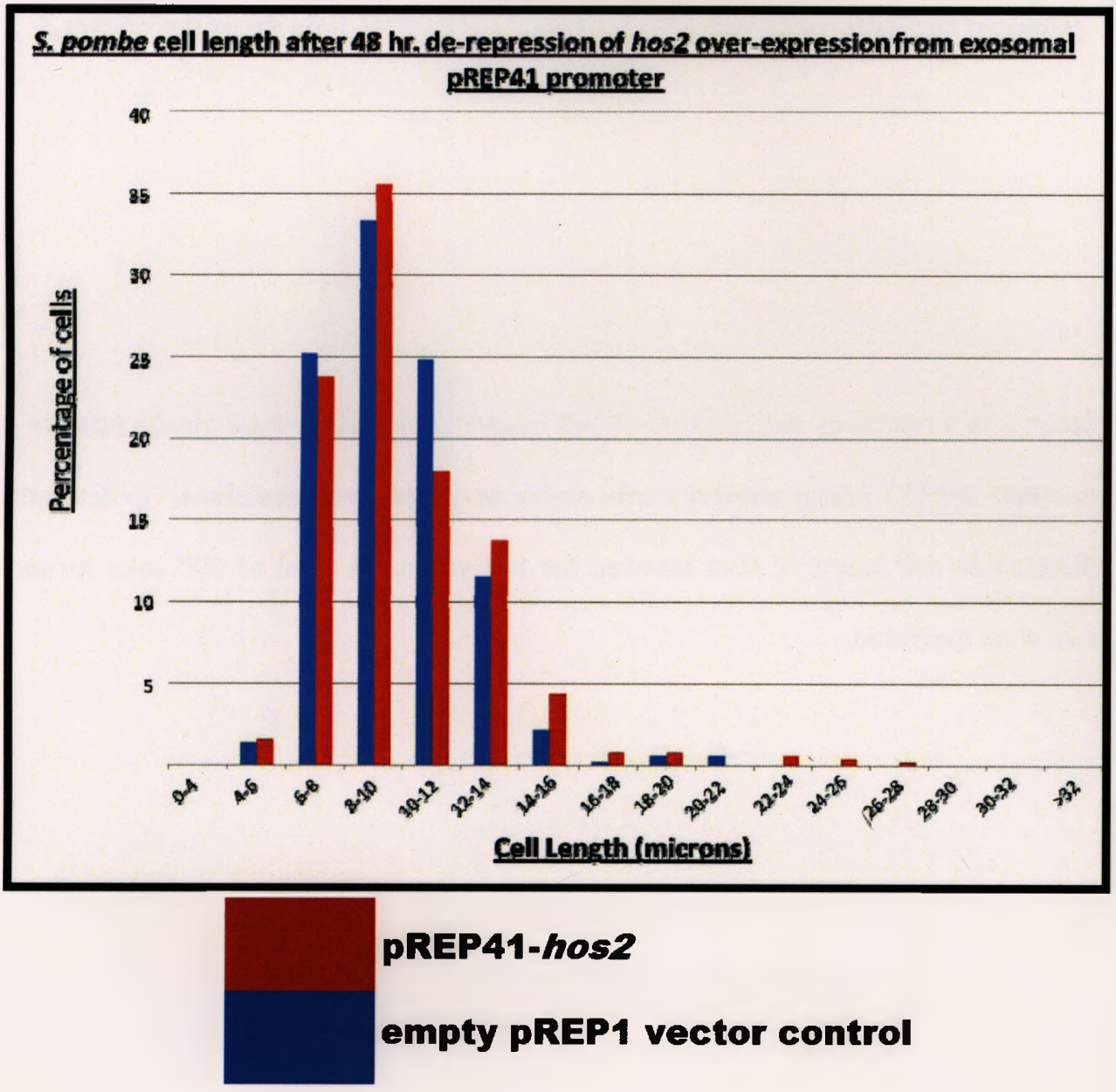
S. pombe cell length after 48 hr. de-repression of hos2 over-expression from exosomal pREP41 promoter
Percentage of cells
40
35
30
25
20
15
10
5
0-4
4-6
6-8
8-10
10-12
12-14
14-16
16-18
18-20
20-22
22-24
24-26
26-28
28-30
30-32
>32
Cell Length (microns)
pREP41-hos2
empty pREP1 vector control

Figure 3.16 Frequency distribution of cell length for pREP81-*hos2* strain relative to the empty pREP1 vector control strain under de-repressive conditions. No detectable difference in cell length is seen between the two strains. A total of 500 cells for each strain were measured.

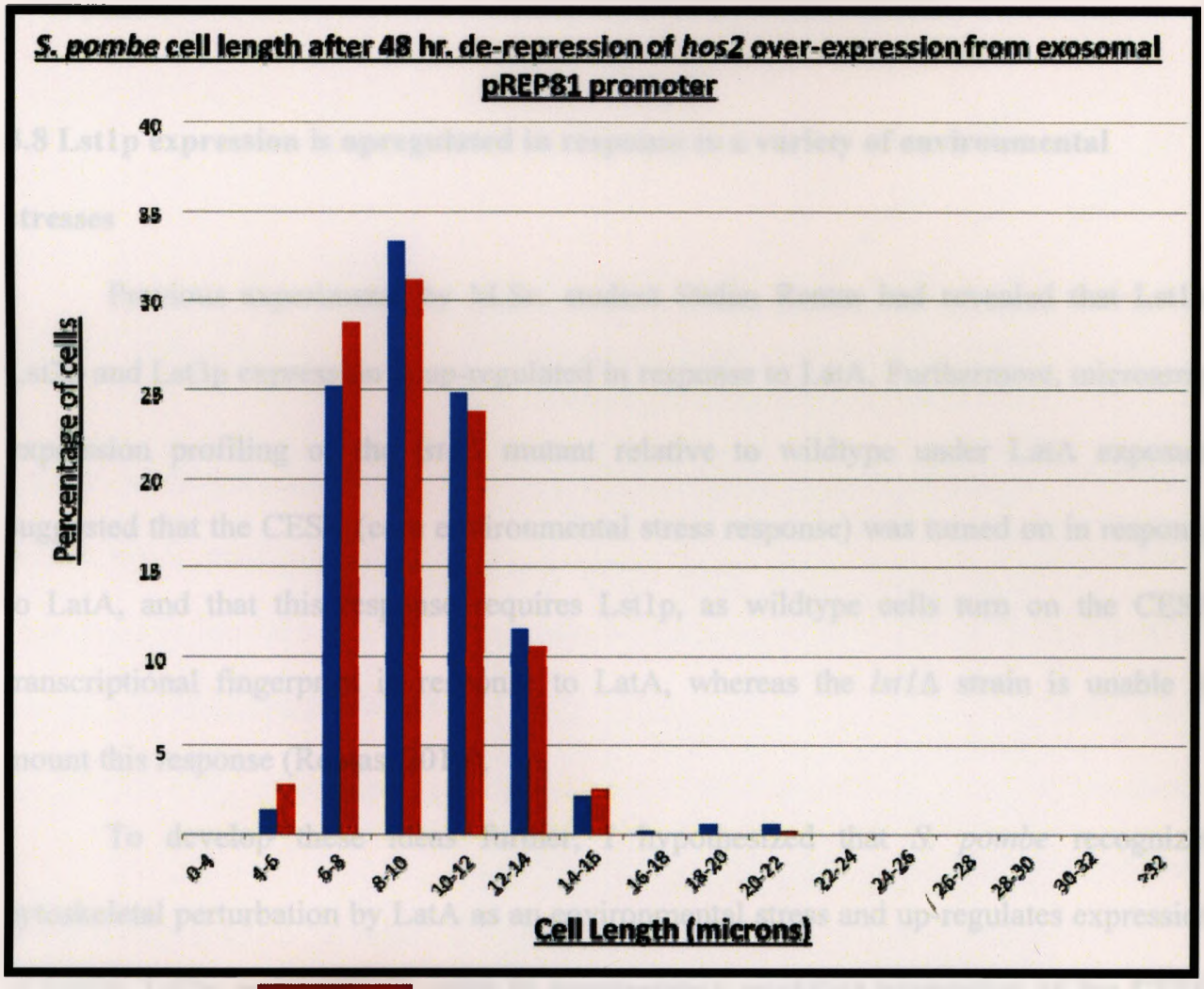
S. pombe cell length after 48 hr. de-repression of hos2 over-expression from exosomal pREP81 promoter
Percentage of cells
40
35
30
25
20
15
10
5
0-4
4-6
6-8
8-10
10-12
12-14
14-16
16-18
18-20
20-22
22-24
24-26
26-28
28-30
30-32
>32
Cell Length (microns)
pREP81-hos2
empty pREP1 vector control

than pREP41-*hos2*, thus suggesting that phenotypes contributing to the formation of hyphae are dose dependent (Fig. 3.14, Fig. 3.15, Fig. 3.16).

3.8 Lst1p expression is upregulated in response to a variety of environmental stresses

Previous experiments by M.Sc. student Stefan Rentas had revealed that Lst1p, Lst2p and Lst3p expression is up-regulated in response to LatA. Furthermore, microarray expression profiling of the *lst1*Δ mutant relative to wildtype under LatA exposure suggested that the CESR (core environmental stress response) was turned on in response to LatA, and that this response requires Lst1p, as wildtype cells turn on the CESR transcriptional fingerprint in response to LatA, whereas the *lst1*Δ strain is unable to mount this response (Rentas, 2010).

To develop these ideas further, I hypothesized that *S. pombe* recognizes cytoskeletal perturbation by LatA as an environmental stress and up-regulates expression of Lst1p, Lst2p and Lst3p in order to appropriately modulate expression of the CESR genes. To test this hypothesis, I did three hour time-course experiments with various environmental stresses to see if Lst1p levels increase in response to a sub-set of the stresses. For each stress, a strain expressing the Lst1-HA fusion protein was allowed to grow to early log phase (OD_{600} = 0.04) in 600 ml of YES; subsequently, 300 ml was subjected to a particular environmental stress while 300 ml was used as a control. A whole-cell protein extract was prepared using 100 ml of each treatment at 10 min., 1 hr.,

Figure 3.17 Lst1p expression was up-regulated under conditions of cellular stress. A strain expressing the HA-epitope tag was grown to early log phase (OD_{600}~ 0.04) in YES. Subsequently, the cells were subjected to the indicated stress conditions; aliquots were taken from the cultures at the indicated time-points and a whole-cell extract was performed. The extracts were then run out using denaturing SDS-PAGE gel electrophoresis. α-Tubulin was used as a loading control.

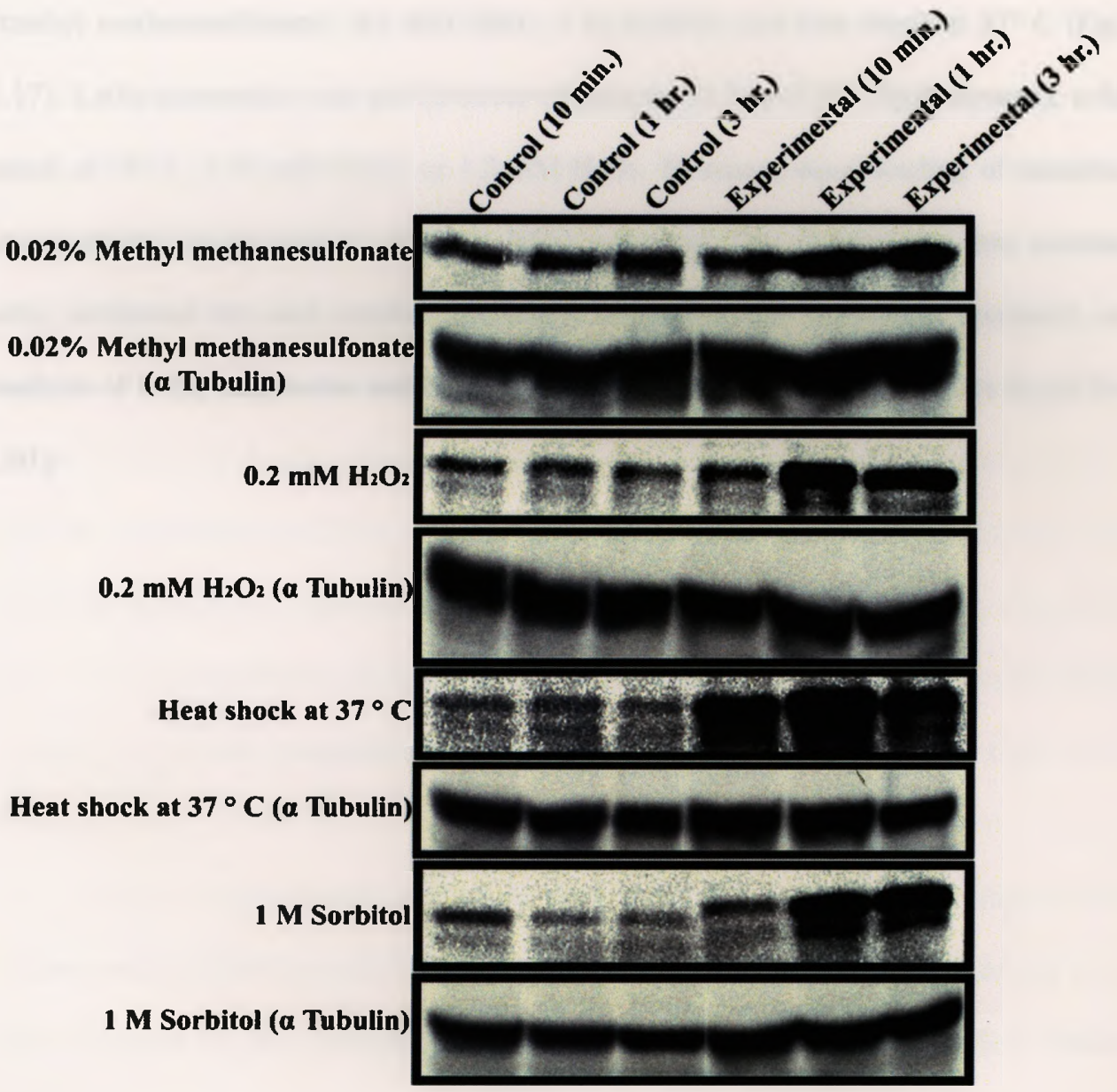
Control (10 min.)
Control (1 hr.)
Control (3 hr.)
Experimental (10 min.)
Experimental (1 hr.)
Experimental (3 hr.)
0.02% Methyl methanesulfonate
0.02% Methyl methanesulfonate (α Tubulin)
0.2 mM H2O2
0.2 mM H2O2 (α Tubulin)
Heat shock at 37 ° C
Heat shock at 37 ° C (α Tubulin)
1 M Sorbitol
1 M Sorbitol (α Tubulin)

and 3 hr. after starting the experiment; 50 μg of protein was subsequently analyzed by SDS-PAGE and Western Blotting to quantify levels of Lst1HA. Strikingly, among the stresses used, Lst1p expression increased several-fold in response to 0.02% MMS (methyl methanesulfonate), 0.2 mM H_2O_2, 1 M Sorbitol, and heat shock at 37° C (Fig. 3.17). Lst1p expression was not however responsive to 5 mM HU (hydroxyurea), cold shock at 18° C, 0.75 mM H_2O_2, or 1.5 mM H_2O_2. To ensure equal loading of samples, anti-α-tubulin monoclonal 1° antibody B512 was used. Two independent time courses were performed for each stressor eliciting a response. Time constraints precluded an analysis of Lst2p expression and Lst3p expression in response to the stressors tested for Lst1p.

CHAPTER 4: DISCUSSION

A complete map of the core, evolutionarily conserved genetic and molecular pathways underlying cytokinesis is essential in the landscape of basic eukaryotic biology. Aspects of this knowledge that are tied to cytokinesis failure (i.e. checkpoint mechanisms) are particularly important for cancer research as cytokinesis failure has been established as an initiating event for tumorigenesis (Fujiwara *et al.* 2005). Despite the importance of understanding cytokinesis, major questions remain to be answered. Recently, a cytokinesis checkpoint was discovered in *S. pombe*. This checkpoint is activated at the G2/M boundary of daughter nuclei as long as an actomyosin ring is present in a mother cell. By maintaining a G2/M boundary arrest, this checkpoint therefore enforces the following dependency relationship: cytokinesis in a mother cell must be completed before the G2/M transition can occur in the daughter nuclei. This checkpoint is also able to sense and corrects perturbations of the ring, thereby stabilizing the ring (Liu *et al.* 2000).

A genome-wide screen of LatA (a drug which can de-stabilize the ring) on the commercially available set of viable *S. pombe* gene deletion mutants, identified *lst1* as a novel regulator of this checkpoint. Follow up experiments by M.Sc. student Stefan Rentas established that Lst1p, Lst2p, and Lst3p form an *in vivo*, nuclear-localized multi-protein complex necessary for normal checkpoint function, and each member is necessary for checkpoint function. More significantly, this complex is orthologous to the mammalian histone de-acetylase complex HDAC3-NCOR2/SMRT (containing the histone de-acetylase, HDAC3) and budding yeast histone de-acetylase complex SET3C

(containing the histone de-acetylase, Hos2) (Rentas, 2010) (Fig. 4.1). There also appears to be functional conservation pertaining to cytokinesis, as HDAC3-NCOR2/SMRT prevents cytokinetic failure in HeLa cells (Kittler *et al.* 2007). Despite all of this, the Lst complex is not fully characterized as an *S. pombe* histone de-acetylase (Hos2p) orthologous to mammalian HDAC3 and *S. cerevisiae* Hos2 exists, but remains uncharacterized in the context of cytokinesis and the Lst complex (Rentas, 2010) (Fig. 3.1, Fig. 3.2). This project aimed to characterize Hos2p within this context, and also, upon accomplishing this, extend knowledge of the Lst complex and Hos2p in order to develop a more complete understanding of this important complex and Hos2p itself.

Before attempting to explain the biological relevance of the data accumulated in this project, it is necessary to review the biochemistry of the previously characterized Lst complex members in order to make a convincing argument for the model derived from this project. Since structural domains confer unique properties to proteins, it is necessary to survey the domains contained within the Lst complex members. Taken as an aggregate, these domains will help develop a biochemical model that can explain how this complex activates the cytokinesis checkpoint. As previously discussed, the Lst complex is orthologous to the mammalian HDAC3/NCOR2-SMRT complex, also consisting of four proteins: HDAC3 (Hos2p orthologue), MLL5 (Lst1p orthologue), NCOR2 (Lst2p orthologue) and TBL1X (Lst3p orthologue) (Rentas, 2010). Bioinformatics analyses by Stefan revealed characteristic domains within the Lst complex members, which are found in the corresponding human orthologues as well. Lst1p contains a PHD domain and a SET domain; the PHD domain is a highly specialized methyl-lysine binding domain found in a number of proteins regulating gene transcription, and the SET domain is a

Figure 4.1 Generalized schematic for an evolutionarily conserved HDAC3 complex. The budding yeast SET3 complex consists of one SET3 subunit, two SNT1 subunits, two SIF2 subunits, and HOS2 histone de-acetylase, recruiting HOS2 to de-acetylate specific substrates. An orthologous complex exists in metazoans (HDAC3/NCOR2-SMRTcomplex) and fission yeast (Lst complex), each of which consist of four different proteins orthologous to the four budding yeast SET3C proteins. Image modified from Kittler *et al.* 2007

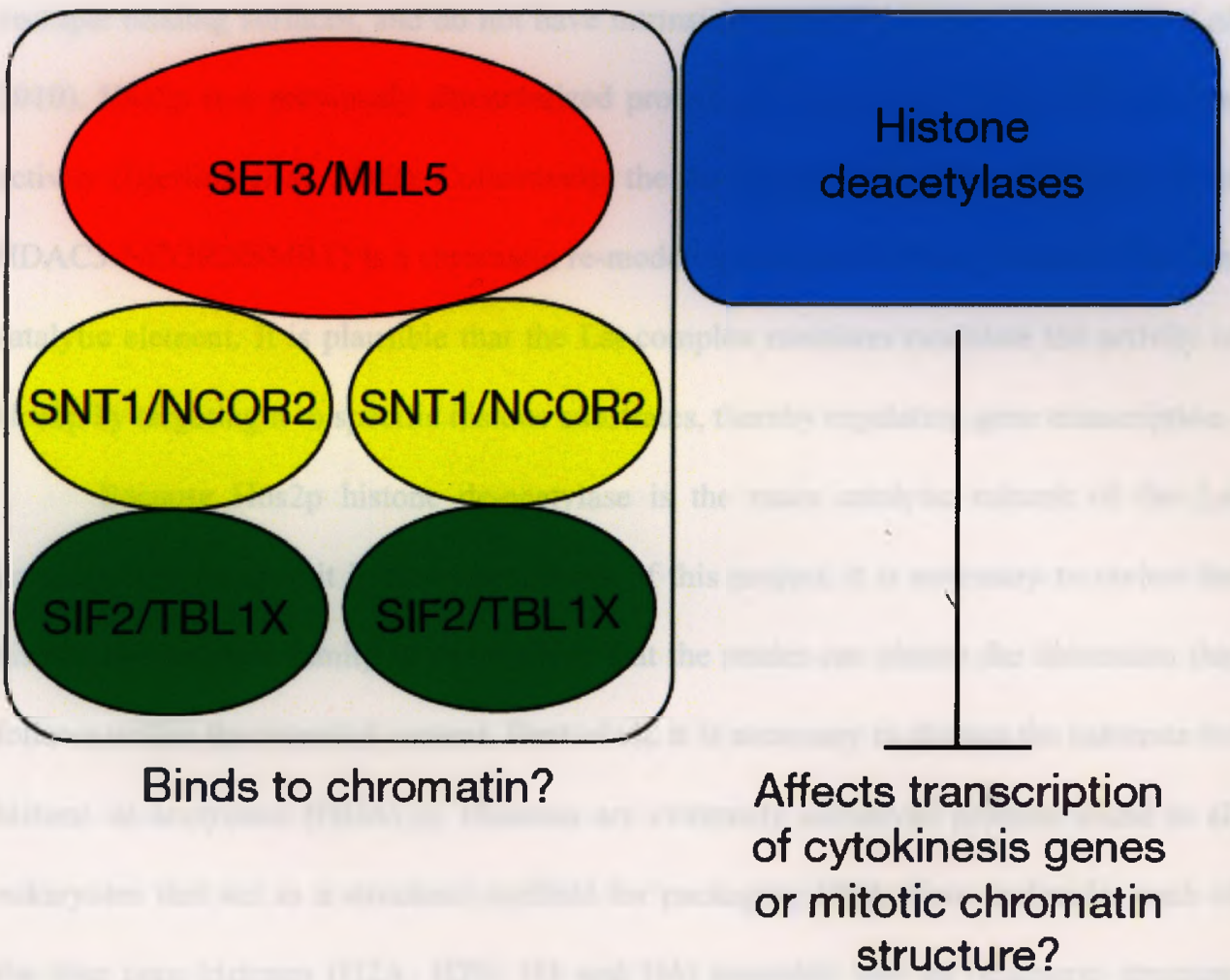
SET3/MLL5
SNT1/NCOR2
SNT1/NCOR2
SIF2/TBL1X
SIF2/TBL1X
Histone deacetylases
Binds to chromatin?
Affects transcription of cytokinesis genes or mitotic chromatin structure?

characteristic domain for histone lysine methyltransferases (Mellor, 2006; Yeates, 2002). Lst2p contains a SANT domain; NCOR2 and SMRT (a NCOR2 paralog) both have a pair of SANT domains, one of which is necessary to activate the de-acetylase activity of HDAC3, and one of which functions asa histone-tail-interaction domain (Boyer *et al.* 2004). Lst3p contains a LisH domain and a WD40 repeat domain; WD40 domains are highly versatile general scaffolds for the formation of protein complexes due to their multiple binding surfaces, and do not have intrinsic enzymatic activity (Stirnimann *et al.* 2010). Hos2p is a previously characterized protein known to have histone de-acetylase activity (Bjerling *et al.* 2002). Collectively, the data suggests that the Lst complex (like HDAC3-NCOR2/SMRT) is a chromatin re-modeling complex in which Hos2p is the core catalytic element. It is plausible that the Lst complex members modulate the activity of Hos2p by targeting it to specific histone substrates, thereby regulating gene transcription.

Because Hos2p histone de-acetylase is the main catalytic subunit of the Lst complex, and because it is the central focus of this project, it is necessary to review the histone de-acetylase family of enzymes so that the reader can absorb the discussion that follows within the intended context. First of all, it is necessary to discuss the substrate for histone de-acetylases (HDACs). Histones are extremely conserved proteins found in all eukaryotes that act as a structural scaffold for packaging DNA. Two molecules each of the four core histones (H2A, H2B, H3 and H4) assemble into an octameric structure called the nucleosome and DNA is wrapped around nucleosomes, repressing transcription *in vivo* and *in vitro* by reducing its accessibility to the transcriptional machinery. This particular chromatin structure is flexible however, because of the potential for histones to be chemically modified, thereby altering their affinity to DNA. The N termini of histones

extend from the nucleosomal core and undergo a variety of chemical modifications throughout the cell cycle, including acetylation and de-acetylation (Grunstein, 1997).

In the traditional model, lysine residues of histone N-termini can have an acetyl group covalently attached to them by a class of enzymes found in all eukaryotes, referred to as histone acetylases. This neutralizes the positive charge on the lysine residue, thereby reducing the overall affinity of the nucleosome for the negatively charged phosphate backbone of the DNA. By opening the conformation of DNA, histone acetylases act as transcriptional activators by increasing the accessibility of DNA to the transcriptional machinery. Conversely, HDACs, which are also found in all eukaryotes, reverse the chemical modification and resulting chromatin architecture produced by histone acetylases, thereby behaving as transcriptional repressors (Grunstein, 1997) (Fig. 4.2).

It should be noted that substrate specificity of HDACs is not restricted to histones. A wide variety of proteins are acetylated, such as transcription factors, nuclear import factors, and α-tubulin, which means that acetylation regulates many diverse functions, including DNA recognition, protein-protein interaction and protein stability. HDACs are a diverse group of proteins, and mammalian HDACs fall into several sub-classes. HDAC3 (the human orthologue of Hos2p) falls into class I, and is most similar to two other class I HDACs, HDAC1 and HDAC2. Class I HDACs possess a highly conserved catalytic domain. Intriguingly, HDAC1 and HDAC2 are more similar to one another than either is to HDAC3, and HDAC3 exists in multisubunit complexes separate and different from other known HDAC complexes, suggesting that HDAC3 has unique functions (Kouzarides, 2000; Kouzarides, 1999; Yang *et al.* 2002).

Before a full characterization of Hos2p in the context of the Lst complex becomes

Figure 4.2 Summary of histone acetylation and de-acetylation. (A) Biochemical mode-of-action of histone de-acetylases (HDACs) and histone acetylases (HATs). The equilibrium of steady-state histone acetylation is maintained by the opposing activities of histone acetyltransferases and deacetylases. Acetyl coenzyme A is the high energy acetyl moiety donor for histone acetylation. Histone acetyltransferases (HATs) transfer the acetyl moiety to the ε-$NH3^+$ group of internal lysine residues of histone N-terminal domains. Reversal of this reaction is catalyzed by histone deacetylases (HDACs). **(B) Biological consequences of histone acetylation and de-acetylation.** Neutralization of the positive charge on histone-tail lysines through acetylation reduces the affinity between nucleosomes and the negatively charged phostphate backbone of DNA, opening up the chromatin architecture for increased access to the transcriptional machinery. De-acetylation of these lysine residues reverses this effect. Figure 4.2 (A) is from Kuo and Allis, 1998. Figure 4.2 (B) is from Pons *et al.* 2009.

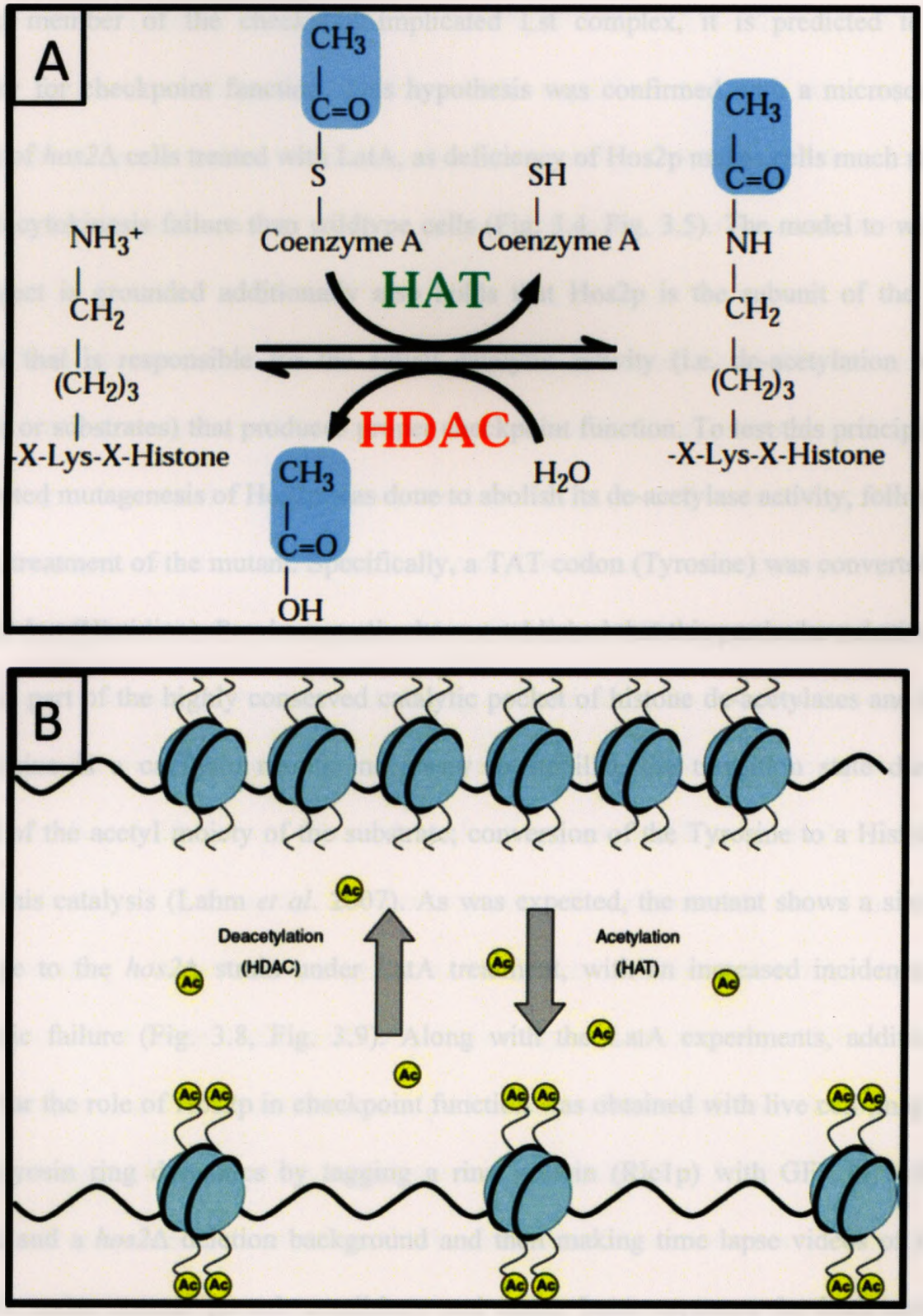
A
CH3
C=O
S
Coenzyme A
SH
Coenzyme A
CH3
C=O
NH3+
CH2
(CH2)3
-X-Lys-X-Histone
HAT
HDAC
NH
CH2
(CH2)3
-X-Lys-X-Histone
CH3
C=O
OH
H2O
B
Deacetylation
(HDAC)
Acetylation
(HAT)
Ac

justified, it is necessary to show that Hos2p is needed to mount a proper checkpoint response under activating conditions (i.e. a low dose of LatA). If Hos2p is indeed an essential member of the checkpoint-implicated Lst complex, it is predicted to be necessary for checkpoint function. This hypothesis was confirmed with a microscopic analysis of *hos2*Δ cells treated with LatA, as deficiency of Hos2p makes cells much more prone to cytokinesis failure than wildtype cells (Fig. 3.4, Fig. 3.5). The model to which this project is grounded additionally also holds that Hos2p is the subunit of the Lst complex that is responsible for the actual catalytic activity (i.e. de-acetylation of a substrate or substrates) that produces proper checkpoint function. To test this principle, a site-directed mutagenesis of Hos2p was done to abolish its de-acetylase activity, followed by LatA treatment of the mutant. Specifically, a TAT codon (Tyrosine) was converted to a CAT codon (Histidine). Previous studies have established that this particular substituted residue is part of the highly conserved catalytic pocket of histone de-acetylases and that the Tyrosine is a catalytic residue necessary to stabilize the transition state during removal of the acetyl moiety of the substrate; conversion of the Tyrosine to a Histidine impairs this catalysis (Lahm *et al.* 2007). As was expected, the mutant shows a similar phenotype to the *hos2*Δ strain under LatA treatment, with an increased incidence of cytokinetic failure (Fig. 3.8, Fig. 3.9). Along with the LatA experiments, additional support for the role of Hos2p in checkpoint function was obtained with live cell imaging of actomyosin ring dynamics by tagging a ring protein (Rlc1p) with GFP in both a wildtype and a *hos2*Δ deletion background and then making time lapse videos of ring dynamics under normal growth conditions and under LatA exposure for both strains (Supplementary Disc, vid. 3.1, vid. 3.2, vid. 3.3, vid. 3.4). The ring dynamics are

consistent with the previously established model for checkpoint activation and cytokinesis failure. Intriguingly, under normal growth conditions, the *hos2*Δ deletion strain executes cytokinesis successfully, but the ring constricts slower than it does in the wild-type under identical growth conditions. The significance of this observation is unknown at the present time. Taken together, these results show that the de-acetylase activity of Hos2p is needed to mount a proper checkpoint response under activating conditions.

In order to set the foundation for more specialized experiments, Hos2p needs to be established as a member of the Lst complex *in vivo*. This was accomplished by live cell imaging to uncover the localization pattern of Hos2p, as well as providing evidence for an *in vivo* interaction with the Lst complex through co-immunoprecipitation experiments. Firstly, Hos2p was tagged with a C-terminal GFP tag and observed under normal growth conditions. As expected, Hos2p co-localized with the other Lst complex members (which are all exclusively nuclear) to the nucleus; additionally, Hos2p was also cytoplasmic; the significance of this dual localization pattern will be touched on later in the discussion (Fig. 3.6). Secondly, co-immunoprecipitation experiments were done using strains possessing a C-terminal epitope tag on Hos2p, and a different C-terminal epitope tag on one of either Lst1p, Lst2p, and Lst3p. Two reciprocal co-immunoprecipitations for each of the three pairwise interactions were performed, each of which indicated a positive interaction between Hos2p and the other Lst complex member (Fig. 3.10). Taken together with Stefan's co-immunoprecipitations, this is powerful evidence for an *in vivo* complex, as all of the six pairwise interactions that are possible between the four proteins have been confirmed to occur.

The data discussed thus far has established the *S. pombe* Lst complex as a histone de-acetylase complex orthologous to the mammalian HDAC3/NCOR2-SMRT histone de-acetylase complex, and both complexes consist of four different proteins, each of which has an orthologue in the corresponding complex present in the other species. Furthermore the Lst complex is necessary for cytokinesis checkpoint function, and a role in cytokinesis appears to be conserved to the mammalian HDAC3/NCOR2-SMRT complex as well, since HDAC3/NCOR2-SMRT members prevent cytokinesis failure. These are now foundational principles of Hos2p and the Lst complex established through empirical evidence rather than untested hypotheses, so more specialized experiments can now be designed to test hypotheses impinging on this knowledge to reveal unknown properties of the Lst complex centered on its core player, Hos2p.

The Lst complex de-acetylates a substrate or substrates to mount the proper checkpoint response under activating conditions, however, the substrates are presently unknown and may either be histones or non-histone nuclear proteins. In either case, the complex may act through regulation of gene activity, a hypothesis that was previously formed and tested by Stefan through microarray profiling experiments. In his studies, Stefan found that Lst1p, Lst2p, and Lst3p expression levels are each up-regulated 2-3 fold during LatA treatment, and he also found that *S. pombe* cells respond to LatA with an Lst1p-dependent transcriptional response that conforms to the transcriptional fingerprint diagnostic of the stereotypical *S. pombe* response to environmental stresses, the *S. pombe* CESR (core environmental stress response). Surprisingly however, cytokinesis genes were not significantly altered in the transcriptional profile (Rentas, 2010). The expression profiling data suggests that LatA is recognized by the cell as an

environmental stressor. Taking all of these observations as an aggregate, I hypothesized that the Lst complex is a stress-responsive gene regulator complex that is necessary to mount the CESR transcriptional response to deal with environmental stress, and increases its ability to do so in the presence of environmental stress by upregulating the expression of its own subunits. If this hypothesis is true, then expression levels of the Lst complex subunits should be up-regulated in the presence of environmental stressors that turn on the CESR transcriptional fingerprint. To test this hypothesis, I used a strain bearing a C-terminal HA epitope tag on Lst1p (*lst1HA)* to quantify Lst1p expression levels under various environmental stresses at set time-points post-exposure to the stressor. Strikingly, Lst1p expression increases upon exposure to a subset of the stressors, and all the stressors eliciting a response (methyl methanesulfonate, heat shock, sorbitol, H_2O_2) have previously been shown to turn on the CESR transcriptional fingerprint (Fig. 3. 17) (Chen *et al.* 2003). Due to time constraints, analogous experiments were not done to quantify Lst2p and Lst3p levels under the same stressors. These experiments validate my hypothesis that the Lst complex is a stress-responsive gene-regulatory complex.

The reader of this discussion will likely ask why the possible existence of expressional control over Hos2p in response to environmental stress was ignored in testing for Lst complex involvement in stress-response, as Hos2p is as much a member of the Lst complex as Lst1p, Lst2p and Lst3p. The reason is that when an analogous attempt was made to quantify Hos2p expression in response to LatA treatment, no change was observed in expression levels (unpublished data). However, another experiment was done, which may shed light in the future on how Hos2p activity is regulated in response to Lst complex activation by environmental stress. Previously, it was mentioned that Hos2p not

only shows the expected nuclear localization, but is also cytoplasmic (Fig. 3.6). There are two obvious hypotheses for this observation, which are not mutually exclusive. The first hypothesis is that Hos2p mediates checkpoint activity as a member of the Lst complex in the nucleus, and shuttling of Hos2p in and out of the nucleus regulates its activity as a member of this complex. The second hypothesis is that Hos2p has cytoplasmic roles that fall outside of the context of the Lst complex. To test the first hypothesis, a time-course live-cell imaging experiment was done using the *hos2GFP* strain under LatA treatment and it was found that Hos2p localizes to the nucleus under checkpoint-activating conditions (Fig. 3.7). This observation, taken together with the stress-response experiments, led me to hypothesize that Hos2p activity in the Lst complex is stress-responsive and regulated by nucleo-cytoplasmic shuttling according to cellular demands. To test this hypothesis, I would perform analogous experiments with *hos2GFP* under environmental stress conditions, although time constraints precluded this important experimental analysis. It is important to note that the Hos2p orthologue, HDAC3, is unique among the class I HDACs in that it is the only one with both nuclear and cytoplasmic localization, owing to both a nuclear import and nuclear export signal in the amino acid sequence. This represents another level at which the Hos2p/HDAC3 histone de-acetylase is conserved across species, and it is exciting to ponder whether HDAC3/NCOR2-SMRT is a stress-responsive complex, and whether HDAC3 localization is also responsive to environmental stress, as the localization pattern is a unique property of HDAC3 (Yang *et al.* 2002).The results convincingly argue for a model whereby the chromatin-modifying activity of the Lst complex is intensified by producing more of the Lst complex in response to environmental stress in order to elicit

the appropriate transcriptional response to deal with the stressor. Furthermore, it should be noted that the SET3 complex of *S. cerevisiae* has been shown to have a role in the *S. cerevisiae* secretory stress response by modifying gene expression, so this function appears to be conserved across eukaryotes (Cohen *et al.* 2008).

The data on Lst1p stress-responsiveness and Hos2p checkpoint-dependent re-localization suggest a possible evolutionarily conserved cross-talk between the environmental stress response and transcriptional regulation by the Hos2p/HDAC3 histone de-acetylase in eukaryotes, because not only is the Lst complex and its role in faithful cytokinesis present in an orthologous form in mammalian systems, but so are the components and mechanisms underlying environmental stress response. The CESR of *S. pombe* is a diagnostic fingerprint of a generalized transcriptional response to various environmental stressors. The CESR is controlled in large part by the Sty1 mitogen-activated protein kinase (MAPK) signaling cascade. Briefly, a variety of environmental stressors are sensed by the cell and relayed to the Sty1 MAPK signaling cascade, which transcriptionally activates a set of co-regulated genes with stress-protective functions. The p38/JNK MAPK signaling cascade in mammals is highly orthologous to the *S. pombe* Sty1 system, and also activates stress-protective genes under various environmental stress conditions

(Chen *et al.* 2003; Toone and Jones 1998).This underscores the possibility that functions of the Lst complex are conserved in eukaryotes beyond the realm of cytokinesis as well.

Although the stress responsiveness of Lst1p gives fresh insight into the functions of the complex, the substrates of Hos2p with respect to checkpoint function and stress response are still unknown. Nor is it clear why LatA induces a transcriptional stress

response but does not alter the expression of cytokinesis genes. In light of these new findings, I suggest several possibilities regarding the substrates for checkpoint activation. The first three possibilities do not argue for or against a relationship between stress response and checkpoint activation. The first possibility is that the Lst complex directly de-acetylates and regulates the activity of nuclear proteins of the cytokinetic machinery (i.e. actin or myosin) rather than regulating their expression levels. The second possibility is that the Lst complex actually does alter expression levels of cytokinesis proteins, but does so at the post-transcriptional level (i.e. by making proteins more stable). The third possibility is that the Lst complex de-acetylates proteins not directly involved in cytokinesis, which when de-acetylated, themselves modify cytokinesis proteins. The fourth and fifth possibilities are very attractive, since they incorporate the observation that checkpoint activation and stress response occur simultaneously during LatA treatment, and suggest a plausible relationship between the two observations. The fourth possibility is that the Lst complex does not directly affect any cytokinesis proteins, but acts in an indirect manner. In the fourth possibility, the complex turns on the CESR as a primary response, and an element or elements of the CESR itself activate(s) the checkpoint as a secondary response. The fifth possibility is that cytokinesis genes and CESR genes are overlapping (i.e. genes are involved in both processes) and fall under the same transcriptional module of the Lst complex, and that the relevant CESR genes were not also identified as cytokinesis genes because they were not annotated as having a role in cytokinesis yet. The sixth and seventh possibilities state there no relationship between stress response and checkpoint function. The sixth possibility is similar to the fifth possibility in that it states that the Lst complex controls a transcriptional module that

modulates expression of both CESR and checkpoint genes, but differs in that it holds that cytokinesis genes and CESR genes are independent and non-overlapping in their functions, despite falling under the same module. The seventh possibility states that checkpoint activity is conferred by a mechanism that doesn't involve gene regulation and is independent from the CESR response. An analysis of these possibilities shows that none of the possibilities are mutually exclusive. This is obviously a complicated problem, and answers to these questions will be important in understanding the Lst complex in the future. A summary of the possible Lst-complex-mediated relationships between cytokinesis checkpoint activation and the CESR transcriptional response is given in Fig. 4.3.

The data that has been discussed so far fits neatly under a unified theme: Hos2p regulates checkpoint function and stress-response as a member of the Lst complex. However, several experiments done in this project generated data that falls outside of this umbrella, and for this reason, they are being discussed last. Specifically, no one to date has studied the effects of Hos2p overexpression, which is an obvious experiment in the complete characterization of Hos2p in *S. pombe*. I wanted to investigate the effects of Hos2p overexpression and determine whether the effects (if present) are dose-dependent. I accomplished this with the pREP series of thiamine-repressible exosomal expression vectors to overexpress Hos2p at a low, moderate and high level of overexpression in three different strains; the plasmids were maintained in the cells with

Figure 4.3 A summary of possible relationships mediated by the Lst complex between cytokinesis checkpoint activation and the CESR transcriptional response. **(A)** Individual elements involved cytokinesis checkpoint activation and the CESR transcriptional response do not have functions that overlap in both processes. **(B)** All individual elements or a sub-set of individual elements in cytokinesis checkpoint activation and the CESR transcriptional response have functions that overlap in both processes. **(C)** The CESR transcriptional response is turned on by the Lst complex as a primary response, and cytokinesis checkpoint activation is a secondary response downstream of an activated CESR transcriptional response; cytokinesis checkpoint activation elements are therefore a sub-set of CESR transcriptional response elements and the Lst complex is not directly responsible for cytokinesis checkpoint activation.

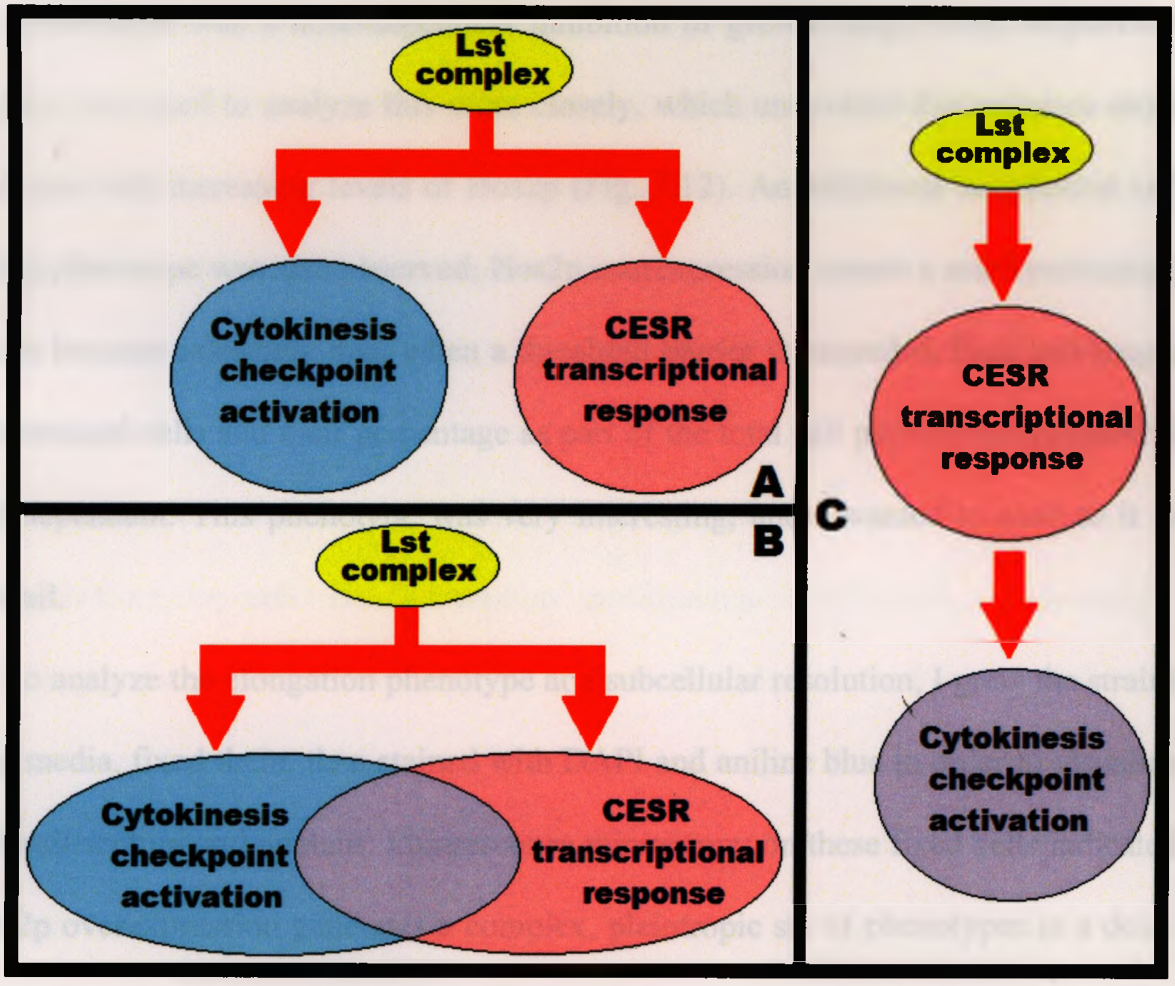
Lst complex
Cytokinesis checkpoint activation
CESR transcriptional response
A
B
Lst complex
Cytokinesis checkpoint activation
CESR transcriptional response
C
Lst complex
CESR transcriptional response
Cytokinesis checkpoint activation

selective media, and the strains were grown and maintained under repression, except during experimental analyses.

Firstly, I sought to determine whether Hos2p overexpression has any effect on growth by streaking the overexpressor strains on media plates in a gradient moving from high to low cell density; these were then allowed to grow. After allowing for growth, an obvious phenotype was a dose-dependent inhibition of growth (Fig. 3.11); bright-field microscopy was used to analyze this more closely, which uncovered that colonies show reduced size with increasing levels of Hos2p (Fig. 3.12). An additional unexpected and surprising phenotype was also observed; Hos2p overexpression causes a small percentage of cells to become extremely long when a threshold barrier is exceeded. Both cell length of these unusual cells and their percentage as part of the total cell population appeared to be dose-dependent. This phenotype was very interesting, and I wanted to analyze it in more detail.

To analyze the elongation phenotype at a subcellular resolution, I grew the strains in liquid media, fixed them, then stained with DAPI and aniline blue in order to visualize the cell wall/septum and nucleus. Fluorescence microscopy on these fixed cells indicated that Hos2p overexpression generates a complex, pleiotropic set of phenotypes in a dose-dependent manner. Additionally, it became clearly apparent that the extremely long cells were actually multi-nucleated hyphae. All of the pleiotropic phenotypes fell into two classes: one class of phenotypes was present globally in both hyphae and non-hyphal cells, whereas another set of phenotypes was responsible for the formation of hyphae, and only found in the hyphae. Additionally, each individual phenotype seen appeared to be dose-dependent above the threshold level of Hos2p needed to produce it (Fig. 3.13).

The global phenotypes included an increase in mean cell length (which was also observed as increased compartment length in the hyphae), the formation of abnormal cell wall deposits, and abnormal spherical morphology of cells and hyphal compartments. Additionally, it appeared that the cell wall deposit phenotype and spherical morphology phenotype were related, as they tended to occur simultaneously within a cell or hyphal compartment (Fig. 3.13 b, c). Hyphae were much longer than non-hyphal cells and often had branches. Phenotypes specific to hyphae included failure of the septum plane to bisect the long axis of the hypha at a perpendicular angle, a failure for hyphal compartments to separate via cytokinesis at the plane of septum deposition, multiple septa forming between two independent nuclei, abnormally shaped septa (i.e. spiraling around the hyphal cortex), and abnormally thick septa (Fig. 3.13 a). The hypha-specific phenotypes all appeared to be responsible for this growth pattern as well, as they all represent defects in cell division/septum positioning; additionally, a frequency distribution generated for cell length (which includes both hyphae and non-hyphal cells) in the three over-expression strains provides additional support for the dose-dependence of hypha-specific phenotypes, as higher levels of Hos2p generate more hypha of a longer length (Fig. 3.14, Fig. 3.15, Fig. 3.16).

The Hos2p over-expression phenotypes are difficult to interpret for several reasons. The phenotypes are pleiotropic, and for this reason, many different cellular processes may be impaired. Also, the results of this experiment are not restricted to confines of the Lst complex-mediated functions of Hos2p; these effects may be within the context of other Hos2p-containing complexes, or Hos2p may be acting on substrates it does not normally target due to its concentration, or any number of other possibilities

could explain these phenotypes. However, the data suggests several speculative hypotheses. The increase in average cell length and hyphal compartment length suggests a cell cycle delay, but does not indicate where this delay may be occurring; it could also represent an aberration in tying size control to cell cycle progression. The cell wall deposits suggest a defect in any of a number of processes involved in cell wall formation; additionally, since it tends to co-occur with spherical morphology, it is possible that the spherical morphology is caused by mechanical stress generated by abnormal cell wall deposition; alternatively, spherical morphology may be due to cytoskeletal abnormalities. Finally, the cell division and septum defects in hyphae suggest defects in the actomyosin contractile ring. One must bear in mind that none of these hypotheses preclude the possibility that other biological processes might be impaired in addition to or as an alternative to the hypotheses presented. More specialized experiments are necessary to disentangle the molecular mechanisms and biological processes underlying the overexpression phenotypes. One simple experiment to test for abnormalities in the actin and/or myosin cytoskeletal subsystems is to fix and stain the overexpressor strains with a fluorescent dye specifically binding actin or myosin, followed by high-resolution fluorescence microscopy.

Having discussed the many complications that hamper interpretation of the Hos2p overexpression phenotypes, I will briefly review research that will give more concrete direction for generating testable hypotheses based around this overexpression study. In one study investigators saw that over-expressing HDAC3 in the human-derived THP-1 cell line increased cell size, which is analogous to the *S. pombe* cell and hyphal-compartment size increase. The researchers also saw an accumulation of G2/M cells; the

hyphal defects in septum positioning and cell division occurred at the G2/M boundary of *S. pombe* as well. That being said however, there are many morphological differences between human cells and *S. pombe*, so it is difficult to determine whether these cross-species similarities are biologically meaningful. However, both studies suggest defects in the integration of components in both the cell cycle and size control when the conserved Hos2p/HDAC3 histone deacetylase is overexpressed. Additionally, there is a cumulative body of data suggesting that HDACs have a role in modulating the G2/M transition via their activity on histone substrates. (Dangond *et al.* 1998)

As this project has now been discussed in its entirety, it is appropriate to make several concluding remarks and put the findings of this project in the scheme of basic eukaryotic cell biology. My project and Stefan's project form two parts of a whole that characterized the Lst complex, and came to the following conclusions. The Lst complex is an evolutionarily conserved, nuclear-localized histone de-acetylase complex needed in a G2/M boundary checkpoint response that prevents cytokinesis failure via its ability to de-acetylate a substrate or substrates and works in a parallel branch to other regulators of this checkpoint. This complex is additionally also needed to respond to environmental stress by transcriptional activation of the CESR. Additionally, the complex increases its capacity for transcriptional control of the CESR genes by up-regulating levels of its Lst1p, Lst2p, Lst3p sub-units (which are exclusively nuclear) and possibly also by shuttling the nucleo-cytoplasmic Hos2p from the cytoplasm into the nucleus. The relationship between stress response and checkpoint activation is presently unresolved, as is the mechanism whereby it regulates functioning of both the checkpoint and CESR response (although the CESR response is likely due to histone or transcription factor de-acetylation). Removing

the activities of Hos2p also appear to slow down normal cytokinesis, a mysterious phenomenon that was not explored further due to its irrelevance in the scheme of this project. It appears that Hos2p over-expression also impairs a process or processes needed for normal cell cycle progression, morphology and growth, but that is the extent to which any conclusions can be made about Hos2p over-expression (Rentas, 2010).

The importance of this project in the context of cytokinesis, stress response and histone de-acetylase research is underscored by the observation that unique properties of Hos2p/HDAC3 histone de-acetylase are conserved from *S. pombe* to metazoans. HDAC3 has many properties not shared by other class I HDACs, suggesting that it has unique functions, and no other human HDAC complexes are similar to HDAC3/NCOR2-SMRT, suggesting it has distinct functions from all other HDACs. (Yang *et al.* 2002) This idea is also supported by data that shows that the budding yeast orthologue of HDAC3 and Hos2p, Hos2, is also unique. Hos2 differs from all other de-acetylases in that it de-acetylates the coding region of active genes and acts as a general activator of transcription. Although this appears to contradict the popular charge-neutralization model, recent research indicates that transcriptional regulation via histone acetylation and de-acetylation is likely more complicated than this simplistic model (Kurdistani and Grunstein, 2003). The conservation and uniqueness of this histone-deacetylase and the Lst complex are indicative of essential biological roles, which make exhaustive research in this area necessary in the future.

LITERATURE CITED

Adams, R. R., A. A. Tavares, A. Salzberg, H. J. Bellen and D. M. Glover, 1998 *pavarotti* encodes a kinesin-like protein required to organize the central spindle and contractile ring for cytokinesis. Genes Dev. **12(10):** 1483-1494.

Alfa, C., P. Fantes, M. Mcleod, E. Warbrick, J. Hyams, 1993 *Experiments with Fission Yeast: A Laboratory Course Manual.* Cold Spring Harbor Press, Cold Spring Harbor, USA

Almonacid, M., J. B. Moseley, J. Janvore, A. Mayeux, V. Fraisier *et al.* 2009 Spatial control of cytokinesis by Cdr2 kinase and Mid1/anillin nuclear export. Curr. Biol. **19(11):** 961-966.

Ayscough, K. R., J. Stryker, N. Pokala, M. Sanders, P. Crews *et al.*,1997 High rates of actin filament turnover in budding yeast and roles for actin in establishment and maintenance of cell polarity revealed using the actin inhibitor latrunculin-A. J. Cell Biol. **137:** 399-416.

Bähler, J., A. B. Steever, S. Wheatley, Y. Wang, J. Pringle *et al.* 1998. Role of Polo Kinase and Mid1p in Determining the Site of Cell Division in Fission Yeast. J. Cell Sci. **143(6):** 1603-1616.

Balasubramanian, M. K., E. Bi and M. Glotzer, 2004 Comparative analysis of cytokinesis in budding yeast, fission yeast and animal cells. Curr. Biol. **14:** R806.

Balasubramanian, M. K., D. McCollum, L. Chang, K. C. Wong, N. I. Naqvi *et al.*, 1998 Isolation and characterization of new fission yeast cytokinesis mutants. Genetics **149:** 1265-1275.

Bement, W. M., H. A. Benink and G. von Dassow, 2005 A microtubule-dependent zone of active RhoA during cleavage plane specification. J. Cell Biol. **170(1):** 91-101.

Boyer, L. A., R. R. Latek and C. L. Peterson, 2004 The SANT domain: a unique histone-tail-binding module? Nat. Rev. Mol. Cell Biol. **5:** 1-6.

Boveri, T., 1929 *The origin of malignant tumors.* Williams and Wilkins, Baltimore, MD.

Bjerling, P., R. A. Silverstein, G. Thon, A. Caudy, S. Grewal *et al.*, 2002 Functional Divergence between Histone Deacetylases in Fission Yeast by Distinct Cellular Localization and In Vivo Specificity. Mol. Cell Biol. **22(7):** 2170-2181.

Chen, D., W. M. Toone, J. Mata, R. Lyne, G. Burns *et al.*, 2003 Global Transcriptional Responses of Fission Yeast to Environmental Stress. Mol. Biol. Cell **14:** 214-229.

Cohen, T. J., M. J. Mallory, R. Strich and T.-P. Yao, 2008 Hos2p/Set3p Deacetylase Complex Signals Secretory Stress through the Mpk1p Cell Integrity Pathway. Eukaryot. Cell **7:** 1191-1199.

Dangond, F., D. A. Hafler, J. K. Tong, J. Randall, R. Kojima *et al.*, 1998 Differential Display Cloning of a Novel Human Histone Deacetylase (HDAC3) cDNA from PHA-Activated Immune Cells. Biochem. Biophys. Res. Commun. **242:** 648–652.

Echard, A., G. R. Hickson, E. Foley and P. H. O'Farrell, 2004 Terminal cytokinesis events uncovered after an RNAi screen. Curr. Biol. **14(18):** 1685-1693.

Egel, R., 2004 *The Molecular Biology of Schizosaccharomyces pombe: Genetics, Genomics and Beyond.* Springer, Heidelberg, Germany.

Eggert, U. S., T. J. Mitchison and C. M. Field, 2006 Animal cytokinesis: from parts list to mechanisms. Annu. Rev. Biochem. **75:** 543-566.

Forsburg, S. L., and N. Rhind, 2006 Basic methods for fission yeast. Yeast **23:** 173-183.

Fujiwara, T., M. Bandi, M. Nitta, E. V. Ivanova, R. T. Bronson, *et al.* 2005 Cytokinesis failure generating tetraploids promotes tumorigenesis in p53-null cells. Nature **437:** 1043-1047.

Ganem, N. J., S. A. Godinho and D. Pellman, 2009 A mechanism linking extra centrosomes to chromosomal instability. Nature **460:** 278-282.

Ganem, N.J., Z. Storchova and D. Pellman, 2007 Tetraploidy, aneuploidy and cancer. Current opinion in genetics & development **17:** 157-162.

Goshima, G., and R. D. Vale, 2003 The roles of microtubule-based motor proteins in mitosis: comprehensive RNAi analysis in the *Drosophila* S2 cell line. J. Cell Biol. **162(6):** 1003-1016.

Grunstein, M., 1997 Histone acetylation in chromatin structure and transcription. Nature **389:** 349-352.

Hartwell, L. H., and T. A. Weinert, 1989 Checkpoints: controls that ensure the order of cell cycle events. Science **246:** 629-634.

Hachet, O. and V. Simanis, 2008 Mid1p/anillin and the septation initiation network orchestrate contractile ring assembly for cytokinesis. Genes Dev. **22(22):** 3205-3216.

Hirose, K., T. Kawashima, I. Iwamoto, T. Nosaka and T. Kitamura, 2001 MgcRacGAP is involved in cytokinesis through associating with mitotic spindle and midbody. J. Biol. Chem. **276(8):** 5821-5828.

Karagiannis, J., A. Bimbo, S. Rajagopalan, J. Liu and M. K. Balasubramanian, 2005 The nuclear kinase Lsk1p positively regulates the septation initiation network and promotes the successful completion of cytokinesis in response to perturbation of the actomyosin ring in *Schizosaccharomyces pombe.* Mol. Biol. Cell **16:** 358-371.

Kim, D. U., J. Hayles, D. Kim, V. Wood, H. O. Park *et al.*, 2010 Analysis of a genome-wide set of gene deletions in the fission yeast, *Schizosaccharomyces pombe.* Nat. Biotechnol. **28:** 617-623.

King, R. W., R. J. Deshaies, J. M. Peters and M. W. Kirschner, 1996 How proteolysis drives the cell cycle. Science **274(5293):** 1652-1659.

Kittler, R., L. Pelletier, A. K. Heninger, M. Slabicki, M. Theis *et al.*, 2007 Genome-scale RNAi profiling of cell division in human tissue culture cells. Nat. Cell Biol. **9:** 1401-1412.

Kouzarides, T., 2000 Acetylation: a regulatory modification to rival phosphorylation? EMBO J. **19:** 1176-1179.

Kouzarides, T., 1999 Histone acetylases and deacetylases in cell proliferation.Curr. Opin. Genetics Dev. **9:** 40-48.

Krapp, A., and V. Simanis, 2008 An overview of the fission yeast septation initiation network (SIN). Biochem. Soc. Trans. **36(Pt 3):** 411-415.

Kurdistani, S. K. and M. Grunstein, 2003 Histone Acetylation and Deacetylation in Yeast. Nat. Rev. Mol. Cell Biol. **4:** 276-284.

Kuo, M.-H. and C. D. Allis, 1998 Roles of histone acetyltransferases and deacetylases in gene regulation. BioEssays **20:** 615-626.

Lahm, A., C. Paolini, M. Pallaoro, M. C. Nardi, P. Jones, *et al.* 2007 Unraveling the hidden catalytic activity of vertebrate class IIa histone deacetylases. Proc. Natl. Acad. Sci. USA **104:** 17335–17340.

Le Goff, X., F. Motegi, E. Salimova, I. Mabuchi and V. Simanis, 2000 The *S. pombe rlc1* gene encodes a putative myosin regulatory light chain that binds the type II myosins myo3p and myo2p. J. Cell Sci. **113:** 4157-4163.

Liu, J., H. Wang and M. K. Balasubramanian, 2000 A checkpoint that monitors cytokinesis in *Schizosaccharomyces pombe.* J. Cell Sci. **113:** 1223-1230.

Low, S. H., X. Li, M. Miura, N. Kudo, B. Quiñones *et al.* 2003 Syntaxin 2 and endobrevin are required for the terminal step of cytokinesis in mammalian cells. Dev. Cell **4(5):** 753-759.

Mabuchi, I., Y. Hamaguchi, H. Fujimoto, N. Morii, M. Mishima *et al.*, 1993 A rho-like protein is involved in the organisation of the contractile ring in dividing sand dollar eggs. Zygote **1(4):** 325-331.

Martin, S. G., and M. Berthelot-Grosjean, 2009 Polar gradients of the DYRK-family kinase Pom1 couple cell length with the cell cycle. Nature **459(7248):** 852-856.

Mellor, J., 2006 It Takes a PHD to Read the Histone Code. Cell **126:** 22-24.

Mishra, M., J. Karagiannis, M. Sevugan, P. Singh and M. K. Balasubramanian, 2005 The 14-3-3 protein rad24p modulates function of the cdc14p family phosphatase clp1p/flp1p in fission yeast. Curr. Biol. **15:** 1376-1383.

Mishra, M., J. Karagiannis, S. Trautmann, H. Wang, D. McCollum *et al.*,2004 The Clp1p/Flp1p phosphatase ensures completion of cytokinesis in response to minor perturbation of the cell division machinery in *Schizosaccharomyces pombe.* J. Cell Sci. **117:** 3897-3910.

Mollinari, C., J. P. Kleman, W. Jiang, G. Schoehn, T. Hunter *et al.*, 2002 PRC1 is a microtubule binding and bundling protein essential to maintain the mitotic spindle midzone. J. Cell Biol. **157(7):** 1175-1186.

Moseley, J. B., A. Mayeux, A. Paoletti and P. Nurse, 2009 A spatial gradient coordinates cell size and mitotic entry in fission yeast. Nature **459(7248):** 857-860.

Nigg, E.A., 2001 Mitotic kinases as regulators of cell division and its checkpoints. Nat. Rev. Mol. Cell Biol. **2(1):** 21-32.

Niiya, F., X. Xie, K. S. Lee, H. Inoue andT. Miki, 2005 Inhibition of cyclin-dependent kinase 1 induces cytokinesis without chromosome segregation in an ECT2 and MgcRacGAP-dependent manner. J. Biol. Chem. **280(43):** 36502-36509.

Nislow, C., V. A. Lombillo, R. Kuriyama and J. R. McIntosh, 1992 A plus-end-directed motor enzyme that moves antiparallel microtubules in vitro localizes to the interzone of mitotic spindles. Nature **359(6395):** 543-547.

Olsson, T. G. S., K. Ekwall, R. C. Allshire, P. Sunnerhagen, J. F. Partridge *et al.*, 1998 Genetic characterisation of *hda1*$^{+}$, a putative fission yeast histone deacetylase gene. Nucleic Acids Res. **26:** 3247-3254.

Pijnappel, W. W., D. Schaft, A. Roguev, A. Shevchenko, H. Tekotte *et al.*, 2001 The *S. cerevisiae* SET3 complex includes two histone deacetylases, Hos2 and Hst1, and is a meiotic-specific repressor of the sporulation gene program. Genes Dev. **15:** 2991-3004.

Pollard, T. D., and J. Q. Wu, 2010 Understanding cytokinesis: lessons from fission yeast.

Nat. Rev. Mol. Cell Biol. **11:** 149-155.

Pons, D., F. R. de Vries, P. J. van den Elsen, B. T. Heijmans, P. H.A. Quax *et al.*, 2009 Epigenetic histone acetylation modifiers in vascular remodelling: new targets for therapy in cardiovascular disease. Eur. Heart J. **30:** 266-277.

Prokopenko, S. N., A. Brumby, L. O'Keefe, L. Prior, Y. He *et al.*, 1999 A putative exchange factor for Rho1 GTPase is required for initiation of cytokinesis in *Drosophila.* Genes Dev. **13(17):** 2301-2314.

Rentas, S., 2010 *A Conserved Histone Deacetylase Complex with a Role in Promoting the Successful Completion of Cytokinesis in Schizosaccharomyces pombe.* The University of Western Ontario, London, ON, Canada.

Schmidt, S., M. Sohrmann, K. Hofmann, A. Woollard and V. Simanis, 1997 The Spg1p GTPase is an essential, dosage-dependent inducer of septum formation in *Schizosaccharomyces pombe.* Genes Dev. **11(12):** 1519-1534.

Stirnimann, C. U., E. Petsalaki, R. B. Russell and C. W. Müller, 2010 WD40 proteins propel cellular networks. Trends Biochem. Sci. **35:** 565-574.

Storchova, Z. and D. Pellman,2004 From polyploidy to aneuploidy, genome instability and cancer. Nat. Rev. Mol. Cell. Biol. **5:** 45-54.

Stoscheck, C.M., 1990 Quantitation of protein. Methods Enzymol. **182:** 50-68.

Tatsumoto, T., X. Xie, R. Blumenthal, I. Okamoto and T. Miki, 1999 Human ECT2 is an exchange factor for Rho GTPases, phosphorylated in G2/M phases, and involved in cytokinesis. J. Cell Biol. **147(5):** 921-928.

Toone, W. M. and N. Jones, 1998 Stress-activated signalling pathways in yeast. Genes Cells **3:** 485-498.

Uyeda, T. Q., A. Nagasaki and S. Yumura, 2004 Multiple parallelisms in animal cytokinesis. Int. Rev. Cytol. **240:** 377-432.

Vavylonis, D., J. Q. Wu, S. Hao, B. O'Shaughnessy and T. D. Pollard, 2008 Assembly mechanism of the contractile ring for cytokinesis by fission yeast. Science **319(5859):** 97-100.

Vernì, F., M. P. Somma, K. C. Gunsalus, S. Bonaccorsi, G. Belloni *et al.*, 2004 Feo, the *Drosophila* homolog of PRC1, is required for central-spindle formation and cytokinesis. Curr. Biol. **14(17):** 1569-1575.

Vernos, I., J. Raats, T. Hirano, J. Heasman, E. Karsenti *et al.*, 1995 Xklp1, a chromosomal *xenopus* kinesin-like protein essential for spindle organization and chromosome positioning. Cell **81(1):** 117-127.

Williams, B. C., M. F. Riedy, E. V. Williams, M. Gatti and M. L. Goldberg, 1995 The *Drosophila* kinesin-like protein KLP3A is a midbody component required for central spindle assembly and initiation of cytokinesis. J. Cell Biol. **129(3):** 709-723.

Wood, V., R. Gwilliam, M. A. Rajandream, M. Lyne, R. Lyne *et al.*, 2002 The genome sequence of *Schizosaccharomyces pombe.* Nature **415:** 871-880.

Wu, J. Q., and T. D. Pollard, 2005 Counting cytokinesis proteins globally and locally in fission yeast. Science **310(5746):** 310-314.

Yang, W.-M., S.-C. Tsai, Y.-D. Wen, G. Fejér and E. Seto, 2002 Functional Domains of Histone Deacetylase-3*. J. Biol. Chem. **277:** 9447-9454.

Yeates, T., 2002 Structures of SET Domain Proteins: Protein Lysine Methyltransferases

Make Their Mark. Cell **111:** 5-7.

Zhu, C., and W. Jiang, 2005 Cell cycle-dependent translocation of PRC1 on the spindle by Kif4 is essential for midzone formation and cytokinesis. Proc. Natl. Acad. Sci. USA **102(2):** 343-348.